POWER MANAGEMENT SYSTEM FOR SMART MICROGRID CONSIDERING METEOROLOGICAL AND LOAD DEMAND DATA

SAM KOOHIKAMALI

THESIS SUBMITTED IN FULFILLMENT OF THE REQUIREMENTS FOR THE DEGREE OF DOCTOR OF PHILOSOPHY

FACULTY OF ENGINEERING
UNIVERSITY OF MALAYA
KUALA LUMPUR

2015

UNIVERSITI MALAYA

ORIGINAL LITERARY WORK DECLARATION

Name of Candidate: Sam Koohikamali (I.C/Passport No:

Registration/Matric No: KHA110043

Name of Degree: Doctor of Philosophy

Title of Project Paper/ Research Report/ Dissertation/ Thesis ("this Work"):

POWER MANAGEMENT SYSTEM FOR SMART MICROGRID CONSIDERING METEOROLOGICAL AND LOAD DEMAND DATA

Field of Study: Power Electronics (Electricity and Energy)

I do solemnly and sincerely declare that:

I am the sole author/writer of this work;

This work is original;

Any use of any work in which copyright exists was done by way of fair dealing and for permitted purpose and any excerpt or extract from, or reference to or reproduction of any copyright has been disclosed expressly and sufficiently and the title of the Work and its authorship have been acknowledged in this work;

I do not have any actual knowledge nor do I ought reasonably to know that the making of this work constitutes an infringement of any copyright work;

I hereby assign all and every rights in copyright to this Work to the University of Malaya ("UM"), who henceforth shall be owner of the copyright in this Work and that any reproduction or use in any form or by any means whatsoever is prohibited without the written consent of UM having been first had and obtained;

I am fully aware that if in the course of making this Work I have infringed any copyright whether intentionally or otherwise, I may be subjected to legal action or any other action as may be determined by UM.

Candidate Signature Date:

Subscribed and solemnly declared before,

Witness's Signature Date:

Name:

Designation:

ABSTRACT

Integration of utility scaled solar electricity generator into power networks can negatively affect the performance of next generation smart grid. Rapidly changing output power of this kind is unpredictable and thus one solution is to mitigate it by short-term to mid-term electrical storage systems like battery. For this purpose, the battery storage system should be dispatched properly by a power management system (PMS) and hence the main objective of this work is to propose a PMS for smart microgrid (MG) applications. Microgrid refers to a cluster of generation, load, and energy storage units which can operate in grid-connected and/or in islanded modes. In this work, a smart microgrid system which consists of diesel, battery storage, and solar plants is suggested as well. Microgrid is able to supply its local load based on operator decision and decline the power oscillations caused by solar photovoltaic (PV) plant together with variable loads.

An algorithm is also proposed which helps to precisely design the battery energy storage plant. A novel application of time domain signal processing approach (i.e. moving average filtering) to filter oscillating output power of the solar PV plant is presented as well. In this case, a power smoothing index (PSI) is formulated, which considers both load and generation, and used to dispatch the battery plant. A droop reference estimator to schedule generation is also introduced where diesel plant can share the local load with grid. A current control algorithm is designed as well which controls the active power smoothing index to ensure battery current magnitude is allowable. Microgrid along with its communication platform and PMS are simulated using PSCAD software. PMS is tested under different scenarios using real load profiles and meteorological data in Malaysia to verify the operational abilities of proposed MG. The results indicate that PMS can effectively manage the MG and satisfies both operator and demand sides.

ABSTRAK

Integrasi utiliti dipertingkatkan penjana elektrik solar dalam rangkaian kuasa boleh mengakibatkan kesan negatif terhadap prestasi generasi grid pintar pada masa hadapan. Perubahan pantas kuasa outputnya tidak dapat dijangka, dan dengan itu, satu penyelesaian adalah dengan mengurangkan kesannya melalui sistem penyimpanan elektrik jangka masa pendek hingga jangka masa sederhana seperti bateri. Untuk tujuan ini, simpanan bateri perlu disalurkan dengan teratur melalui sistem pengurusan kuasa (PMS) dan oleh yang demikian objektif utama kajian ini ialah untuk mencadangkan sebuah sistem pengurusan kuasa (PMS) untuk applikasi grid mikro (MG) pintar. Grid mikro merujuk kepada sebuah kluster penjanaan, beban dan unit penyimpanan tenaga yang dapat beroperasi sama ada di dalam mod sambungan grid atau mod 'terpulau'. Sebuah sistem grid mikro pintar yang terdiri daripada diesel, simpanan bateri, dan loji solar turut dicadangkan dalam kajian ini. Grid mikro berupaya untuk membekal beban tempatan berdasarkan keputusan operator dan mengelak ayunan kuasa yang dihasilkan oleh loji fotovoltek (PV) solar bersama dengan beban pembolehubah.

Satu algoritma turut dicadangkan bagi membantu mereka bentuk loji simpanan tenaga bateri tersebut dengan tepat. Applikasi baru menggunakan kaedah pemprosesan signal domain masa (i.e. penyaringan purata bergerak) untuk menyaring kuasa output ayunan yang dihasilkan loji PV solar turut dibincangkan. Dalam kes ini, satu indeks pelicinan kuasa (PSI) turut diformulasi, dengan mengambil kira kedua-dua beban dan penjanaan, yang kemudiannya digunakan untuk penghantaran loji bateri tersebut. Sebuah penganggar rujukan 'droop' untuk menjadualkan penjanaan juga diperkenalkan di mana loji diesel dapat berkongsi beban tempatan dengan grid. Satu algoritma kawalan arus yang mengawal indeks pelicinan kuasa aktif turut direka bagi memastikan magnitud arus bateri adalah dalam kadar yang dibenarkan. Grid mikro bersama dengan platform komunikasinya dan PMS disimulasi menggunakkan perisian PSCAD. PMS diuji

melalui pelbagai senario dengan menggunakan profil beban sebenar dan data meteorologi di Malaysia bagi mengesahkan kebolehoperasian MG yang dicadangkan. Hasil kajian menunjukkan bahawa PMS tersebut mampu mengurus MG dengan efektif selain memenuhi kehendak kedua-dua belah pihak operator dan pengguna.

ACKNOWLEDGEMENTS

I am heartily grateful to my dear parents and my dear sister who gave me the moral support during my studies.

To my dear supervisors **Prof. Dr. Nasrudin Abd Rahim** and **Assoc. Prof. Dr. Hazlie Mokhlis** whose recommendations and supports encouraged me to put my ideas forward here and develop such relevant results.

To **High Impact Research Secretariat (HIR)** which provided me with research funds and facilities in order to complete this work.

I also would like to appreciate **University of Malaya Faculty of Engineering** and **UM Power Energy Dedicated Advanced Centre (UMPEDAC)** administrative and technical personnel who collaborated on this project.

And the last but not the least, to my classmate **Ms. Syahirah Abd Halim** who helped me to translate my thesis abstract to Malay language.

Sam Koohikamali
October 2014

TABLE OF CONTENTS

LIST OF FIGURES

LIST OF TABLES

LIST OF SYMBOLS AND ABBREVIATIONS

APSI	Active Power Smoothing Index
BES	Battery Energy Storage
BESS	Battery Energy Storage System
CC	Central Controller
CERTS	Consortium for Electric Reliability Technology Solutions
COE	Cost of Electricity
CT	Current Transformer
DER	Distributed Energy Resource
DG	Distributed Generation
DNO	Distribution Network Operator
DOE	Department of Energy
DR	Demand Response
DS	Distributed Storage
DSP	Digital Signal Processor
e-FiT	Online feed-in tariff
EI	Electronically Interfaced
EIDG	Electronically Interfaced Distributed Generation
EMM	Energy Manager Module
EMS	Energy Management System
ESS	Energy Storage System

EV	Electric Vehicle
FiT	Feed-in tariff
G.C	Grid-Connected
GA	Genetic Algorithm
GW	Giga Watt
IC	Internal Combustion
IEA-PVPS	International Energy Agency-Photovoltaic Power Systems Program
IED	Intelligent Electronic Device
IGBT	Insulated Gate Bipolar Transistor
LAB	Lead Acid Battery
LC	Local Controller
LTC	Load Tap Changer
LVRT	Low Voltage Ride-Through
MAF	Moving Average Filtering
MBIPV	Malaysia Building Integrated Photovoltaic
MC	Microsource Controller
MCC	Microgrid Central Controller
MG	Microgrid
MO	Market Operator
MPP	Maximum Power Point
MPPT	Maximum Power Point Tracking

MW_p	Mega Watt Peak
PC	Point of Connection
PCC	Point of Common Coupling
PCM	Protection Co-ordination Module
PI	Proportional Integral
PLL	Phase Locked Loop
PMA	Power Management Algorithm
PMS	Power Management System
PT	Potential Transformer
PV	Photovoltaic
PVDG	Photovoltaic Distributed Generation
PWM	Pulse Width Modulation
rad/sec	Radian Per Second
RE	Renewable Energy
RES	Renewable Energy System
ROCOF	Rate of Change of Frequency
rpm	Round Per Minute
RPSI	Reactive Power Smoothing Index
SEDA	Sustainable Energy Development Authority
SOC	State of Charge
TNB	Tenaga National Berhad

TOV	Temporary Overvoltage
TWh	Terra Watt Hour
UPS	Uninterruptible Power Supply
VA	Volt Ampere
VCO	Voltage-Controlled Oscillator
VR	Voltage Regulator
VSC	Voltage Sourced Converter

LIST OF APPENDICES

CHAPTER 1: INTRODUCTION

1.1. Overview

Modern social needs necessitate extracting energy from the burning fossil fuels. This fact leads to propagation of greenhouse gases (carbon dioxide, nitrous oxide, methane) into the atmosphere and hence changes the climate globally. To avoid disastrous harm to the planet, forceful carbon decline must begin today. Electricity constitutes about 24% of greenhouse gas emissions. Electricity consumption is expected to grow from 18 trillion kWh in 2006 to 32 trillion kWh in 2030 (which means 77% growth). This means that 4800 GW of new electricity generation plants must be constructed and more than 50% of this amount would be from developing nations. China is responsible for 28% of this raise by itself. Therefore, the extreme decrease of global carbon emission cannot be achieved without an effective collaboration from the electricity sector (Varaiya, Wu, & Bialek, 2011).

To supply the ever growing electricity demand, utilities can contribute in generation of electricity by exploiting renewable energy (RE) based power plants instead of fossil fuel plants. Renewable energy resources must create bigger contributions in generation of electrical power since generation of electrical power through renewable energy resources declines environmental emissions. Most rapidly growing renewable resources are wind and solar. In the U.S., wind is anticipated to increase from 31 TWh in 2008 (1.3% of total supply) to 1160 TWh by 2030 (Moslehi & Kumar, 2010). From 2005 to 2008, worldwide gain, in (grid-connected) solar energy, grew six fold to 13 GW.

In 2008, 5.4 GW of solar were added globally. China also met its target of 10 GW of installed wind power capacity two years ahead of schedule. In 2009, China renewed its goal for 2020 onward to generate 100 GW of wind power (from 30 GW set in the 2007 plan) and 20 GW of solar (from 1.8 GW set in the 2007 plan) (Varaiya et al., 2011).

Considering the ever growing global interest to generate electricity by utilization of renewable energy resources, new generation of utility networks have to include both renewable energy and fossil fuel plants. Public needs in modern societies beside optimal consumption and/or generation of electricity also necessitate to manage energy resources from any kind in a coordinated manner. Therefore, it is necessary to integrate power management systems (PMSs) into deregulated power networks. This matter has brought a new concept which is so-called “Smartgrid”. Smartgrid incorporates advanced measurement technologies, control algorithms, and communication platforms into present power grid configuration. These features are helpful to optimally exploit renewable energy (RE) systems in large scales along with fossil fuels plants (Acharjee, 2012, 2013).

A smart power grid can be composed by several areas and each region can be taken into account as a micro power grid. Microgrid (MG) refers to a combination of distributed storage (DS), RE distributed generation (DG) systems, and loads which can operate in parallel with the main smartgrid or in autonomous modes. Microgrid is an issue that has been investigated globally in the recent decade. Remarkable attention was paid to microgrid concept by the IEEE Std P1547.4 on Guide for Design, Operation, and Integration of Distributed Resource Island Systems with Electric Power Systems (Benjamin Kroposki et al., 2008). This guide was initially drafted to deal with the missing information in IEEE Std 1547-2008 about intentional islanding.

For the time being, the research works on microgrids have commonly relied on test-beds or simulations using different microgrid configurations. There are some typical microgrid topologies that have been discussed by (Lidula & Rajapakse, 2011) in detail.

Microgrid can be considered as a cluster of load and generation in smartgrid and brings many advantages for the grid which is connected to. The benefits can be pointed out i.e. increasing RE sources depth of penetration, decreasing environmental emissions, utilizing waste heat, providing ancillary services, making the balance between generation and consumption, and bringing continuous backup power supply for redundant and sensitive processes (Cornforth, 2011; Eckroad & Gyuk, 2003).

However, utilities must deal with technical challenges resulted by utilization of renewable resources beside fossil fuels. For example, in the case of photovoltaic plants, the availability of solar resource is highly affected by changes in meteorological variables such as solar irradiation and cell operating temperature. These variables are stochastic and hence the power generated by a solar plant is intermittent. The capacity factors for a photovoltaic plant are usually about 10% or 20% of its total generation capacity (Moslehi & Kumar, 2010). Therefore, solar power plants generally have adverse impacts on grid reliability because of their fluctuating output power.

Microgrid operation can be improved by exploiting energy storage systems (ESSs). To alleviate the power fluctuations caused by a photovoltaic power plant, the energy ESS can be considered as a proper solution. Therefore, the main applications of energy storage devices are to balance between generation and demand as well as to provide the power grid with ancillary services e.g. voltage regulation and spinning reserve (Eckroad & Gyuk, 2003; Koohi-Kamali, Rahim, & Mokhlis, 2014; Koohi-Kamali, Tyagi, Rahim, Panwar, & Mokhlis, 2013).

In a microgrid, the coordinated operation and control of distributed energy resources (DERs) through a central power management system (PMS) improves system reliability, power quality, and reduces emissions and costs.

This work mainly focuses on the functionalities of microgrid power management system (PMS) in order to decline power oscillations caused by photovoltaic plant using energy storage systems. In this case, a coordinated power management algorithm is proposed to optimally schedule dispatchable distributed energy resources (i.e. both renewable energy and fossil fuel based plants) in the microgrid.

1.2. Problem Statement

The resources inside of a deregulated distribution network have to be controlled smartly through a power management system (PMS). This matter helps the system operator to manage the power grid devices such as distributed photovoltaic (PV) plants, energy storage systems (ESSs), and voltage regulators in a coordinated manner. In a large-scale distribution network, the probability of system sectionalizing into different autonomous areas forming microgrids is quite high. In this case, each microgrid should be able to optimally satisfy technical and economical requirements through its PMS for both operator and demand sides.

Different functionalities should be defined for PMS by the system operator and customers. Power smoothing capability is one example brought to this end. The operator should be able to handle all distributed energy resources (DERs) in such a way that to decrease their adverse impacts on the main supply. For example, solar PV plant in high penetration levels can modify the load profile (from the operator's view) and create technical and economical challenges for the system in steady-state and transient operating modes. The fluctuating output power is one example of this kind (Daud, Mohamed, & Hannan, 2013; Shah, Mithulananthan, & Bansal, 2013). Ramp ups/downs

in solar plant output power are completely unpredictable. These fluctuations can be governed by several factors i.e. passing clouds, PV power plant placement, depth of penetration, and power network topology. If these power fluctuations are uncontrollable, main AC network equipments such as motors, generators, and voltage regulating devices can be affected adversely (Daud et al., 2013; Koohi-Kamali et al., 2013; Steffel & Dinkel, 2013). This oscillatory nature may create voltage and angle instability in the main grid as well.

To address the problem due to the unpredictable manner of photovoltaic power plants, different methods have been proposed in the literature (Ahmed, Miyatake, & Al-Othman, 2008; Omran, Kazerani, & Salama, 2011; Teleke, Baran, Bhattacharya, & Huang, 2010; Teleke, Baran, Huang, Bhattacharya, & Anderson, 2009). For instance, in (Omran et al., 2011), generation curtailment, dump load usage, and exploiting energy storage systems have been recommended as the solutions for this problem. However, the role of load real-time variation based on an actual profile has not been considered in this research.

In order to suppress addressed oscillations, the use of energy storage systems along with fuel cell (Ahmed et al., 2008) has also become very popular recently (Teleke et al., 2010; Teleke et al., 2009). In this case, battery energy storage (BES) has mostly been proposed by the researchers for short-term to mid-term applications (Daud et al., 2013; Teleke et al., 2010; Teleke et al., 2009). Batteries are expensive equipments and thus elaborated control strategies must be adopted to exploit battery energy storage (BES) systems efficiently. A conventional inertial filter has been utilized in (Yun-Hyun, Soo-Hong, Chang-Jin, Sang Hyun, & Byeong-Ki, 2011) to smooth output power of a wind farm and make a reference value for current controlled inverter of a BES plant. In (Daud et al., 2013; Yoshimoto, Nanahara, & Koshimizu, 2006), state of charge (*SOC*) feedback controllers for BES have been suggested which limit battery

charging/discharging currents within the acceptable range. However, finding an accurate time constant for state of charge by these two methods is not a straightforward task and hence highly depends on assumptions made by the planner which may not be the same at all times. In (Daud et al., 2013), genetic algorithm (GA) has also been used to optimize the control parameters for solar plant which may increase the computational burden instead.

Power management system (PMS) should be designed so that it handles DGs and loads in any kind considering plug and play ability. PMS also should manage the system based on real-time data. In all above mentioned literatures, there has not been considered the role of rotary based DG systems such as diesel generator power plant in conjunction with the intermittent RE sources where the system supplies variable loads based on actual profiles. The lack of an embedded PMS (in microgrid supervisory system) which can govern a MG including RE sources together with the conventional DGs is completely obvious as well. In (Tan, Peng, So, Chu, & Chen, 2012; Tan, So, Chu, & Chen, 2013), coordinated energy management algorithms have been proposed which can control a MG consisting of only electronically interfaced (EI) DGs. However, the role of rotary based DG has not been investigated and smoothing power fluctuations of solar plant together with a real load profile has not been addressed in these two works as well.

As another issue, batteries are expensive equipments and hence a battery bank has to be designed and sized to effectively minimize power fluctuations in the network. The previous methods (Lin, Xinbo, Chengxiong, Buhan, & Yi, 2013; Yu, Kleissl, & Martinez, 2013) rely on optimization algorithm which increase computational burden instead. However, a straightforward algorithm is proposed for this purpose in this thesis which considers the ramp rate limits of the main power grid. This algorithm is easy to implement and requires trivial computation.

Therefore, the need for a centralized PMS is crucial in managing a smart microgrid system that is able to adapt itself with real-time changes in meteorological and load demand data. In this case, a well-designed energy storage system, properly scheduled by the PMS, can compensate for the power oscillations.

1.3. Research Objectives

In this thesis, the main objectives are:

- To propose and evaluate a smart microgrid system consisting of both rotary and electronically interfaced distributed energy resources (DERs);
- To develop a power management algorithm to control proposed microgrid system through a hierarchical communication platform;
- To develop controllers for distributed generation (DG) plants in order to exploit them based on operator commands delivered through power management system (PMS);
- To develop a battery sizing algorithm based on proposed power smoothing index (PSI);

1.4. Scope of Study

This work only focuses on technical issues associated with the power management system (PMS) and hence economical aspects are not taken into account at all. Proposed microgrid consists of both rotary (diesel power plant) and electronically interfaced (EI) distributed generation (DG) plants.

In addition, a new power smoothing index is formulated to mitigate the fluctuations resulted by intermittent solar PV system together with the variable load. In this case, moving average filtering (MAF) which is a time domain signal processing approach is utilized to smooth out these oscillations. This index can be applied on any kind of

intermittent renewable energy (RE) sources since it is easy to implement and has not relied on complicated computational methods.

A load model is also designed which can be suitable for real-time applications where the actual load profile has to be simulated for dynamic studies. A current control algorithm is proposed as well to ensure the battery charge/discharge current is within the specified limitation.

This work also suggests an algorithm for the purpose of the battery house sizing taking into account the ramp rate limits of the main network. Moreover, a power management algorithm (PMA) is suggested which helps the system owner to exploit the battery plant in the most efficient way.

The concept of agent is included in this algorithm to define different level of hierarchy where a communication channel acts as the platform to exchange information between the operator, DGs, and loads. To dispatch diesel and BES plants a new application of droop control mechanism is also introduced which makes it possible for the operator to schedule the generation units for both active and reactive powers. A droop mechanism for diesel plant excitation controller is also designed so that it can share the local reactive power with battery energy storage (BES) plant proportional to their ratings.

Proposed microgrid system including dynamic model of distributed generation plants (diesel and photovoltaic) and energy storage system together with their controllers are simulated and implemented in PSCAD/EMTDC software.

PSCAD is the simulation tool for professional applications. This software makes it possible to analyze transients of power system and study the dynamic behavior of grid components. This software is also recognized as PSCAD/EMTDC. EMTDC refers to the simulation engine which is currently the integral part of PSCAD.

1.5. Thesis Outline

In this thesis, Chapter 2 summarizes the theoretical frameworks associated with this thesis i.e. distributed generation (DG) concepts, photovoltaic DG system technical considerations, smart microgrid concept, power management techniques, energy storage system applications, and control of smart micro power grid.

Chapter 3 presents the proposed microgrid (MG) configuration and dynamic model of system components. In this chapter, the data collection approach (associated with load and generation) and the proposed power management algorithm (PMA) are presented. Battery storage bank design algorithm and the proposed charging/discharging current controller are also discussed in detail. This chapter also highlights the role of moving average filtering (MAF) in smoothing out the active power fluctuations.

In Chapter 4, simulation results are brought to the readers and technical matters are investigated in depth. In this chapter, four test cases are studied to validate effectiveness of proposed algorithms and controllers.

In the first test case, power smoothing index is evaluated and the ability of diesel and battery plants in order to share the load reactive power between themselves is assessed.

In the second test case, the capability of power management system (PMS) to dispatch the diesel plant and to shift up or down the AC network active power profile is examined. Battery storage plant is supposed to smooth out active power fluctuations and reactive power is shared between diesel and battery plants.

In the third test case, the ability of diesel plant to charge the battery is tested while smoothing function of battery plant is acting and grid is supplying average local reactive power demand.

In the last test case, active and reactive powers are supposed to be supplied locally. Battery plant is supposed to be charged locally by the diesel plant.

Chapter 5 concludes this work and the future research opportunities in this filed are presented in this chapter.

CHAPTER 2: LITRATURE REVIEW

2.1. Introduction

In this chapter, microgrid concept is discussed in detail. Some existing microgrid test-beds in the world are investigated briefly as well. The deregulated power system is also introduced and the related technical challenges are pointed out. The concept of distributed energy resource (DER) is also analyzed in terms of prime mover (i.e. the sources of energy either renewable resources or fossil fuels) type and the generation capacity (i.e. utility, medium, and small scales). Distributed generation (DG) systems are categorized in two groups, namely, dispatchable and non-dispatchable DGs. In the case of dispatchable DGs, electrical energy storage (EES) systems are introduced and the necessity of using such devices in microgrids is described. Applications of diesel generator power plants (diesel gen-sets) in power systems are explained and recent researches are summarized in this domain.

In the case of non-dispatchable distributed generation systems, photovoltaic distributed generation (PVDG) is investigated in depth. The current status of solar energy and general policy of government to promote it in Malaysia is discussed completely. Technical impacts of PVDG systems on distribution network are also pointed out and recent article are investigated in this field.

Distributed generation (DG) systems are also classified into electronically and rotary interfaced DGs based on the type of interfacing unit between their prime mover and the main power grid.

For the electronically interfaced DGs (EIDGs), different operating modes of voltage sourced converters (VSCs) together with corresponding control schemes are reviewed in detail.

The concept of power management system (PMS) is presented as well. Various kinds of PMS i.e. centralized (remote) and decentralized (local) controllers are discussed accordingly. The meaning of a hierarchical supervisory channel is analyzed and the tasks associated with each level of hierarchy are described accordingly. Load sharing control mechanisms and recent literatures in this field are reviewed in detail. Agent concept is also investigated in this section.

2.2. Microgrid Concept

A microgrid (MG) may be referred to an intelligent power grid (or entity as a region in a power system) which contains distributed generation (DG), energy storage, and load units (Kroposki, Basso, & DeBlasio, 2008). From the view of utility network operator, the microgrid can be considered as a controllable load which is able to support the main supply and keep the system stability during the transients. The microgrid also brings many advantages for the customers i.e. reducing feeder losses, improving voltage profile of the system, continuity of power supply (UPS application), increasing the efficiency by using the waste heat and correction of voltage sag (Lasseter, 2002).

Microgrid can specify a portion of utility network which is located in downstream of the distribution substation. Microgrid may include in different types of loads and distributed energy resources (DERs). Microgrid can supply different types of customers such as residential, commercial, and industrial. Generally, commercial and industrial loads are most vital and sensitive in terms of high quality power that they need.

This categorization of loads is necessary in order to define the microgrid expected operating strategy i.e. facilitating load/generation shedding within the microgrid to

control the net power flow (in grid-connected mode) and voltage or frequency (in islanded mode), improving the power quality and reliability for the vital and sensitive loads, and the last not the least, reducing the peak load to optimize DER rating. In this case, a portion of loads which is non-sensitive can be considered as controllable load in order to perform mentioned strategies (Farid Katiraei et al., 2008). Also, a microgrid should be capable of operating in:

- Grid-connected mode;
- Islanded (autonomous) mode;
- Transition mode between grid-connected and islanded modes;
- Ride-through (through voltage sags) for each DER in either grid-connected.

Ride-through capability is the ability of a power source to deliver usable power for a limited time interval during a power loss. A microgrid (as a power source) should be able to provide low-voltage ride-through (LVRT) capability when the voltage is temporarily drops due to a fault or load change in one, two or all the three phases of the AC grid.

Since there are two load categories i.e. electrical and thermal, a microgrid should be able to serve both of them properly. In grid-connected mode, the utility grid can be taken into account as an electric “swing bus” which absorbs and/or supplies any power discrepancy in the microgrid to maintain the balance between the generation and demand. Generation or load shedding within a microgrid is also an option if the net import/export power limit does not meet operational limits or contractual obligations. In autonomous mode of operation, load/generation shedding is often required to stabilize the microgrid voltage and angle (frequency). Also, the operating strategy must ensure that the critical loads of microgrid receive service priority. Load shedding and demand

response (DR) are normally run and supervised through energy management controller of microgrid (Farid Katiraei et al., 2008; Lidula & Rajapakse, 2011).

Microgrid is connected to the utility network through an interconnection switch. Technological advancements merge different power and switching functions (e.g., protective relaying, power switching, metering, and communication) together in a single system which is so-called in digital signal processor (DSP). To determine operational condition, the grid conditions are measured in both sides of interconnection switch through potential transformers (PTs) and current transformers (CTs). DSPs are designed to be capable of working with any type of switch (i.e. circuit breaker and semiconductor-based static switches) because this matter causes to increase DSP functionality (Benjamin Kroposki et al., 2008).

2.3. Existing Microgrid Test-beds

As described in previous section, microgrid can be considered as a cluster of generation, load, and energy storage units in a power system. There exist some microgrid test-beds around the world and two microgrid test-beds are discussed in this section. One of these tests-beds belongs to the group of intentional islanding experiences and another one belongs to the group of simulation studies (Lidula & Rajapakse, 2011). In the following subsections, two popular test-beds are investigated briefly.

2.3.1. The CERTS test System in the United States

The CERTS stands for "**Consortium for Electric Reliability Technology Solutions".** This test-bed has been built close to Columbus, Ohio and managed by American Electric Power. As shown in Figure 2.1, this microgrid contains three feeders. From the top, the first feeder includes two 60 kW electronically interfaced DGs (EIDGs) driven by natural gas. The second feeder is also connected to one EIDG and its specifications are similar to DGs at the first feeder. Third feeder is connected to the main grid.

This feeder could be powered by the DGs when static switch is closed while no power is being injected to the utility grid. Each DG plant is equipped with a battery energy storage unit connected to the inverter DC bus.

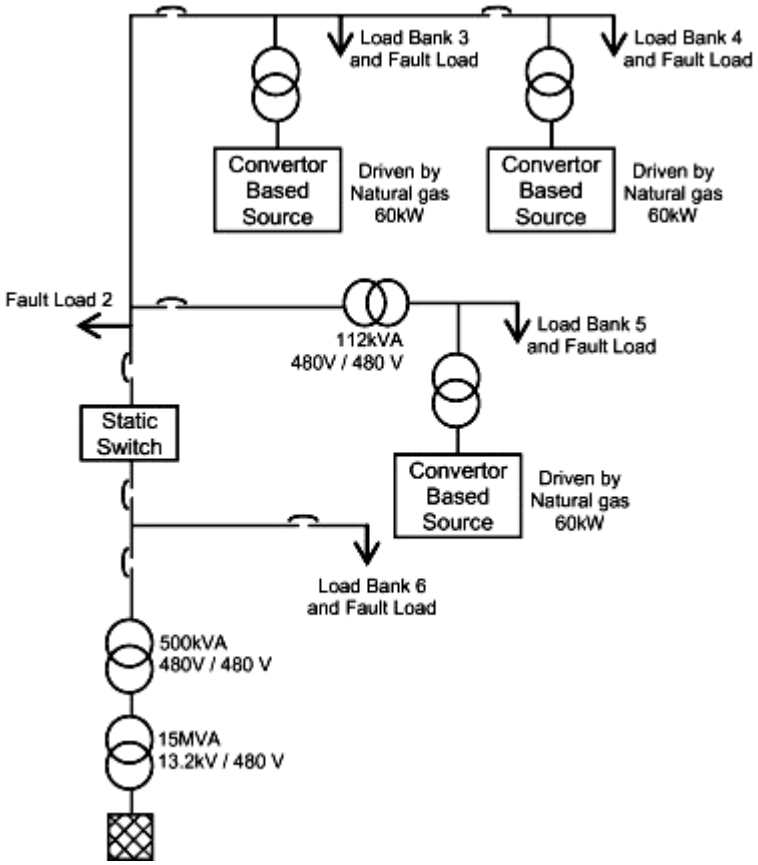

Figure 2. 1: The CERTS microgrid test-bed one-line diagram (Lidula & Rajapakse, 2011).

To set DG dispatching references, an Energy management system (EMS) has been allocated to this microgrid. EMS communicates with system components through an Ethernet network. However, this communication network is not applicable when the microgrid is controlled dynamically. DGs can be controlled independently which gives them plug-and-play capability. There is no central controller (CC) in the CERTS microgrid and DGs operate in peer-to-peer fashion (i.e. N + 1 DGs in operation). Therefore, loss of one DG has no harm for the microgrid operation.

In CERTS microgrid, frequency of system is controlled by power versus frequency droop (coordinated) controllers implemented in each DG unit. Voltage (at each DG

terminal) is controlled by reactive power versus voltage droop mechanism which is also implemented in controller of each DG unit. Reactive power versus voltage droop controller assures that there is no circulating reactive power between DG units.

The thyristor based static switch makes it possible to autonomously disconnect the microgrid at disturbances (e.g. IEEE 1547 or power quality events). Microgrid is also able to reconnect itself to the main grid (resynchronization).

2.3.2. Low Voltage (LV) microgrid benchmark

This microgrid model has been simulated based on the CIGRE low voltage (LV) distribution benchmark network. As illustrated in Figure 2.2, this microgrid is composed by distributed generation (DG) units i.e. micro-turbines (CHP generation), solar photovoltaic plant, fuel cells, and wind turbines. The total installed capacity of the microsources is about two third of the maximum load demand which is 100 kW.

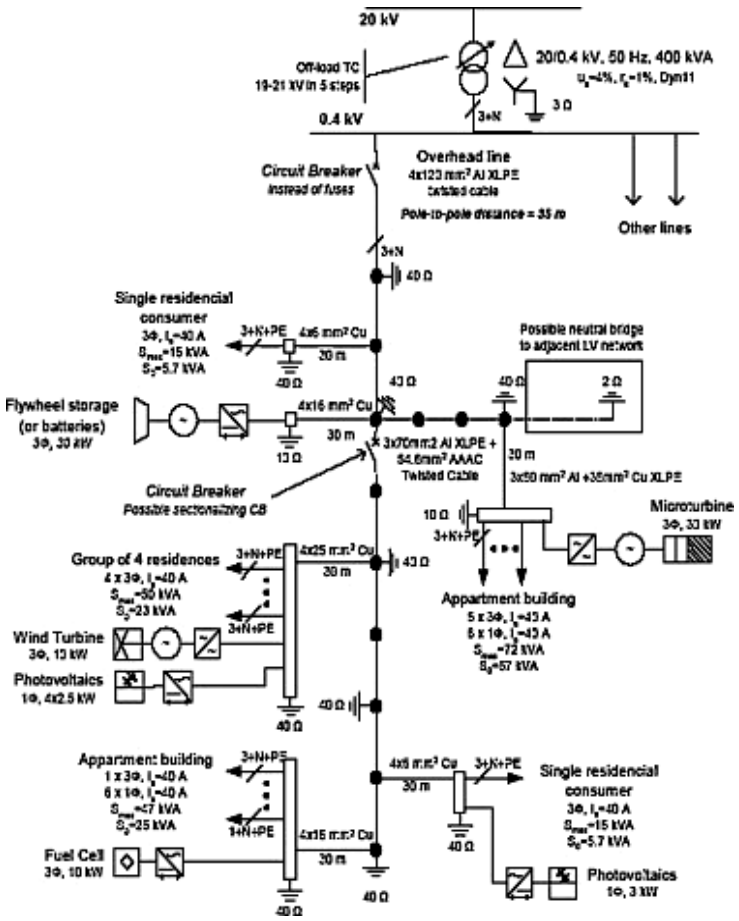

Figure 2. 2: Low voltage microgrid benchmark (Lidula & Rajapakse, 2011).

A fast-acting central energy storage system (e.g. a flywheel or a battery inverter) has been allocated to keep stable the microgrid frequency during its islanded operating mode. The microsources and DGs are controlled by a central controller (CC). However, autonomous control of microgrid is also possible if a local storage (e.g. batteries or ultra-capacitors) unit and a suitable controller are allocated to each DG.

2.4. Distributed Energy Resources (DERs)

A Distributed Energy Resource (DER) refers to a distributed generation (DG) unit, a Distributed Storage (DS) unit or any combination of DG and DS units. In terms of prime mover (e.g. sunlight and wind) availability, DG systems are classified to two groups which are “Dispatchable” and “Non-Dispatchable” entities. In the former case, DG guarantees the amount of power requested by the system operator provided that this value is within its power capability. Diesel gen-set plant or redundant UPS systems are two examples brought to this end. However, in the latter case, as much as power (uncertain amount) which is available from the prime mover (such as sun and wind) can be transferred to the AC grid or stored in a storage system. DERs are divided in two groups based on their interfacing unit to the AC power grid. The first group is interconnected through the conventional rotary systems such as synchronous generators and the second group is coupled through power electronic converters.

For an electronically interfaced (EI) DG (EIDG) unit, the interfacing converter provides a fast dynamic response for the system. Interfacing converter also is capable of limiting short-circuit current of the unit to less than 200% of rated current and thus extra fault current sent form the EIDG is practically prohibited by the VSC.

Against to a rotary based DG unit, an EIDG unit does not exhibit any inertia during the microgrid transients and hence has no inherent tendency to keep the frequency of microgrid stable.

Interfacing converter can also minimize the dynamic interactions between the primary source of power and the distribution system (these reactions are normally severe in the case of conventional DG units) (Chowdhury & Crossley, 2009).

2.4.1. Utility Scale Distributed Energy Resource

A utility scale DER refers to a distributed energy power plant with a same capacity which is defined for a conventional fossil fuel power plant. For example, we can point out to a utility sized solar photovoltaic distributed generation (PVDG) system. This type of power plant is constructed from plenty of single solar cells which are mounted on a PV module/panel. Solar modules are usually installed in groups and each set have a separated supportive structure. PVDG systems can be designed in order to track the sun in the sky through single or double axis tracking mechanisms (Bhatnagar & Nema, 2013; Eltawil & Zhao, 2013). In double tracking system the solar radiation input is higher but it is more complex and expensive than the first type. In short, the utility scaled DG system term reflects a large commercial or industrial DG based power plant which is able to supply the three-phase loads more than 1 MW ("IEEE Application Guide for IEEE Std 1547, IEEE Standard for Interconnecting Distributed Resources with Electric Power Systems," 2009; "IEEE Recommended Practice for Utility Interface of Photovoltaic (PV) Systems," 2000; F. Katiraei, Agu, x, & ero, 2011; Sorensen et al., 2008).

2.4.2. Medium and Small Scale Distributed Energy Resource

Medium scale DER refers to an electricity generation plant which can supply electrical power for both single and three phase loads between 10 kW to 1 MW.

The next definition backs to small scale DERs which their capacity of generation is less than 10 kW and hence they are commonly prone to supply single-phase loads ("IEEE Application Guide for IEEE Std 1547, IEEE Standard for Interconnecting Distributed

Resources with Electric Power Systems," 2009; "IEEE Recommended Practice for Utility Interface of Photovoltaic (PV) Systems," 2000; F. Katiraei et al., 2011; Sorensen et al., 2008).

2.5. Dispatchable Distributed Energy Resources and Related Issues

A dispatchable unit refers to a DER whose output power can be set externally through an external supervisory channel such as the system operator. A dispatchable DER can be either a slow-response or a fast-acting unit (Chowdhury & Crossley, 2009).

2.5.1. Electrical Energy Storage

Beside distributed generation in a power grid other components such as batteries, fly-wheels and super-capacitors can be exploited to bring ancillary services for the power grid. Such units are so-called distributed storage (DS) devices and support the power grid in order to operate properly (Díaz-González, Sumper, Gomis-Bellmunt, & Villafáfila-Robles, 2012; Koohi-Kamali et al., 2013; Roberts & Sandberg, 2011).

Energy storage units assure to balance between generation and demand in a power grid during load or generation fluctuations and transients (Carbone, 2011; Divya & Østergaard, 2009; Droste-Franke et al., 2012; Haruna, Itoh, Horiba, Seki, & Kohno, 2011; Nasiri, 2008; S. Barnes & G. Levine, 2011; Vazquez, Lukic, Galvan, Franquelo, & Carrasco, 2010).

Electrical energy storage system can provide ride-through capability when intermittent energy sources vary dynamically. Also, these elements can bring a smooth changeover between grid-connected and autonomous operating modes (Brown, Peas Lopes, & Matos, 2008; Chang et al., 2009; Mercier, Cherkaoui, & Oudalov, 2009; Oudalov, Buehler, & Chartouni, 2008; Rabiee, Khorramdel, & Aghaei, 2013).

2.5.2. Battery Energy Storage Operation and Principles

Batteries are electrochemical energy storage devices which convert chemical energy into electrical energy. A typical battery cell comprises two electrodes (plates) plunged in an electrolyte solution (see Figure 2.3). If a circuit is formed between the electrodes, a current passes through the circuit. The reversible chemical reactions between electrolyte and plates cause this current to flow. Some batteries can only be used one time and they are so-called "primary batteries" (i.e. dry cells). However, other types of batteries are so-called "secondary batteries" that are rechargeable. In this section and this thesis only the rechargeable batteries are investigated. During the process of battery charging, electric energy is stored as chemical energy in the battery. When the battery is supplying electrical power and being discharged, stored chemical energy is being released from the battery.

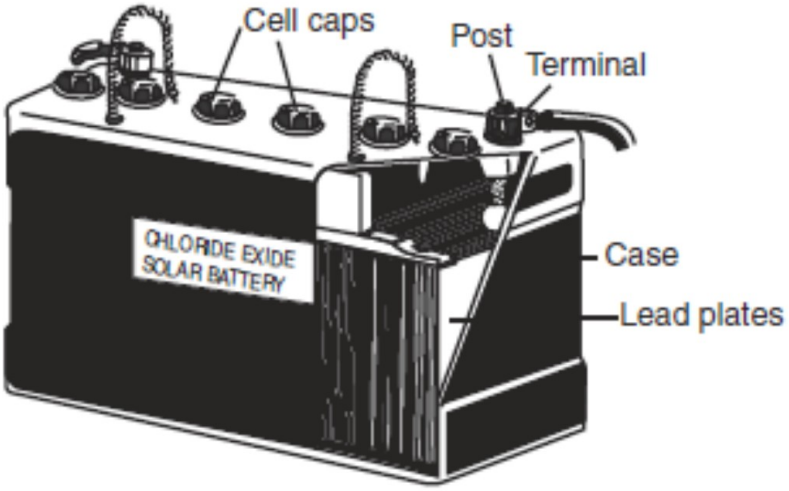

Figure 2. 3: Typical structure of lead-acid battery (Hankins, 2010).

On the current world market, the most commonly offered rechargeable batteries are lead-acid, nickel metal hydride, nickel cadmium, and lithium ion. Lead-acid batteries are most affordable, accessible, and appropriate solutions for power system applications between all of those. Other kinds of batteries are generally exploited for electric

appliances such as notebook computers, cell phones, radios, and lanterns (A. Huggins, 2010; Hankins, 2010; S. Barnes & G. Levine, 2011).

Chemical reactions between the negative lead plate (Pb), positive lead dioxide plate (PbO_2), and electrolyte cause the lead-acid battery to operate. Electrolyte is composed of water (H_2O) and sulphuric acid (H_2SO_4). During the charging process, spongy lead accumulates on the negative electrode and lead dioxide on the positive electrode. The relative amount of sulphuric acid in the electrolyte grows as well. During the discharging process, lead sulphate ($PbSO_4$) accumulates on the negative electrode and the relative amount of water in the electrolyte increases (see equation 2.1).

In a lead-acid battery, each cell generates a voltage about 2.1V if it is fully-charged and hence a fully-charged 12V lead-acid battery generates a voltage of 12.6V in open-circuit position. The battery terminal voltage increases when it is being charged and decreases when it is being discharged (Hankins, 2010).

$$Pb + PbO_2 + 2H_2SO_4 \underset{\overrightarrow{Discharge}}{\overset{\overleftarrow{Charge}}{\leftrightarrow}} 2PbSO_4 + 2H_2O \qquad (2.1)$$

Based on discharging capabilities, lead-acid batteries are categorized into two groups which are “deep discharge” and “shallow discharge”. Deep discharge batteries are suitable candidates to be used with solar power systems. In this case, the whole energy stored in the battery can be delivered easily while the discharge process is not damaging the battery and shortening its lifetime. Shallow discharge batteries are suitable for automotive applications and are designed to be dischargeable in a short while. Drawing too much power from shallow discharge batteries can damage their plates inside.

If this type is chosen for solar power systems, they have to be managed very carefully and never deeply discharged (Hankins, 2010).

Based on physical structure, lead-acid batteries are classified in two types which are flooded (or vented) lead-acid battery and valve regulated lead-acid (VRLA) battery. In the former, the plates are immersed in reservoirs of excess liquid electrolyte. In the latter (see Figure 2.4), the electrolyte is immobilized in an absorbent separator or in a gel. Valve regulated batteries are maintenance-free (no need to add acid). During the process of charging, the gas given off is recombined into the battery as electrolyte (water). There is also a safety valve which vents electrolyte and prevents to increase the gas pressure inside the battery if the battery is overcharged (Eckroad & Gyuk, 2003).

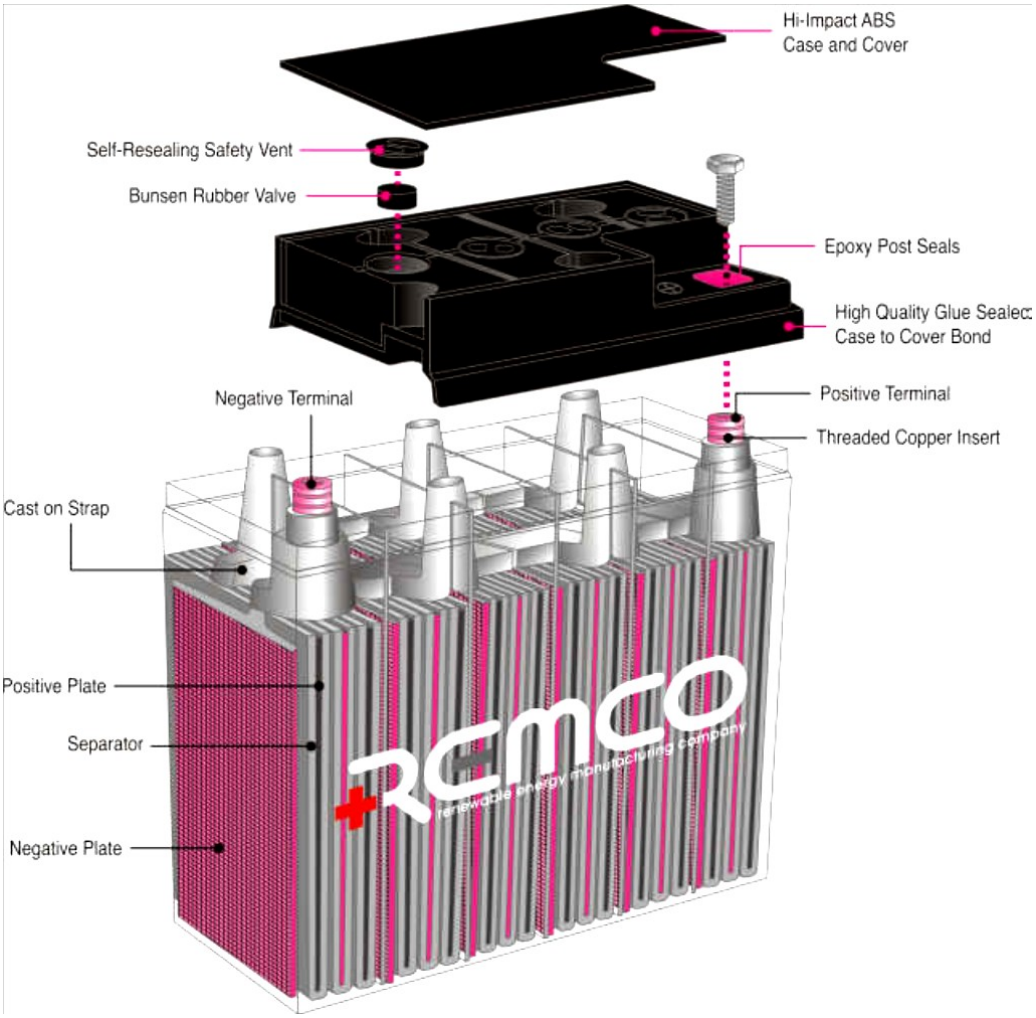

Figure 2. 4: REMCO 12V valve regulated (sealed) lead-acid battery construction (Remco Ltd., 2012).

2.5.3. Battery Energy Storage and Charge Controller

If a battery is fully charged and still left connected without charge controller to a source of power, it can become overcharged. Continual overcharging leads to the electrodes destruction and electrolyte loss (that both shorten the cyclic lifetime). In overcharge state, the electrolyte of a battery is lost by gassing (see Figure 2.5). In fact, a fully charged battery cannot accept more charge from the power source and hence the additional charge converts the electrolyte water to the hydrogen. Battery gasification leads to two problems since it escapes as bubbles from the electrolyte. Firstly, the electrolyte level drops in each cell and the cells must be refilled by distilled water. Secondly, the hydrogen is an explosive gas and can be dangerous. To prevent the explosion of hydrogen, the gas must gas must be vented from the battery storage area (Hankins, 2010).

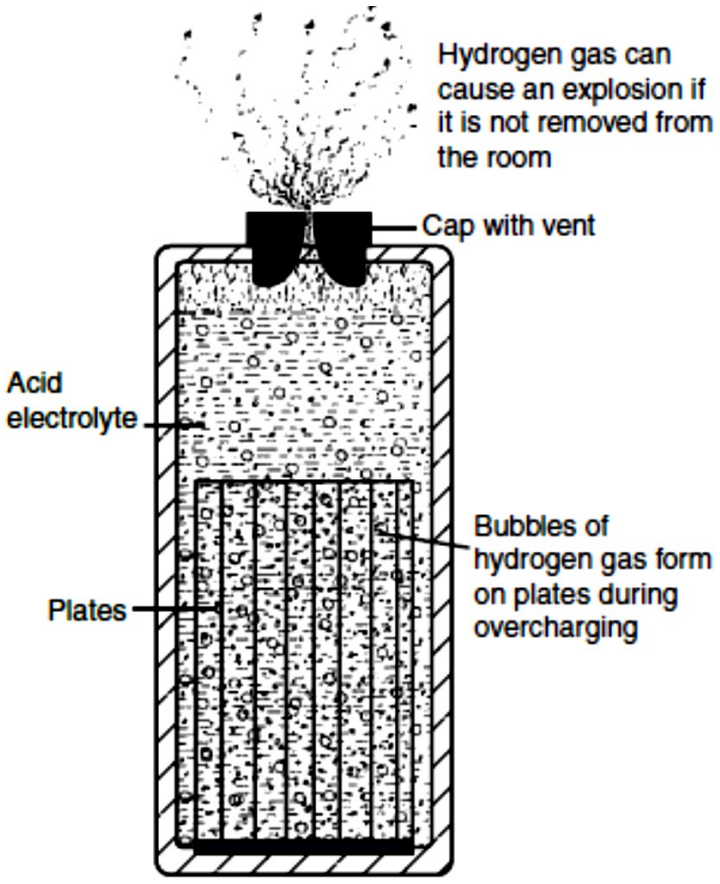

Figure 2. 5: Gassing phenomena in a battery cell due to overcharging (Hankins, 2010).

On the other hand, depth of discharge (DOD) is a term used by manufacturers to denote how much battery is discharged in a cycle before it is re-charged. A battery at 20% DOD is similar to a battery with 80% state of charge (SOC). The SOC of a battery equals to 25% if its DOD is equal to 75%. If the DOD reduces, the battery cycle life increases. For instance, the battery cyclic lifetime is more for 30% DOD than 70% DOD (see Figure 2.6). Lead-acid batteries that left discharged for long term may lose their capacities as a result of sulphation. A battery which is left more than one month at low stage of charge may not hold or accept its rated capacity.

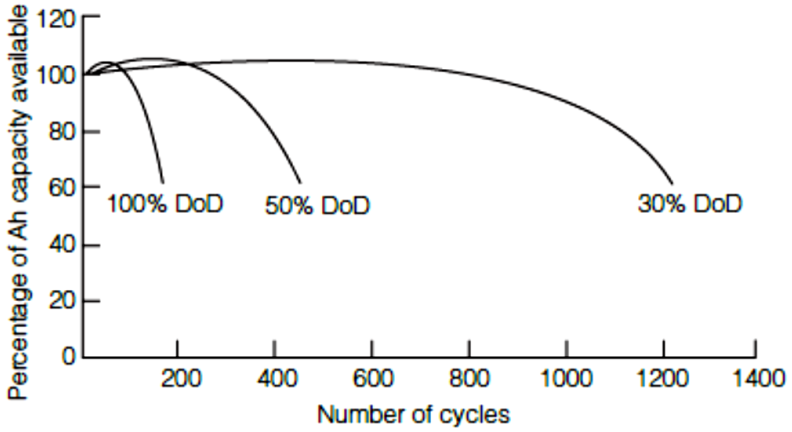

Figure 2. 6: Impact of DOD on a battery cycle life (Hankins, 2010).

In order to avoid damaging the battery by overcharging and over discharging, a charge controller can be implemented between the power source and battery. In this case, if the battery is fully-charged, the charge controller decreases the charge amount or stops charging the battery. Likewise, if the battery is being discharged, the charge controller takes care of discharge level to supply the battery with an absorbing power or to stop it from over discharging.

To increase a battery lifetime, it must be charged appropriately and kept in a high SOC. The energy being absorbed by the battery during the day must be closely equal to the energy being delivered by it at night (Hankins, 2010).

2.5.4. Diesel Power Plant

Diesel generator can be classified as the rotary interfaced DG which is dispatchable. This means that the operator can decide about the amount of power can be delivered by the diesel plant at anytime provided that this power is within the power plant operational limits. In the case of diesel generator operation together with RESs such as wind and solar PV many works have been reported in the literature (Abbey, Wei, & Joos, 2010; Alegria, Brown, Minear, & Lasseter, 2014; Datta, Senjyu, Yona, Funabashi, & Chul-Hwan, 2011; El Moursi, Weidong, & Kirtley, 2013; Elmitwally & Rashed, 2011; Mipoung, Lopes, & Pillay, 2014; Mishra, Ramasubramanian, & Sekhar, 2013; Nayar, Ashari, & Keerthipala, 2000). A hybrid power system including diesel, solar PV, and battery storage power plants was investigated by (Nayar et al., 2000). This work presented an uninterruptible power supply (UPS) system which exploited the diesel generator as a backup. This system was also able to provide voltage stabilization beside demand side management (DSM), and hence declined the main grid blackouts.

In another work by (Datta et al., 2011), a fuzzy-based method was reported to control the frequency in a hybrid PV-diesel power system in which energy storage is utilized as well. PV output power command is issued through this fuzzy approach. By the use of PV generator, this hybrid system was designed to compensate for the increase of fuel price and to reduce the environmental pollutants propagated by the conventional diesel plant.

Elmitwally and Rashed (Elmitwally & Rashed, 2011) proposed a control method to capture maximum power from the PV generator in a microgrid consists of diesel and solar power plants without any storage system. The suggested controller also regulates the load voltage and unbalance viewed by diesel generator power plant.

A combination of wind and diesel generator was utilized to examine the performance of a controller, introduced by Mursi et al. (El Moursi et al., 2013), where a utility-scaled solar PV power plant is integrated to the main AC network. This controller is able to improve the ride-through capability of PV system based on PV characteristics, positive and negative sequence controllers.

Abbey et al. (Abbey et al., 2010) presented a two-level controller to manage energy storage system and smooth out the power fluctuations generated by a wind power plant. This controller is also useful to decrease diesel generator fuel consumption and reduce ramp ups/downs. Mipoungh et al. (Mipoung et al., 2014) suggested a hybrid power system including wind and diesel power plants in order to relief system frequency oscillations which may lead to load shedding. In this work, a power versus frequency droop scheme has been introduced that mitigates the power fluctuations produced by wind plant and load. Thus, the stresses on diesel plant as the master unit are minimized in islanded mode.

Mishra et al. (Mishra et al., 2013) introduced a seamless control approach to manage a microgrid including diesel and PV plants in both grid-connected and autonomous modes. A second order sliding mode controller has been utilized to control VSC of PV plant.

Diesel generator plant is adjusted by the frequency of microgrid. PV system sets the voltage at PCC and in the case of diesel failure it keeps stable the microgrid frequency.

2.6. Non-Dispatchable DERs

A non-dispatchable unit refers to a DER that its output power is normally controlled based on the optimal operating state of its primary source of power. The availability of prime mover (e.g. sunlight and wind) is unpredictable and hence the system operator cannot decide about the power that can be absorbed from the unit at a certain moment.

The DG units which use intermittent renewable energy resources such as wind and solar PV plants are often non-dispatchable systems. In order to maximize the delivery of their output power, maximum power point tracking (MPPT) methods have been suggested to be exploited (Bhatnagar & Nema, 2013; Chowdhury & Crossley, 2009; Eltawil & Zhao, 2013).

2.6.1. Solar Photovoltaic Status in the World

Solar energy is the fundamental source for all sorts of energy resources on the earth with only a few exemptions such as nuclear and geothermal energy. There are generally two ways to produce electrical power from sunlight i.e. through solar thermal and photovoltaic (PV) systems. In this section and this dissertation, only solar PV system would be discussed.

Solar PV is a rapid developing renewable energy technology. Though the total capacity of solar PV installed in worldwide is much less than wind power (about 50%), it has grown even faster than wind power throughout the past decade (from 2004-2013). About 32% growth in solar PV systems applications was reported in the IEA-PVPS countries in 2013. The global installed PV capacity increased to more than 35 times from 3.7 GW in 2004 to 140 GW in 2013 (International Energy Agency, 2014; Renewable Energy Policy Network for the 21st Century, 2014).

Due to improvements in semiconductor materials, device designs, product quality, and the expansion of production capacity, initial investment for PV modules have been declined significantly, from about $1.0/W in 2001 to about $0.52/W in 2013. The cost of electricity (COE) generated by solar PV systems keeps on dropping. It has decreased from $0.90/kWh in 1980 to about 0.20$/kWh today. In the U.S., the department of energy (DOE) goal is to reduce the COE of PV to $0.06/kWh by 2020 (International Energy Agency, 2014).

There are many applications for which a PV system is the most economic long-term solution, particularly in inaccessible areas such as power for remote lighting and signs, remote telecommunications, remote houses, and recreational vehicles (Wang, 2006). In general, energy from the solar PV is still more costly than energy from the local utility. Currently, the capital cost of a PV system is also higher than that of an engine generator.

2.6.2. Solar Photovoltaic Status in Malaysia

By the end of 2011, total capacity of solar PV system installed in Malaysia was about 13.5 MW. 2.5 MW of this amount was grid-connected PV systems. More than 60 % of the grid-connected solar PV plants in Malaysia are domestic installations and the rest is related to educational and commercial applications (PVPS, 2012).

In 2011, there was installed about 1 MW of grid-connected PV systems and a trivial amount of off-grid systems. Although the capital financial support from the Malaysia Building Integrated Photovoltaic (MBIPV) project expired in 2010, the installation of grid-connected solar PV systems grew in order to complete the outstanding financially supported projects (PVPS, 2012).

PV policy developed significantly in 2011 in Malaysia. In this case, the Government passed to approve the Renewable Energy (RE) Act 2011, the Sustainable Energy Development Authority (SEDA) Act 2011, and the associated implementation of a feed-in tariff (FiT) scheme. The opening share allocated to solar PV was 150 MW over three years (50 MW for every of years 2012, 2013 and 2014), with 90% assigned for commercial sector developments and 10% for households. House owners are permitted to install up to 12 kW solar PV for each application whereas the commercial entities are permitted up to 5 MW for each purpose.

The countries' major national electricity utility, Tenaga National Berhad (TNB) is one of the key stakeholders in order to impalement the feed-in tariff scheme (TNB adds 1%

extra charge on the electricity bill for those consumers who use above 300 kWh of electricity monthly) (PVPS, 2012). This is put down into the RE Fund which is governed by SEDA Malaysia and will be utilized to pay FiT. A feature of the Malaysian FiT scheme is the e-FiT online System that provides the users with an online FiT processing system. This system gives this facility to the public to submit their applications through the internet within three hours. Three hours starts counting once the quota for any commercial sector project is completed (PVPS, 2012).

2.6.3. Technical Impacts of Solar Photovoltaic Plant

Technical impacts of photovoltaic distributed generation (PVDG) on distribution network have also been investigated widely in the literature (Brinkman, Denholm, Drury, Margolis, & Mowers, 2011; Ellis, Behnke, & Keller, 2011; Hernandez et al., 2014; F. Katiraei et al., 2011; Mills et al., 2011; Sechilariu, Baochao, & Locment, 2013; Silva, Severino, & de Oliveira, 2013; Steffel & Dinkel, 2013; Tamimi, Canizares, & Bhattacharya, 2013; von Appen, Braun, Stetz, Diwold, & Geibel, 2013).

As a general practice, distribution networks have been conventionally designed to operate in a radial fashion. In this case, the flow of power was only in one direction from upstream power plants to the loads in down streams. Integration of DG systems into utility power grid brings new technical challenges that have to be studied in depth (Eftekharnejad, Vittal, Heydt, Keel, & Loehr, 2013; Hernández, Ruiz-Rodriguez, & Jurado, 2013; Hoke, Butler, Hambrick, & Kroposki, 2013; Lee, Shin, Yoo, Choi, & Kim, 2013; Marra et al., 2013; Miret et al., 2012; Ramasamy & Thangavel, 2012; Sadineni, Atallah, & Boehm, 2012; R. Tonkoski, Turcotte, & El-Fouly, 2012; Urbanetz, Braun, & Rüther, 2012).

Impact studies are generally proposed to qualify the scope of the issues and provide utilities with guidelines, tools, and processes which the predictable steady-state and

transient behavior of PVDG can be handled through. Most important outcomes of these studies are to evaluate mitigation measures for any problems found out and to decide about the cost and effectiveness of different solutions (Al-Smairan, 2012; Albuquerque, Moraes, Guimarães, Sanhueza, & Vaz, 2010; Batista, Melício, Matias, & Catalão, 2013; Ghoddami, Delghavi, & Yazdani, 2012; Kauhaniemi & Kumpulainen, 2004; KoohiKamali, Yusof, Selvaraj, & Esa, 2010; Matallanas et al., 2012; Menti, Zacharias, & Milias-Argitis, 2011; Ramasamy & Thangavel, 2011; Shahnia, Majumder, Ghosh, Ledwich, & Zare, 2011; Reinaldo Tonkoski & Lopes, 2011; Widén, Wäckelgård, Paatero, & Lund, 2010; Zahedi, 2011).

The utilization of PVDG is looked forward to keeps on growing in coming decades. In planning and operating view points, it is mandatory for distribution utilities to be aware of potential effects of PVDG integration onto distribution network. PVDG depth of penetration can affect the distribution network locally (e.g. at single substation or feeder level) or system-wide (e.g. affecting a number of feeders and substations throughout the utility network that consists of sub-transmission and transmission facilities) (F. Katiraei et al., 2011).

The intermittency nature of PVDG system can affect the operation of main distribution power grid by creating steady-state and/or transient problems. Due to this unpredictable manner, solar PV plant can adversely affect system operation and power quality. Some of these impacts can only be explored through dynamic/transient studies that investigate the time-varying behavior of loads, fast-acting generators (inverters), and automatic voltage regulators on the feeders. Utilities are less motivated to deal with solar PV plant compared to other types because this kind is quite new and more complex than the others. Also, the engineers are not familiar adequately to identify mitigation measures and effects of the solar PV plant.

In small-scale PVDG systems, the problem to be studied is more complicated than large scale. The location of interconnection, time of use (ToU) based on market availability, and possible interactions with active loads such as electric vehicles (EVs) are all those kind of issues that increase the boundary of uncertainties (F. Katiraei et al., 2011).

Solar PV plant impacts on distribution systems can be consistent (in steady-state mode) or temporary (in transient mode) in nature. These impacts are listed in the followings as (F. Katiraei et al., 2011):

(a) Changing the voltage profile of feeders i.e. voltage increase and imbalance;
(b) Modifying the feeders loading i.e. potential overloading of components and equipments;
(c) Causing numerous operation of voltage controllers and regulators, such as load tap changers (LTCs), capacitor banks, and line voltage regulators (VRs);
(d) Causing oscillations in flow of reactive power as a results of switched capacitor banks unfavorable operation;
(e) Creating power quality problem e.g. voltage oscillation (due to intermittency of solar PV plant);
(f) Causing failure of over-current and over-voltage protecting devices and temporary over-voltage (TOV);
(g) Causing reverse power flow which may leads to increase the losses;
(h) Making power factor of a feeder or system variable and hence economically affecting local distribution companies that purchase their needful power from larger utilities;
(i) In general, robustness and operation of the system can be affected.

Solar PV plant penetration level and location of interconnection as well as utility grid electrical characteristics are those important factors which determine the severity of

these impacts. For example, A PVDG plant with high penetration level can behave as an active feeder and delivers power back to the main grid (reverse power flow).

This matter may influence voltage profiles, over-current protection, and capacitor bank operation. This kind of problem may happen where several utility scale PVDG systems are interconnected to a feeder. Since both PVDG plant output power and feeder load fluctuate during the day, it is essential to study effects associated with power fluctuations due to different levels of solar PV plant penetration and feeder loading. Study cases should justify cyclic (e.g. every season) oscillations in both PVDG system output power and feeder load demand (F. Katiraei et al., 2011).

There are several issues related to voltage which can be exacerbated along with the increase of penetration level. Firstly, feeder voltage rise which is resulted by positive power mismatch between the generation and load demand when feeder is low-loaded. Secondly, voltage flicker which can be considered as a result of sudden cloud movements. In this case, solar PV plant output power sharply ramp ups/downs in close vicinity of feeder and thus creates voltage flickers. Other probable areas of distress consist of phase current balance deterioration, voltage regulation, power factor (PF) adjustment, and harmonics injection. A recent PEPCO HOLDING INC. (PHI) analysis of data from a new 1.9 MW solar installation indicates that inverters are able to effectively follow feeder voltage, maintain unity power factor, and keep the current balanced on each phase (Steffel & Dinkel, 2013).

Another technical matter that has to be considered (for planning stage) is to pick up the cold-load properly. This can become a problem even after a temporary electricity interruption when the feeder full load is reconnected but the solar PV plant does not return for about five minutes. For this kind of power grids which include in distributed automatic restoration schemes, the presence of generation must be checked before the cold-load pickup (Steffel & Dinkel, 2013).

The integration of intermittent renewable energy systems to supply the load demand will intensify the uncertainty and variability that must be handled by system planners and operators. Figure 2.7 shows data exploited in an interconnection study of wind and solar DG systems and a flexible conventional power plant is also utilized to supply the load or the net load during a morning when the demand ramps up (Mills et al., 2011).

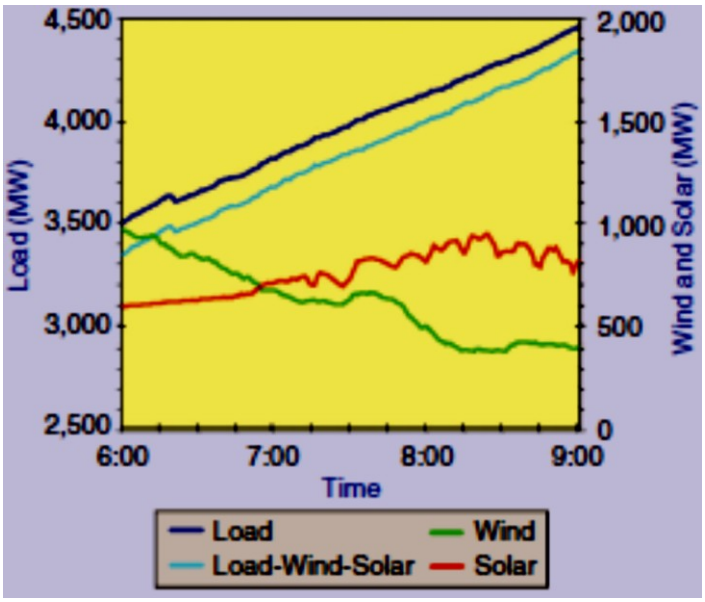

Figure 2. 7: Analysis of the technical concerns that the operator must be able to manage them. Operator need to use dispatchable resources to manage the system including load, wind, and solar plants (Mills et al., 2011).

System planners and operators employ various methods such as scheduling, economic dispatch, forecasting, and reserves to guarantee the system performance (i.e. technically and economically complies with standards). In this case, the system planners and operators have a good knowledge in advance about the uncertainties that they have to encounter. They should evaluate and consider many solutions and thus select the most reliable and cheapest between those. In planning stage, the future needs of transmission and generation systems are also evaluated based on the estimated load growth. Therefore, generation and transmission capacity can be designed to be expandable in order to match with the load demand growth in future (Mills et al., 2011).

Generation flexibility is another issue that has to be considered and is determined in terms of factors such as ramp rates, allowable start-up and shut-down times as well as minimum fixed generation. Also, planners must schedule for periodic maintenance of generation units in order to meet forecasted load demand. These units commit to supply power required in the grid from hourly to daily time scale. In the 10-min-to-hours time scale system, operators have to change the power set-points of committed units in order to track the load variations during the day. The generation units must be able to commit any additional capacity needed at any time and to guarantee that the power difference in forecasts or unpredicted events can be settled without jeopardizing the reliability of power system. In the sub-hourly time scale, system operators plan sufficient regulating reserves to balance minute-by-minute variations between load demand and generation (see Figure 2.8) (Mills et al., 2011).

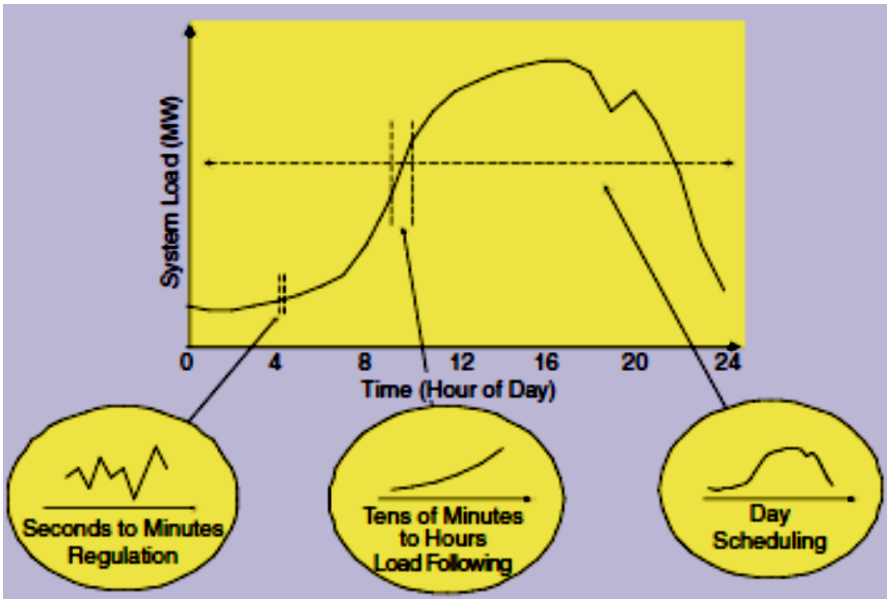

Figure 2. 8: Time scales related to the power system operation (Mills et al., 2011).

Solar power plant output power should be forecasted days ahead down to hours and tens-of-minutes ahead (see Figure 2.8). Forecasts should consist of data about the estimated output power and their accuracy in order to especially monitor missing periods.

Short-term PV plant generation forecasting can be examined through the observation of clouds in the sky. Sky image recorders next to PVDG plants can be exploited to detect approaching clouds and hence the effects of clouds on solar PV plant output power can be forecasted. In this case, images taken so far by satellite have given helpful information regarding velocity and direction of approaching clouds (Mills et al., 2011).

For longer time scales, numerical models of weather can be utilized to estimate sunlight intensity for several days. PVDG plant generation forecasting is mandatory to properly manage both the intermittency and the uncertainty of solar PV plant output power and thus it should be taken into account carefully in power system planning and operation stages (Chow, Lee, & Li, 2012; Fernandez-Jimenez et al., 2012; Inman, Pedro, & Coimbra, 2013; Mandal, Madhira, haque, Meng, & Pineda, 2012; Mellit, Massi Pavan, & Lughi, 2014).

2.7. Power Management Systems (PMSs)

A microgrid should allow the system operator to treat it like as a controllable load inside of the distribution network. The current practice in the area of designing control system for distributed generation (DG) units is to adopt control mechanisms imbedded in each DG unit. These controllers can interchange their information through a central controller which is so-called agent. This arrangement forms a flexible network where plug and play facility is required without re-engineering the system and uses peer-to-peer model (interactive N+1 distributed energy resources).

Many research works have been conducted in the field of microgrid systems to present that such entities are useful for main power grids. In (Milosevic, Rosa, Portmann, & Andersson, 2007), the main concentration is on DG units which are capable of working on both grid-connected and islanded modes which provides the critical loads with consistent power supply.

In (Li & Kao, 2009; Hassan Nikkhajoei & Lasseter, 2009; Salamah, Finney, & Williams, 2008; Sao & Lehn, 2008; Shahabi, Haghifam, Mohamadian, & Nabavi-Niaki, 2009), many types of microgrid control and power management systems (PMSs) have been presented as well. In a microgrid, a reliable high quality power (i.e. premium power) can be generated through the power electronic devices, UPSs, and multi utility feeders to keep supplying the critical loads. In the case of non-inertial prime movers (excluding wind turbines which can be connected either through inverter or directly), there is a need for an interfacing units. This unit is a kind of voltage sourced converter (VSC) which can be two or three levels. The main duty of VSC is to generate sinusoidal voltage waveform at the same frequency (50 or 60 Hz) and magnitude of grid voltage. The interfacing unit can be controlled either through pulse width modulation (PWM) techniques or a vector controller (De Doncker, Pulle, & Veltman, 2010).

In (Bae & Kim, 2007; Gil & Joos, 2008; Haffner, Pereira, Pereira, & Barreto, 2008), the power management, economic operations, reliability, and planning of microgrid have been investigated. In these works, there are some fundamental concepts which can be addressed in the followings:

(a) **Control strategy:** In any microgrid system the controlling scheme related to each distributed generation (DG) unit plays an important role. In this case, the interaction between microsources during the grid-connected and stand-alone modes is necessary to be studied;

(b) **Operation and economic issues:** DG units with large capacity of electricity generation are more economic than microsources with small capacity. For example, adding protection systems gives much as 50% additional cost (Hassan Nikkhajoei & Lasseter, 2009) and hence a DG with a rating more than three to five times the rating of a microsource is more reasonable as long as the cost of protection system is same;

(c) **Power management, quality, and reliability:** DG units provide the power grid with decentralized generation of electricity. Thus, the power flows into the network is reliable and high quality if the DGs can operate continuously during the transients (Hassan Nikkhajoei & Lasseter, 2009).

Control schemes for distributed energy resources (DERs) inside of a microgrid are defined based on the required functions and possible operational scenarios. Control mechanisms of a DER unit are also designed taking into account how it naturally interacts with the system and other units. The main control strategies for a DER unit can be pointed out in here are voltage/frequency and active/reactive power (current control) control schemes. In general, there are two major categories i.e. noninteractive and interactive methods. Each category is divided in two control strategies i.e. grid-following and grid-forming controls (Table 2.1). In noninteractive strategy, a DER output power is controlled independently so that there are no interactions between the generation units and/or loads (i.e. MPPT which is a local control). In contrast, in interactive method, DER unit is dispatched (through the set-point) by a supervision system (e.g. network operator) to deliver or absorb active (in the case a storage unit) and reactive powers.

Table 2. 1: Classification of control strategies for electronically coupled DER units (Farid Katiraei et al., 2008).

	Grid-Following Controls	Grid-Forming Controls
Noninteractive Control Methods	Power export (with/without MPPT)	Voltage and frequency control
Interactive Control Methods	Power dispatch Real and reactive power support	Load sharing (droop control)

In the case of electronically based DGs, there are two kinds of control strategies exploited to run a voltage sourced converter (VSC) in a microgrid as (Jiayi, Chuanwen, & Rong, 2008):

(a) **PQ control mode:** The inverter is used to meet a given active and reactive power set-point;

(b) **Voltage and frequency control mode:** The inverter is controlled to "feed" the load with preset values for voltage and frequency.

Grid-following (power export control or grid-connected mode) scheme is mostly exploited to control the DER output power within the voltage and frequency limits as determined by the microgrid. Current control strategy determines the reference voltage waveforms for the pulse-width modulation (PWM) of the VSC. The reference signals are also synchronized to the frequency of microgrid by tracking the point of common coupling (PCC) voltage waveform by phase locked loop (PLL) controller.

Grid-forming scheme imitates behavior of a "swing source" in an islanded microgrid. A grid-forming unit inside of a microgrid can adjust the voltage at point of common coupling (PCC) and dominantly regulate the microgrid frequency (Farid Katiraei et al., 2008).

In power electronic based microgrids which include in non-inertial DERs and the *R/X* ratio is high, the control schemes taken into account differ from those utilized in those power grids with low *R/X* ratio.

In order to control a microgrid, zero to three hierarchical control levels can be defined i.e. tertiary, secondary, primary controls and inner control loop. Each level has the duty of a command level and provides supervisory control over lower-level systems.

The three levels hierarchical supervision channel is organized as follows (Guerrero, Vasquez, Matas, de Vicuna, & Castilla, 2011):

(a) **The primary control** handles the inner control of the DG units;
(b) **The secondary control** is exploited to bring back the frequency and voltage amplitude deviations;
(c) **The tertiary control** regulates the power flow.

All the mentioned features and duties can be implemented inside of a management unit that is so-called power or energy management system (PMS or EMS). This network assigns real and reactive power references for the DER units to:

(a) share real/reactive power among the DER units;
(b) respond to the microgrid disturbances and transients;
(c) determine the power set-points to restore the frequency;
(d) enable the resynchronization of microgrid.

In addition, PMS/EMS unit can receive the real-time data associated with the present and the forecasted values of load, generation, and market information in order to impose proper controls on power flow. This control unit should accommodate both short-term power balancing and long-term energy management requirements. In the PMS/EMS, a subsystem which is so-called microgrid central controller (MCC) performs different tasks ranging from maximization of microgrid value to coordination of local controllers

(LCs). LC controls both DERs and controllable loads. Distribution network operator (DNO) or market operator (MO) systems can also be added to this group through each MCC where there exists more than one microgrid in a power network (Farid Katiraei et al., 2008).

2.7.1. Local (Decentralized) Control of Smart Microgrid

Microgrids should be equipped by wide-range control systems in order to ensure system security, emission reduction, optimal operation and seamless transfer from one operating mode to another according to regulatory requirements ("IEEE Application Guide for IEEE Std 1547, IEEE Standard for Interconnecting Distributed Resources with Electric Power Systems," 2009; "IEEE Standard for Interconnecting Distributed Resources With Electric Power Systems," 2003). This control over a microgrid is attained using the central controller (CC) together with microsource controllers (MCs).

MC looks after the local control functions which govern the microsource (or DER). The key features of MC design are listed in the followings as:

(a) The microsources cannot interact unless through CC. This enables each MC to respond effectively to the system changes and hence it does not need any data to be exchanged between MCs;
(b) Although MC is designed to communicate with CC and perform commands issued by this unit, it should be able to reject unacceptable CC commands.

The embedded control functions in a microsource controller (MC) are classified as follows:

(a) Voltage control;
(b) Load sharing through *P-f* control;
(c) Active and reactive power control;
(d) Storage requirement for fast load tracking.

These control functions should ensure that DERs pick up their share of load rapidly whenever the microgrid disconnects itself from the utility.

In a decentralized environment, the maximum autonomy of DERs is guaranteed if local controllers are intelligent and communicate with each other to form a larger entity.

The main target of each controller is not necessarily to maximize the revenue of the corresponding unit but to improve the overall performance of microgrid.

2.7.2. Grid-Connected Mode Control of Voltage Sourced Converter (VSC)

In the case of grid-connected (grid-following) mode, one solution to control voltage sourced converter (VSC) is to determine a reference voltage through controlling the current. This method can be implemented in a synchronous *dq*-Frame which denotes the direct (d-axis) and quadrature (q-axis) components of converter output currents. These two components correspond to the real and reactive output powers, respectively (see Figure 2.9).

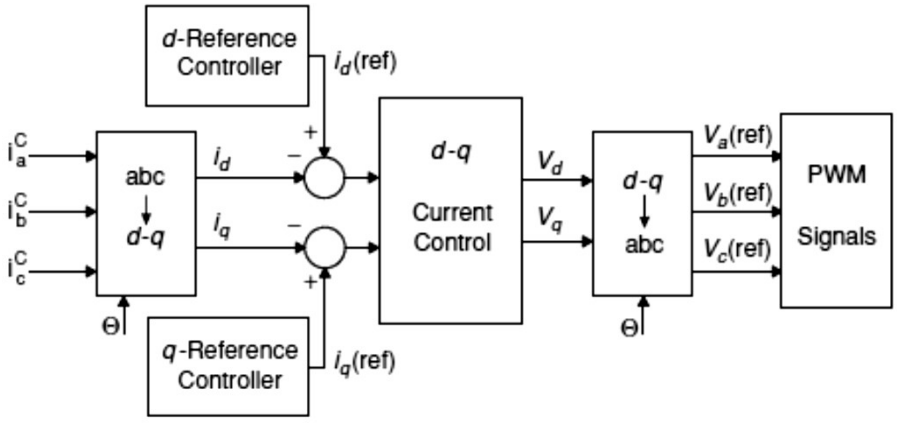

Figure 2. 9: *dq*-Frame current controller for an electronically interfaced (EI) DER (Farid Katiraei et al., 2008).

As another method, DC link voltage is regulated to control the flow of active power. Reactive power is also controlled through the outer power loop shown in Figure 2.10. The power which is drawn from the renewable energy source (RES) is fed into DC link that boosts up the voltage at DC side of VSC.

This controller ensures that the instantaneous power generated in DC side is transferred to the AC side and the DC voltage is regulated properly.

The voltage controller compensates for the voltage rise by determining an adequate value of the d-axis inverter current to balance the power in-flow and out-flow of the DC link. A reference value can be allocated to the q-component of the converter current by the reactive power outer control loop. For example, $Q_{(ref)}$ value is set to zero if VSC is supposed to operate in unity power factor.

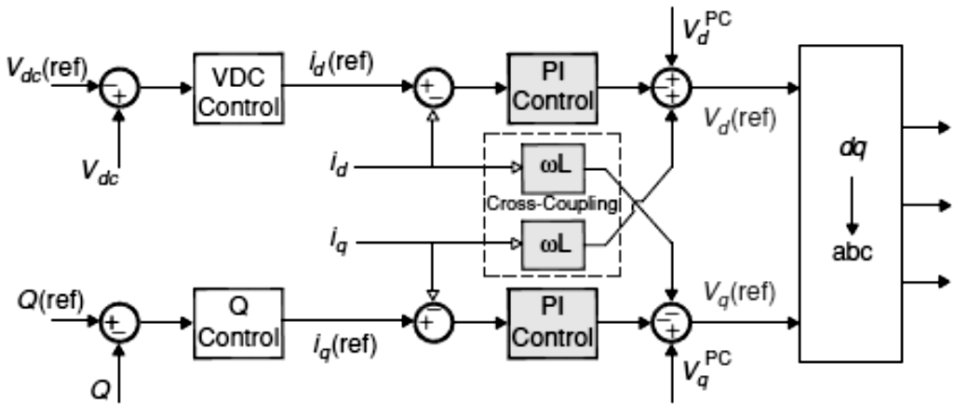

Figure 2. 10: Grid-connected mode power controller of VSC (Farid Katiraei, Iravani, Hatziargyriou, & Dimeas, 2008).

Figure 2.10 also gives more information about *dq*-Frame current control that consists of two proportional-integral (PI) controllers to set for d-axis and q-axis current components, respectively. There is also the voltage feed-forward path that is added by the cross-coupling elimination term and voltage feedback from the point of connection (pointing out to the inherent feature of VSCs which is current limiting during the fault).

In another approach, real/reactive power control strategies are applied to control the output power of a dispatchable DER. In this case, pre-specified dispatching references (set-points) for real and reactive powers are determined by the system operator. As shown in Figure 2.11, $P_{(ref)}$ and $Q_{(ref)}$ values can be set by a supervisory power management unit or locally calculated according to a predetermined power profile to optimize real/reactive power export from the unit.

There are also other common methods to control the active/reactive power flow which can be categorized based on compensating variations in the local load, peak shaving profile and/or smoothing out fluctuations in the feeder power flow (Farid Katiraei et al., 2008).

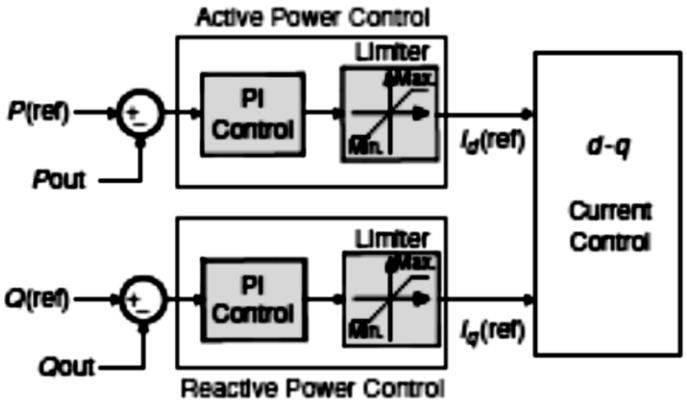

Figure 2. 11: Active and reactive power dispatching controller (Farid Katiraei et al., 2008).

The reactive power compensation is commonly performed based on power factor compensation strategy through voltage regulation at the point of connection (PC). To supply the active power balance in grid-forming mode (autonomous operation), the unit should be sufficiently large and have enough reserve capacity.

2.7.3. Stand-alone Mode Control of Voltage Sourced Converter (VSC)

All microgrids are equipped by a control system which satisfies the safely operation of the system in grid-connected and stand-alone (autonomous) modes. This system may be implemented inside a central controller or embedded as a structural part of each DER.

DC-to-AC conversion is carried out by a voltage source inverter (VSI). VSI controls both magnitude and phase angle of the output voltage at its own terminal (PCC). The active power (P) is controlled by adjusting δ which is the difference between sending end angle (δ_S) and receiving end angle (δ_R). The reactive power (Q) is controlled by sending voltage magnitude. The control functions use output power P and microgrid bus voltage magnitude E (voltage magnitude at receiving end) as feedback states.

2.7.3.1. Load sharing through Active Power vs. Frequency (*P-f*)

All the controllers inside of microgrid must ensure automatic and smooth change over from grid-connected mode to stand-alone mode and vice versa as per necessity. During transition to stand-alone mode, the microsource controller (MC) of each DER unit employs local *P-f* control to change the operating point in order to achieve local power balance at the new loading condition. The drooping *P-f* characteristic used by the MCs for *P-f* control is shown in Figure 2.12.

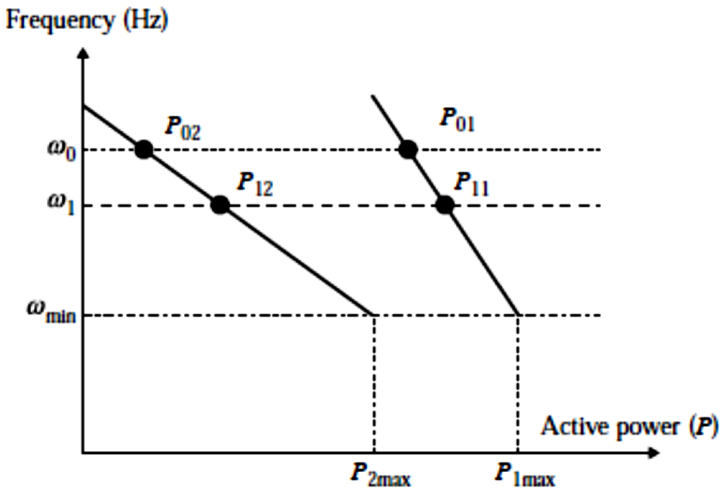

Figure 2. 12: Active power versus frequency droop characteristics.

When a power outage happens (as a result of any contingency), the microgrid seamlessly changes over to the autonomous mode. During this time, the voltage phase angles of the DER units also start changing and hence it leads to obvious drops in the amount of power that they deliver. Consequently, the local frequency also changes. In such cases each microsource rapidly picks up its own portion of load without any new power dispatch schedule from the central controller (CC). For instance, it is assumed that two DERs operate at a common minimum frequency with their maximum capacities P_{1min} and P_{2max}. In grid-connected mode, they operate at a base frequency and deliver powers P_{01} and P_{02}, respectively. With the change in load demand, the DERs operate at different frequencies and thus this matter leads to a change in relative power angles.

In this case, the frequency of operation drifts to a lower common value with different proportions of load sharing. This happens as per the droops of the *P-f* characteristics (see Figure 2.12). Droop mechanism emulates the conventional generators behavior and decreases the frequency and MC must include a control scheme to bring back the microgrid frequency of operation to its nominal value.

2.7.3.2. Load Sharing Reactive Power vs. Voltage (*Q-V*)

Microgrids with plenty of microsources also experience reactive power oscillations where there is no suitable voltage control mechanism. Since a microgrid is generally a radial network, the impedance between the generators inside of microgrid is small so the level of generated circulating current would be high. The value of circulating current can exceed a DER rated current. The circulating current can be controlled using voltage-reactive power (*V-Q*) droop controller with droop characteristic as shown in Figure 2.13. This controller changes the local voltage set-point according to the reactive power which is delivered (capacitive) or absorbed (inductive). In the former the controller decreases the voltage at point of common coupling (PCC), but in the latter it increases the local voltage set-point.

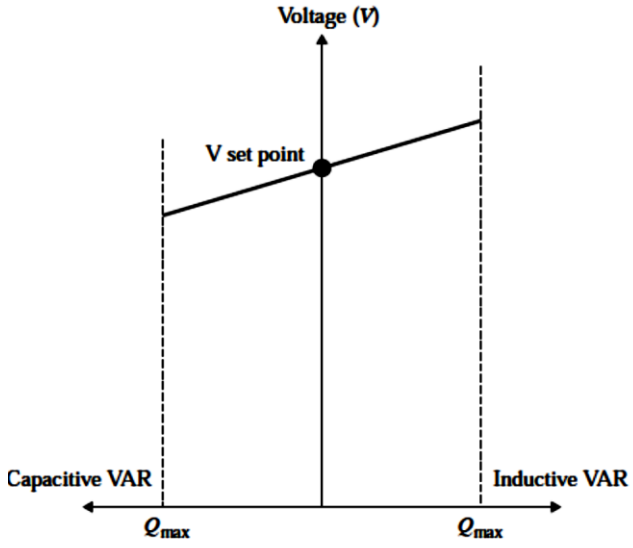

Figure 2. 13: Droop characteristic for *V-Q* droop controller.

As another important point, in grid-forming (islanded) control the unit should be adequately large and have sufficient reserve capacity to supply the power balance. If two or more DERs actively take part in the stabilization of power microgrid and the voltage regulation, frequency and voltage droops control schemes are exploited to share real and reactive power components between the units. Figure 2.14 shows frequency-droop (*f-P*) and voltage-droop (*v-Q*) characteristics. Each is specified through its slope (k_{fP} or k_{vQ}) and a base-point representing either the rated frequency (f_0,P_0) or the terminal voltage (V_0,Q_0), respectively.

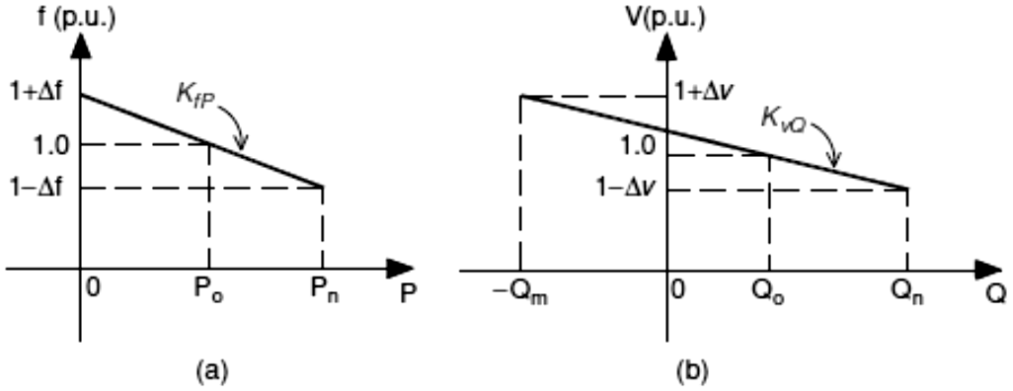

Figure 2. 14: Droop characteristic for load sharing among multiple DER units: (a) *f-P* droop, (b) *v-Q* droop (Farid Katiraei et al., 2008).

The droop coefficients and the base-point can be controlled through a restoration process which dynamically adjusts the operating points of the units.

Figure 2.15 shows a block diagram of a droop control strategy. The locally measured deviations in the frequency and the terminal voltage of the unit are used as the inputs for the controller. If the microsources are not similar in their capacities, the slope of each droop is determined proportional to the nominal capacity of the related microsource to prevent overloading.

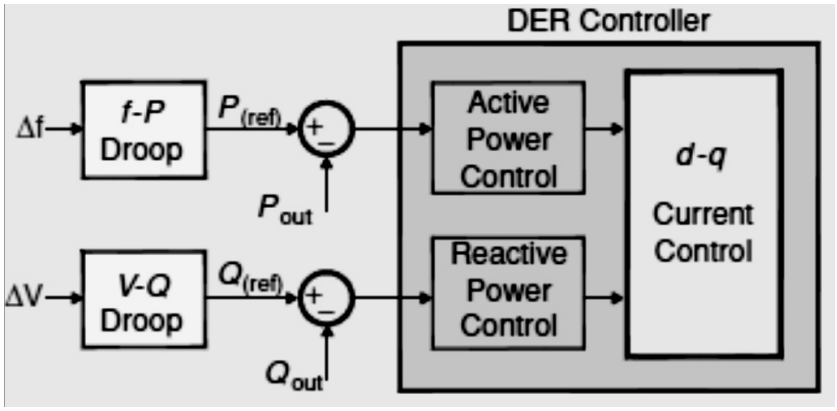

Figure 2. 15: Droop control mechanisms (Farid Katiraei et al., 2008).

2.7.4. Remote (Centralized) Control of Smart Microgrid

The central controller (CC) performs the overall control of microgrid operation and protection through microsource controllers (MCs). The main application of CC is to keep reliability and power quality through voltage-reactive power (*Q-V*) control, power-frequency (*P-f*) control, and protection coordination. This unit also schedules the microsources generation based on economic constraints and helps to maintain power intake from the main grid at bilateral agreed contract points (Prema & Rao, 2014). Thus, the CC ensures energy optimization for the microgrid and stabilizes the specified frequency and voltage set-points for all the MCs to meet the customers' needs. This controller is designed in order to operate in both automatic and manual modes. Also, this unit continuously monitors the operating status of MCs using two modules which are energy manager module (EMM) and protection coordination module (PCM) (Chowdhury & Crossley, 2009).

EMM controls the microsource generation and domestic processes such as heat ventilation air conditioning (HVAC), water heating and chilling optimization, energy storage control, maintaining power quality for industrial processes, and providing ancillary services.

For example, microgrid could support the power network by peak shaving capability. In general, an energy manager module (EMM) should start performing only the basic tasks.

It can opt for complicated duties through intelligent electronic devices (IEDs) and Ethernet communication protocols. Another important role of EMM would be smoothing out the electrical load profile by proper scheduling of loads including the charging of energy storage devices and shifting individual load peaks. Microsource controller should be able to (Chowdhury & Crossley, 2009):

(a) detect new microsources added to existing system without any modification (plug and play capability);
(b) switch seamlessly and quickly between grid-connected and islanded modes;
(c) control the flow of active and reactive powers;
(d) correct the system imbalances and voltage sags;
(e) handle the faults without loss of stability;
(f) provide the utility power grid with the load dynamics' requirements.

In a centralized power management system (PMS) or energy management system (EMS), microgrid central controller (MCC) can be assigned to optimally dispatch distributed energy resources (DERs) and control the loads (Amin et al., 2014; Wei, Jinfeng, Xianzhong, & Christofides, 2011). Thus, it maximizes the local electricity generation according to the market price and security constraints. In this case, local controllers (LCs) issue bids for their demands (for a time interval and get prepared for the subsequent interval) and consider their priorities to serve their customers (Parisio & Glielmo, 2011; Valverde, Bordons, & Rosa, 2012). The functions can be embedded in a central controller (CC) may include load, generation, and heat forecasting as well as functions associated with the unit commitment (Parisio, Rikos, & Glielmo, 2014).

2.7.5. Agent Concept

A supervisory channel which controls a microgrid operation may consist of several agents. The supervision system which includes several agents is so-called multi agent system (MAS) (Colson & Nehrir, 2011). Agent is an intelligent entity composed by software and/or hardware (Suryanarayanan, Mitra, & Biswas, 2010). All information associated with a distributed energy resource can be recorded in its agent. Information such as local measurements, availability of energy resources, and feedback signals for controllers are some example brought to this end. As described in Table 2.2, agents can be dispersed in the microgrid (decentralized control) or interconnected to each other through a central agent (centralized control).

Table 2. 2: Centralized versus decentralized MAS (Colson & Nehrir, 2011).

	Centralized MAS	Decentralized MAS
Characteristics	Sophisticated central supervisor; remote agents with limited capabilities dependent on supervisor for decision-making.	No central supervisor; sophisticated distributed agents organize and make decisions collectively.
Communication Infrastructure	Client-server; *n* communication paths†. *n* minimum communication paths.	*n* minimum communication paths; *n(n-1)/2* maximum if fully networked†.
"Plug & Play"	Entrance and exit from system dictated by supervisor.	Framework facilitates agents to enter and leave the system as conditions permit.
Survivability	System control totally dependent on central supervisor.	Control responsibilities are dispersed and not dependant on a single node.
Reliability	Single node of failure; central supervisor must be redundant.	Decision-making not dependant on a single node.
Synchronization	Central supervisor dictates; control actions issued serially.	Agents act independently; communications and control actions occur asynchronously and in parallel.

†: *n* represents the number of agents within a particular MAS.

Agent based system facilitates both centralized coordination and local control as it operates in different hierarchical levels. This configuration allows utilizing both centralized and decentralized controllers together inside of smart grid and thus makes a robust control channel (Lidula & Rajapakse, 2011).

The tasks associated with local controller (LC), microsource controller (MC), and microgrid central controller (MCC) can be assigned to an agent as an internal function. Each agent can accept different tasks based on the agreement between the customer and power grid operator. In a centralized system, the tasks done by an agent depends on the hierarchical level allocated to that agent such as producer agent, consumer agent, and observer agent (Colson & Nehrir, 2011).

Agents can also be assigned to optimize certain performance measures (e.g. power quality and efficiency) in the system. Agents can exchange their information to do complicated tasks e.g. microgrid resynchronization or to meet a common target e.g. voltage regulation in smartgrid (Ghosn et al., 2010). Therefore, the presence of agents in a microgrid as data banks and communication platform between DERs is necessary.

2.7.6. Challenges in Microgrid Control

Although *P-f* and *Q-V* techniques give high reliability and flexibility, they have several drawbacks that restrict their applications. For example, the conventional droop method is not suitable when the paralleled system must share nonlinear loads (Guerrero et al., 2011). In this case, new control loops have been proposed by (Guerrero et al., 2011; Jiayi et al., 2008; Kakigano, Miura, Ise, & Uchida, 2006) that adjust the output impedance of DER units by adding output virtual reactors or resistors embedded in droop mechanism to share the current harmonic content properly.

Another disadvantage of droop method is its load-dependant frequency deviation which implies a phase deviation between the output-voltage frequency and the main utility.

This matter can cause loss of synchronization during the transition between grid-connected and islanded modes (Guerrero et al., 2011). To improve the droop-control method, in (Kundur, 1994), a local controller shifts up the droop function to restore the initial frequency of the inverters by using an integrator to avoid frequency deviation. However, this method is not applicable in practice when the inverters are not connected to a common AC bus at the same time to be initialized and as a consequence the power sharing is degraded. Another possibility is to wait for accidental synchronization but it is hazardous and can take a lot of time (Guerrero et al., 2011). To solve this problem, an inverter can be located physically near the bypass switch. This inverter can be synchronized with the main grid for seamless reconnection. As a drawback, during the synchronization process, this inverter will be overloaded if there are plenty of inverters supplying the microgrid. In this case, the use of communications seems to be necessary and thus DER controllers should be connected together through a low-bandwidth communication channel. Hierarchical control applied for power dispatching in AC power systems is well known and it has been used extensively for decades. Nowadays, these concepts are applied on wind-power parks and isolated photovoltaic (PV) plants. Therefore, with the proliferation of power electronic based microgrids, presence of hierarchical controllers and energy management systems is mandatory (Guerrero et al., 2011).

In (Marwali & Keyhani, 2004) a low-bandwidth communication channel has been proposed beside locally measureable signals for each distributed generation (DG) unit. This supervisory channel is formed by combining two control methods, namely, droop control and average power control. The average power strategy is used with a slow update rate to relief sensitivity of the system in relation to current and voltage measurement errors.

In this article, a droop characteristic relying on harmonics has also been proposed which enables the system to share the harmonic content of the load currents. However, the communication among the DG units is not possible everywhere in the system due to the physical distance between the units.

In (Marwali, Jin-Woo, & Keyhani, 2004), a method has been presented to control the converter based DGs where a number of such units are being operated in parallel. A controller with a modular structure is presented in this work as well. This controller can be modified to match the control system requirements associated with other AC systems. In this method, a P-I controller has been proposed to specify the set-points for the generator angle and flux.

The application of a robust or adaptive controller in DG systems has been investigated by (Salomonsson, Soder, & Sannino, 2008; Yun Wei, Vilathgamuwa, & Poh Chiang, 2007). In this case, a critical analysis and optimizing techniques have also been proposed in (Ault, McDonald, & Burt, 2003; Senjyu, Miyazato, Yona, Urasaki, & Funabashi, 2008) to control the voltage for DG systems. Voltage sourced converter (VSC) which acts as an interfacing module between a DER and a microgrid can be a source of harmonics. The non-linear loads are also another source of harmonics. Hence, the inverter compensator should be able to supply the electrical power to the microgrid while it is compensating for the no-linearity or imbalance. Generating a high quality power is one of major concerns and various filtering techniques have been suggested in (Tzung-Lin & Po-Tai, 2007; Tzung-Lin, Po-Tai, Akagi, & Fujita, 2008). The level of penetration as a factor can affect the amount of harmonics injected by a distributed energy resource (DER) unit into a microgrid and this issue has been investigated by (Bhowmik, Maitra, Halpin, & Schatz, 2003).

Microgrid stability in another important issue that should be investigated especially where the system is islanded. The system stability during the load sharing has been

investigated by (Chandorkar, Divan, & Adapa, 1993; Reza, Sudarmadi, Viawan, Kling, & Van Der Sluis, 2006; Slootweg & Kling, 2002). The transient stability of a microgrid including electronically interfaced DG (EIDG) with high penetration level has also been studied in (Reza et al., 2006) but this study is based on the presence of an infinite bus (grid-connected mode). Another drawback in this work is that the autonomous operation of power network has been overlooked.

Similar to small signal stability of conventional power systems, the effectiveness of a control system to stabilize a microgrid in oscillatory modes (which may result in a poor damping) has been investigated by (Lopez, de Vicuna, Castilla, Matas, & Lopez, 2000). To determine the possible feedback signals for controllers, a sensitivity analysis has also been carried out in this paper.

A low frequency stability problem during the period of power demand variation has been addressed in (Vilathgamuwa, Poh Chiang, & Li, 2006). It is proved that the changes in power demand move the low-frequency oscillation to a new area in which the relative stability of system is affected. Some decentralized control strategies towards controlling the parallel interconnected DGs have been presented in (Guerrero, Matas, de Vicuna, Castilla, & Miret, 2006; Guerrero, Matas, Luis Garcia de, Castilla, & Miret, 2007).

In (Marwali, Min, & Keyhani, 2006), the robustness of voltage and current control solutions in an isolated microgrid has been analyzed through structured singular values that results in a discrete-time sliding mode current controller. A combination of droop and average power method for load sharing has been discussed in (Marwali, Jin-Woo, & Keyhani, 2007). The small signal stability analysis associated with this scheme was carried out and the result obtained from the small signal model has been compared to the original non-linear model.

Dynamic modeling and autonomous operation of converter-based microgrid along with voltage and frequency droop controllers has been analyzed in (Barklund, Pogaku, Prodanovic, Hernandez-Aramburo, & Green, 2008; Pogaku, Prodanovic, & Green, 2007). In this paper, firstly, each part of this system is modeled in state-space form. Secondly, all the modules are combined together and evaluated in terms of a common reference frame. This model only presents the control loops but not switching operation. Common P-I controller are utilized in order to control the voltage and current.

Another challenge about the microgrids is ancillary services that they can provide the main grid with them. One of those services is to locally supply the loads through DERs and hence reduce the power losses. In this case, optimization techniques have been exploited by (El-Khattam, Hegazy, & Salama, 2005; Golshan & Arefifar, 2006; Khodr, Vale, & Ramos, 2009) to plan and decrease energy losses using DG systems. A single-phase high frequency AC (HFAC) microgrid as a solution has also been recommended by (Puttgen, MacGregor, & Lambert, 2003) to utilize renewable energy sources (RESs) efficiently.

To achieve an acceptable level of reliability, performance of operation, and efficient management of energy, it is necessary to control the flow of power between a microgrid (MG) and the main power grid. A perfect solution can be a bidirectional control over the flowing power. In this case, it is possible not only to define the exact amount of power supplied by the utility but also the fed-back power from microgrid to the main grid during the times when the demand is less than the generation.

Designing a reliable system is a major task in microgrid operation. The concepts such as DG unit location, dynamic load changing, and intermittent output power (in the case of intermittent resources) have been always challenging issues. As a solution, frequency isolation between the utility and microgrid is recommended in order to obtain a reliable system.

Isolation between the microgrid and the main network ensure a safe operation where several DG units together with the loads are interconnected in a large microgrid. Any variation in voltage and/or frequency at the utility side affects the microgrid state causing the load power and voltage oscillations. To obtain safely operation, the sensitive loads inside of microgrid should not be encountered with any abrupt changes in voltage and frequency. The isolation between the grid and microgrid can resolve such problem and hence prevents the direct impact of microgrid load change or change in a DG output voltage on the utility side.

Microgrid protection is another major concern regarding the microgrid and its distribution network which is connected to (Al-Nasseri, Redfern, & O'Gorman, 2005; Brahma & Girgis, 2004; H. Nikkhajoei & Lasseter, 2007; Vieira, Freitas, Wilsun, & Morelato, 2006). Integrating DG units into an existing power grid can modify the set-points of protective relays. DG units can supply a portion of fault current which cause to decrease a relay threshold current setting instead. In another case, if a reverse power flows from downstream to upstream in a feeder (due to presence of DG units), it is not detectable by unidirectional relays. An adaptive protection scheme has been proposed by (Brahma & Girgis, 2004) to consider the impact of a DG penetration on coordination of protective devices. A method has also been introduced by (Vieira et al., 2006) to determine the coordination of the rate of change of frequency (ROCOF) in under or over frequency relays.

In rural area the electricity should be continuously available and the distributed generation inside of a microgrid system is the best solution to provide the people in such regions with adequate electrical energy. In this case, the interconnection location of microsources is very important. Any consideration regarding the technical issues should be studied since the failure and success of rural electrification are highly dependent to such systematic analyses. Power electronic converters are able to provide the rural

electrification in lower cost than the current electrification cost but in weak systems it may cause poor voltage regulation.

In rural networks, a highly resistive low or medium voltage transmission lines affect the performance of controller in power sharing. Since there is a strong coupling between active and reactive powers, the matter leads to inaccurate load frequency control. In weak system, the use of high values of droop gain is recommended to share the load properly. However, in very resistive networks the high droop gains may results in an unstable system and hence it cannot sometimes guarantee a proper load sharing. In such cases, the main concept of load sharing which is the decoupled control of active and reactive powers is violated and the conventional droop control schemes are not applicable (Chandorkar et al., 1993). In (De Brabandere et al., 2007), the droop equations have been modified for a line with high *R/X* ratio in order to decouple the control of active and reactive powers but the choice of droop gains for rating based power sharing has not been investigated at all.

In the case of electronically interfaced DGs, since the output angle can vary instantaneously, drooping the angle to share the load is more accurate than the drooping frequency (Majumder, Ghosh, Ledwich, & Zare, 2009a). The constraints that limit the allowable range of frequency droop may results in the oscillation of frequency during the frequent load changes in a microgrid. In (Majumder, Ghosh, Ledwich, & Zare, 2009b), it is assumed that the lines are mainly resistive and conventional droop can work with real power controlled by voltage and reactive power by angle. But in rural network with a high *R/X* ratio and a strong coupling between active and reactive powers, it is not possible to control them independently only by using the frequency and voltage. To cope with such a problem, it is necessary to modify the droop equations and the real power droop coefficient can be chosen depending on the load sharing ratio.

It is often difficult to install extensive distribution network since the customer density in the rural areas can be dispersed. Distributed generation (DG) is an appropriate solution to resolve this problem. In (Agalgaonkar, Kulkarni, & Khaparde, 2006; Blyden & Wei-Jen, 2006; De Brabandere et al., 2007), a typical medium voltage rural distribution network is planned for different loading conditions. The bottom up approach through an evaluation of autonomous or non-autonomous modified microgrid concept to provide electricity to local residents is proposed in (Blyden & Wei-Jen, 2006). The policy and prospective planning achievements for rural electrification are hindered in many countries that are described in (Balakrishnan, 2006; Downer, 2001; F. Katiraei, Abbey, Tang, & Gauthier, 2008; Lewis, 1997; Mackay, 1990; Mukhopadhyay & Singh, 2009; Munasinghe, 1990; Owen, 1998; Samuels, 1946; Townsend, 1985).

CHAPTER 3: RESEARCH METHODOLOGY

3.1. Introduction

The proposed microgrid configuration is introduced in this chapter. The technical specifications of distributed energy resources (DERs) and loads pointed out as well. The agent concept applied on this microgrid is also discussed. Voltage sourced converter (VSC) dynamic model, Phase locked loop (PLL) controller, and current controller implemented in PSCAD/EMTDC are described in detail.

In addition, the dynamic models of DERs (implemented in PSCAD/EMTDC) together with their controllers are analyzed. Solar photovoltaic plant dynamic model is described along with its controllers. The improved dynamic model of battery bank (improved version of Shepherd model) is presented. The proposed battery sizing algorithm is investigated as well. This chapter also presents the proposed charging and discharging current controller of battery bank. Dynamic models of diesel power plant as well as the improved excitation and governor controllers are discussed. A load model is designed and its design procedure is investigated in this chapter.

3.2. Proposed Microgrid Configuration and Operation

3.2.1. Overview

The proposed microgrid (MG) configuration is almost similar to MG systems which have been evaluated by (Daud et al., 2013; Tan et al., 2012; Tan et al., 2013). The only difference is that in this, microgrid incorporates both rotary and electronically interfaced

distributed energy resources (see Figure 3.1) to study interactions between both types. Microgrid is subject to operate in grid-connected (G.C) mode.

The primary source of power is a diesel engine which provides the mechanical torque required for a 1.28 MVA synchronous generator. Another distributed energy resource (DER) is a 1080 kVA (1026 kWh, 1125 Ah) battery energy storage system (BESS) which consists of a Lead-acid battery bank connected to the grid through a three-phase bi-directional voltage sourced converter (VSC). BESS is capable of operating as either source or sink of power.

As a load demand, a six steps AC load in two categories (i.e. industrial and domestic loads) are interconnected to the load bus and each group consists of three similar feeders. The load demand is supposed to vary throughout the day. A 1 MW_p photovoltaic distributed generation (PVDG) plant is also considered to inject the available power from the sun into the microgrid in unity power factor during the day.

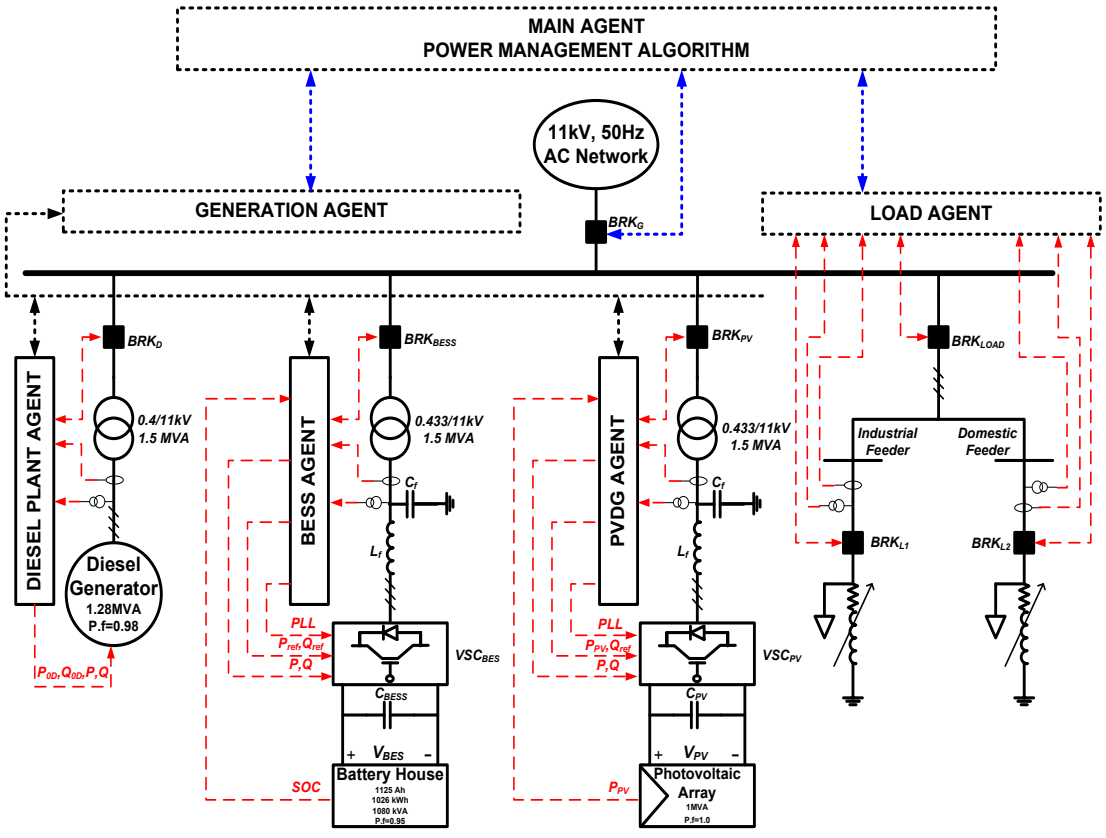

Figure 3. 1: Smart microgrid configuration.

Battery plant is dispatched to smooth out the power fluctuations in system caused by solar plant together with loads and hence it is subject to limit the ramp rate stresses on the main AC network. Diesel plant is dispatched to shift up or down the grid active power profile and thus shares the load active power with AC network.

Depending on the power management strategy, BESS operates either in inverting or rectifying modes. Diesel plant is assumed to decrease or increase its active power generation according to power management system (PMS) commands. Battery energy storage and diesel plants can also be dispatched in order to share the load reactive power proportional to their nominal capacities. As shown in Figure 3.1, there exist four agents in microgrid with different hierarchical levels, namely, unit agents, generation agent, load agent, and main agent.

3.2.2. Main Agent

All the information collected from generation and load agents is sent to the main agent (which is in the highest level of hierarchy) to inform the operator about the system states (dotted blue lines). Then, the operator calculates the dispatching references and issues required commands for the dispatchable plants and breakers of loads.

3.2.3. Generation Agent

Generation agent is assigned to receive and/or send the data from/to DG unit agents through the communication channel (bus) indicated by dotted black line.

3.2.4. Unit Agent

Each DER has an agent under its own name (e.g. PVDG agent) which is so-called “unit agent”. This agent collects the local information such as DG plants breakers statuses, output voltage and current, and availability of prime mover (i.e. sunlight and engine fuel). There is a forecasting module embedded in solar PV plant unit agent and along

with this module the estimated solar pattern is sent to the main agent to be filtered yielding averaged solar irradiation profile.

In BESS, unit agent calculates *SOC* of battery and sends it to generation agent. All this information is recorded in generation agent and then sent to the main agent. Local agents also generate and compute the feedback signals required for the internal controllers (red dotted lines) such as current or power loops, governor, and excitation controllers.

3.2.5. Load Agent

Load agent also registers the status of load breakers and the power which is flown in each feeder together with the forecasted load profile.

3.2.6. Voltage Sourced Converter (VSC)

Two-level three-leg converter topology is utilized in this work. This topology consists of six insulated gate bipolar transistor (IGBT) semiconductor switches. There exist two IGBTs in each leg and hence they supposed to be switched on/off in a complementary manner to prevent the short circuit at the VSC terminal. The gate firing signals are generated through pulse width modulation (PWM) technique which benefits from high frequency modulation saw-tooth waveform crossing the reference signal which oscillates at fundamental frequency (50 Hz).

To prevent the propagation of high switching frequency harmonics into the main network, VSC is connected to point of common coupling (PCC) through a LC filter and delta-star step-up isolation transformer. LC filter includes in equivalent inverter line inductance in parallel with a capacitor bank (design value). Bandwidth of LC filter should be lower than the VSC controller bandwidth to make sure that the noiseless states are fed back into the controller. Thus, the control loops would be in charge of attenuating the low frequency disturbances which pass through the filter.

3.2.6.1. Phase Locked Loop (PLL)

To measure the frequency of an AC signal, phase locked loop mechanism can be used. PLL controller can be explained in this way that the measured three-phase AC signal is transformed to *dq*-frame using Park's Transformation. The quadrature component of AC signal (V_q) is considered as the input of PLL controller and is compared to zero. The error between these two values passes through a PI regulator whose output is considered as the input for voltage-controlled oscillator (VCO) unit (see Figure 3.2). This method of PLL implementation forces V_q to become zero and thus the direct component of signal (V_d) is aligned with the reference phasor rotating at the same frequency. In another method proposed by (Zhang & Ooi, 2013), the difference between the PLL output angle and its input reference angle can turn into zero if it is limited to between 0° and -180°.

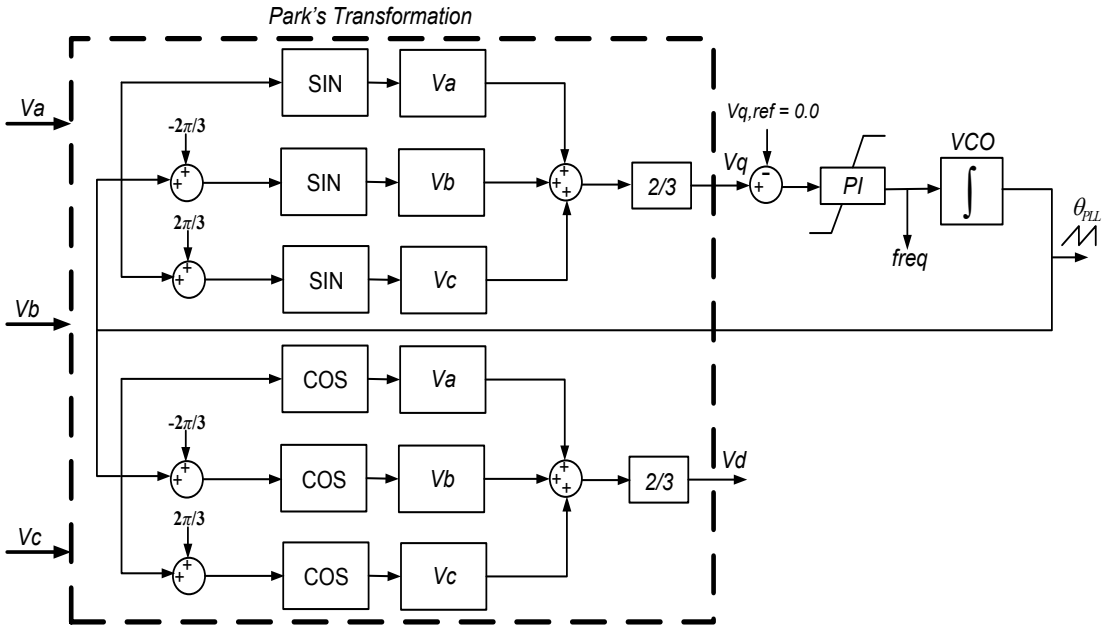

Figure 3. 2: PLL controller model used in this work.

3.2.6.2. Current Control

The most common technique utilized to control an electronically interfaced DG in the presence of a master grid (AC network) is so-called "current control" scheme. In current control mode, the flow of power can be in two directions i.e. from the VSC to the master network or vice versa. The master AC network is assumed to be robust enough to provide constant frequency and voltage at PCC and thus voltage sourced converter (VSC) can easily follow the reference phasor using the PLL controller (Amirnaser Yazdani & Iravani, 2010).

To model current controller, states of the system should be measured and transformed to *dq* rotating synchronous frame. Park's transformation is applied for this purpose (see Figure 3.2). The angle of this conversion is generated by PLL controller which simultaneously oscillates along with the instantaneous alternating voltage phasor measured at point of common coupling (PCC).

As shown in Figure 3.3, current controller is composed by a fast inner current loop which tracks the reference current value (I_{ref}). Direct and quadrature components of reference current can be calculated either through Eqs. 3.1 and 3.2 (Amirnaser Yazdani & Iravani, 2010) or can be generated using an outer slower power loop in *P-Q* control mode (see Figure 3.4). The outer power loop follows the given power references which are either negative (in rectifying mode) or positive (in inverting mode).

$$I_{d,ref} = \frac{2}{3V_d} P_{ref} \tag{3.1}$$

$$I_{q,ref} = -\frac{2}{3V_d} Q_{ref} + C_f \omega_0 V_d \tag{3.2}$$

where V_d is the direct component of VSC output voltage (in kV), C_f is the capacitor value in LC filter (in F), P_{ref} and Q_{ref} are the desired set-points for active and reactive powers (in MW and MVAR), respectively.

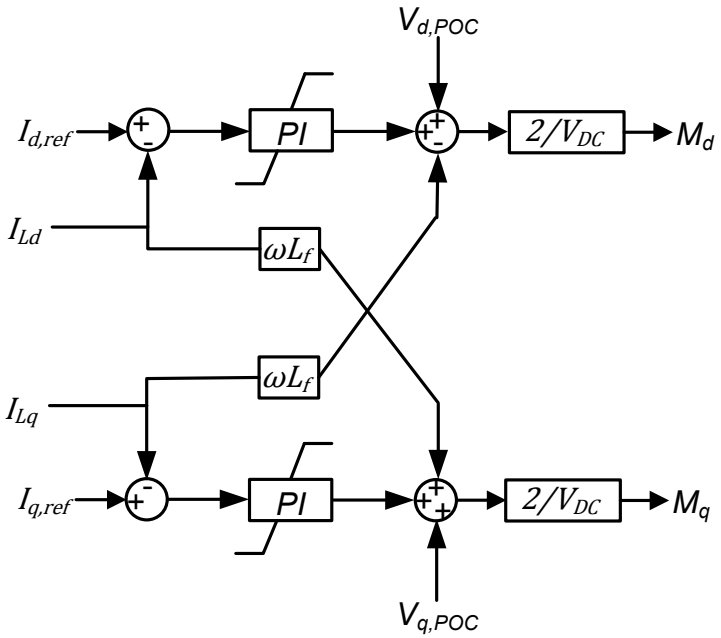

Figure 3. 3: Inner current loop regulator.

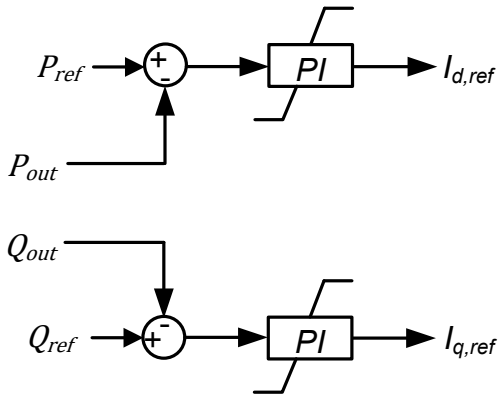

Figure 3. 4: Outer power loop regulator in *P-Q* control mode.

3.2.7. Solar Photovoltaic Generator Dynamic Model

Photovoltaic (PV) generator has to be modeled accurately because the dynamics of VSC and controllers highly depend on the model of PV array. For the circuitry based modeling techniques of PV cell, single-diode, double-diode, and three-diode models have been suggested in the literature.

The single-diode model can be further improved by adding a second diode in parallel with the first diode. The second diode represents the recombination effect of carriers in depletion region of semiconductor where output current value of PV cell is low (Taheri, 2011). In three-diode model, a third diode is added to the double-diode model to represent the current flows through the peripheries (Nishioka, Sakitani, Uraoka, & Fuyuki, 2007). However, single-diode model has shown a reasonable trade-off between accuracy and simplicity. This model is generally utilized in power system studies since determination of parameters becomes slightly complicated for double-diode and three-diode models (Carrero, Amador, & Arnaltes, 2007; A. Yazdani et al., 2011).

In single-diode model, a current source is anti-parallel with a diode. As depicted in Figure 3.5, shunt and series resistances are also considered in this equivalent circuit.

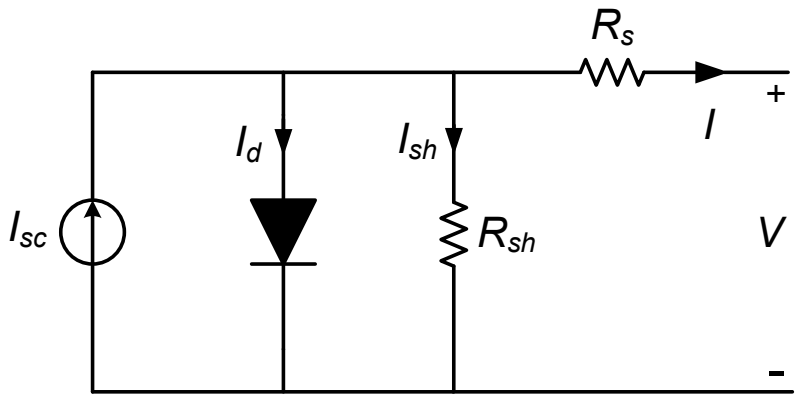

Figure 3. 5: Equivalent single-diode model of solar PV cell.

When the PV cell is illuminated by the sun, it generates DC photo-current (I_{sc}). Photo-current varies linearly against changes in solar irradiance. The current through the anti-parallel diode (I_d) is responsible for non-linearity of *I-V* characteristic. Applying the Kirchhoff's current law based on equivalent circuit shown in Figure 3.5 yields (Rajapakse & Muthumuni, 2009):

$$I = I_{sc} - I_d - I_{sh} \tag{3.3}$$

and hence,

$$I = I_{sc} - I_0 \left[exp\left(\frac{V + IR_s}{nkT_c/q}\right) - 1 \right] - \left(\frac{V + IR_s}{R_{sh}}\right) \tag{3.4}$$

I_{sc} can be calculated as:

$$I_{sc} = I_{scR} \frac{G}{G_R} [1 + \alpha_T (T_c - T_{CR})] \tag{3.5}$$

where

G_R: reference solar radiation

T_{CR}: reference cell temperature

I_{scR}: short circuit current at G_R and T_{CR}

α_T: temperature coefficient of photo current

and I_0 is dark current and can be calculated as:

$$I_0 = I_{oR} \left(\frac{T_c^3}{T_{cR}^3}\right) exp\left[\left(\frac{1}{T_{cR}} - \frac{1}{T_c}\right)\right] \frac{qe_g}{nk} \tag{3.6}$$

where

I_{oR}: dark current at T_{CR}

q: electron charge

k: Boltzman constant

e_g: band gap energy

n: diode ideality factor (between 1 and 2, a typical value for silicon solar cell is 1.3)

The basic unit of PV generator is the solar cell which is able to generate electrical power about 1 to 2 Watt. Series and/or parallel electrically coupled PV cells make PV modules

and further PV arrays. A PV array encompasses series and parallel connected modules and hence the single cell equivalent circuit can be scaled up in order to rearrange for any series/parallel configuration.

In this work, total number of 160 strings that each consists of 24 modules in series ($V_{oc,Plant} = 1221.6V$) have been connected in parallel ($I_{sc,Plant} = 891.2A$) to build up 1 MW solar PV power plant. Parameters of PV module used in this thesis are given in Table 3.1.

Table 3. 1: Electrical specifications of solar module (HIT-N210A01) (SANYO North America, 2010).

Parameter	Value
Rated Power (P_{max})	$210\ W$
Maximum Power Voltage (V_{pm})	$41.3\ V$
Maximum Power Current (I_{pm})	$5.09\ A$
Open Circuit Voltage (V_{oc})	$50.9\ V$
Short Circuit Current (I_{sc})	$5.57\ A$
Temperature Coefficient (V_{oc})	$-0.142\ V/℃$
Temperature Coefficient (I_{sc})	$1.95\ mA/℃$
NOCT (Normal Operating Cell Temperature)	46℃

3.2.7.1. Maximum Power Point Tracking (MPPT)

The amount of power which can be captured from the solar cell depends on its operating point on *I-V* characteristic. To draw as much power as possible from the PV generator, different MPPT techniques have been introduced in the literature (Bhatnagar & Nema, 2013; Eltawil & Zhao, 2013; Ishaque & Salam, 2013; Salas, Olías, Barrado, & Lázaro, 2006). MPPT algorithm is designed to set reference voltage value for the controller based on PV module output current as well as voltage and hence keep the operating point about the knee point on *I-V* curve (see Figure 3.6).

The main duty of MPPT algorithm is to match impedance at the PV generator terminal where the load impedance varies and force the operating point to move away the knee point.

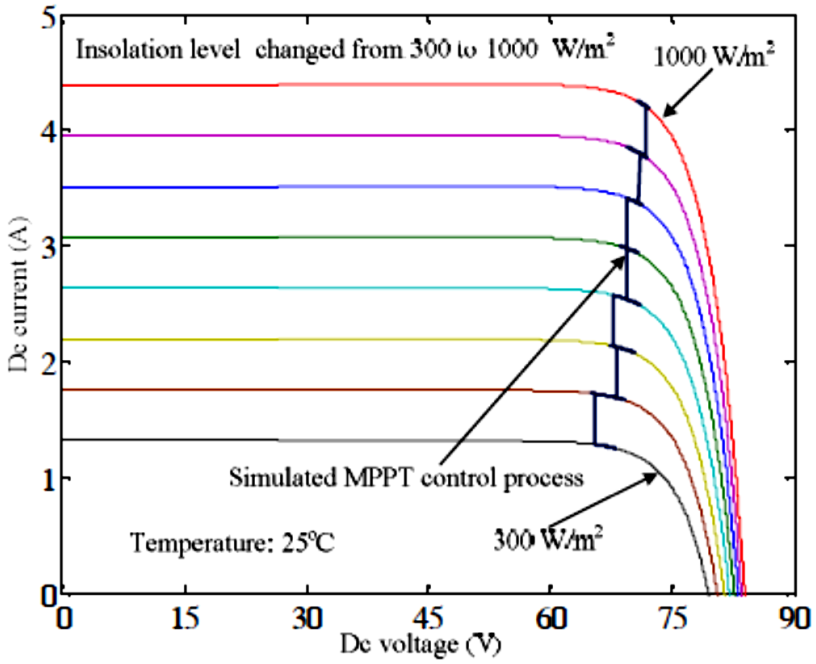

Figure 3. 6: An example of simulated MPPT mechanism which tracks the knee point (Zhou, Zhao, Eltawil, & Yuan, 2008).

A commonly used algorithm is Perturb and Observe (P&O) technique. However, this method has its own limitations. For example, the exact maximum power point (MPP) can never be found and hence the power oscillates around MPP (Rajapakse & Muthumuni, 2009; A. Yazdani et al., 2011). The method adopted in this work is Incremental Conductance (IC) algorithm. Figure 3.7 shows the flowchart of this algorithm which is implemented in PSCAD/EMTDC. The IC algorithm is designed to evaluate Eq. 3.5 at the MPP as:

$$\frac{dP}{dV} = \frac{d(VI)}{dV} = I + V\frac{dI}{dV} = 0 \tag{3.7}$$

where I and V are the output current and voltage at the terminal of PV generator ,respectively. The logic behind this algorithm is given in Table 3.2.

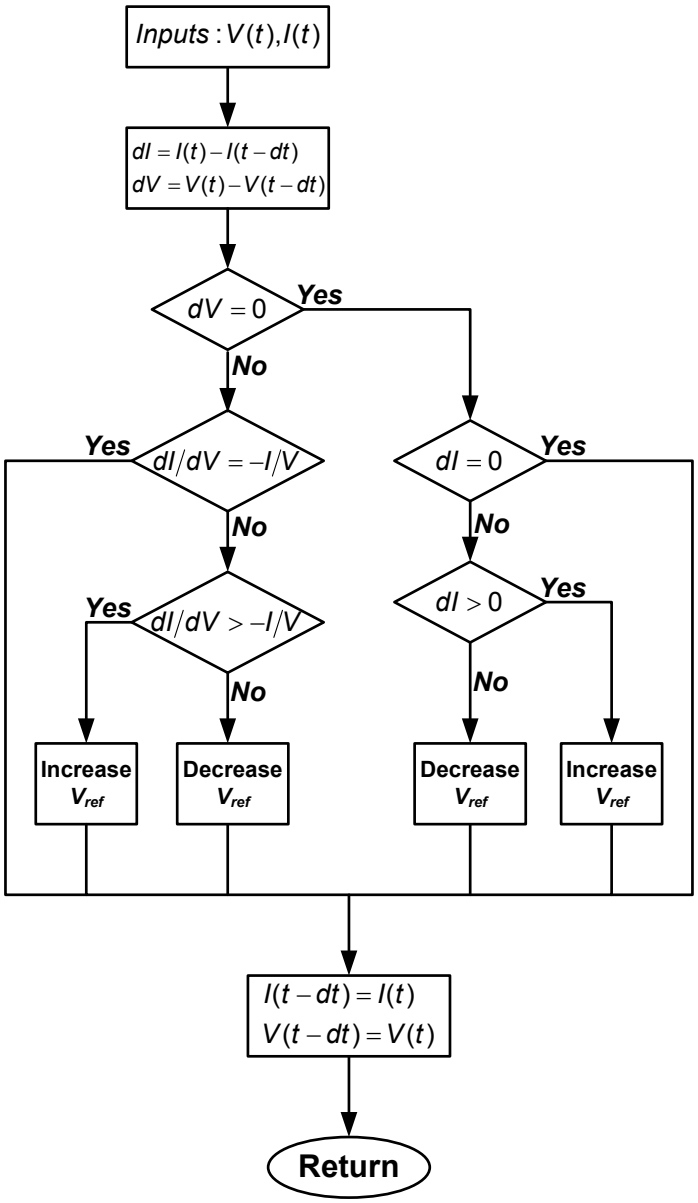

Figure 3. 7: IC algorithm in order to the estimate V_{ref} for DC bus controller.

Table 3. 2: Logic behind the IC MPPT algorithm.

$\frac{dI}{dV}$	$\frac{dP}{dV}$	Operating point with respect to *MPP*
$= -\frac{I}{V}$	$= 0.0$	at *MPP*
$> -\frac{I}{V}$	> 0.0	Left side
$< -\frac{I}{V}$	< 0.0	Right side

3.2.7.2. Photovoltaic Generator Control Mechanism

According to ("IEEE Application Guide for IEEE Std 1547, IEEE Standard for Interconnecting Distributed Resources with Electric Power Systems," 2009; "IEEE Recommended Practice for Utility Interface of Photovoltaic (PV) Systems," 2000), a photovoltaic distributed generation (PVDG) system is not allowed to participate in voltage regulation and thus it can only operate in unity power factor. By forcing the reactive power to zero in steady-state, the DC bus equation which shows relationship between input power (P_{PV}) and output power (P_{VSC}) can be written as:

$$\frac{d}{dt}V_{dc}^2 = \frac{2}{C}(P_{PV} - P_{VSC}) \tag{3.8}$$

PVDG system is assumed to operate in current control mode at all the times. To regulate the voltage at DC bus, there are two techniques i.e. single-stage and double-stage methods. In this work, single-stage controller has been adopted through which only the inverter is controlled. There is no interfacing unit between the PV array and inverter except DC link. In single-stage mechanism, whole power generated in DC side by PV generator is instantaneously transferred to AC side and hence the voltage at DC link gets regulated. MPPT unit sets the voltage reference for DC link voltage regulator. As illustrated in Figure 3.8, the error between the square of set-point and square of measured DC bus voltage passes through a PI compensator. PI regulator output is added to instantaneous power generated by PV array making up P_{ref} for the inner power loop. Assuming that P_{VSC} to be the input power for the inverter and if the switching losses is ignored, the V_{dc}^2 and P_{PV} would be the controller inputs and hence P_{ref} would be the controller output. P_{VSC} would become equal to P_{ref} in steady-state so that the variation of DC link voltage would be forced to become zero and the feed-forward path including the P_{PV} ensures that the whole power is transferred to the AC side.

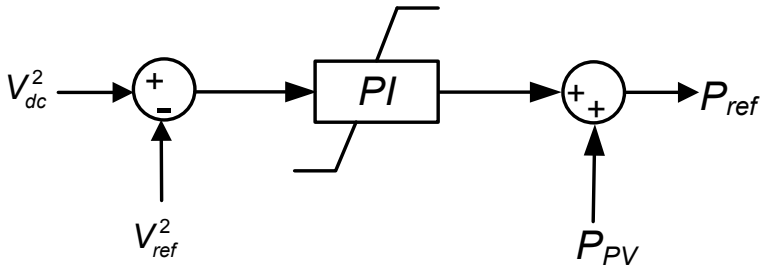

Figure 3. 8: Outer power loop in PVDG controller.

On the other hand, in double-stage approach a DC-DC converter is exploited which regulates for the DC bus voltage at a desired value by tracking the MPPT reference. DC-DC converter should be controlled separately and so one control level has to be added to the controller with additional filtering and switching hardware.

3.2.8. Battery Energy Storage System (BESS)

3.2.8.1. Proposed BESS Sizing Algorithm

In this thesis, a algorithm is proposed to accurately design and size the battery storage plant taking into account the technical and empirical aspects. In conventional rotary based generators, the high inertia of rotating mass is capable of supplying for any transient power mismatch between the load and generation. By contrast, in low or non-inertial systems (e.g. an inverter based DG) any changes in the load or generation results in abrupt power oscillations. To compensate for this drawback, BESS can be exploited in power networks (Barton & Infield, 2004; Beaudin, Zareipour, Schellenberglabe, & Rosehart, 2010; Carbone, 2011; Koohi-Kamali et al., 2013; Ribeiro, Johnson, Crow, Arsoy, & Liu, 2001; Vazquez et al., 2010). BESS can also bring ancillary services for AC network such as dispatching ability, ride-through capability, and network stability.

For the utility applications, lead-acid battery is a proper solution in terms of technical aspects and its cost per kilo watt (Poullikkas, 2013). Lead-acid battery (LAB) is able to meet the ramp rate requirements of the grid as well.

Lead-acid battery can be used for deep-cycle applications where the power is supplied for a long duration. Lead-acid battery is also suitable to be charged or discharged in a short period of time (e.g. for the purpose of power smoothing).

The time taken for BESS to ramp up or down depends on the application which BESS is designed for. In grid-connected (G.C) mode, BESS is responsible for smoothing out the power fluctuations caused by photovoltaic distributed generation (PVDG) plant and the loads. Smoothing index is considered to be the dispatching reference for the battery plant voltage sourced converter (VSC) and hence BESS should be sized based on this index.

The ramp rate of a PVDG unit is very fast because it is an electronically interfaced DG (EIDG) and a sudden change in solar radiation level results in abrupt solar PV plant output power oscillations. Load also changes which exacerbate the situation. In this case, generation and load forecasting can be proper remedies in order to denote what would be the boundary of these fluctuations beforehand. In this work, the load and generation profiles are assumed to be forecasted one day ahead. For example, it is possible to consider a noise of ±10% about the PVDG average output power. In this case, if the PVDG is designed for 1 MW_p, the peak time generation would vary from 0.9 to 1.1 MW_p. Hence, BESS is designed and sized so that it can supply or absorb 100 kW within several seconds.

To determine the charge or discharge rate of a battery cell, *C* rate is defined. *C* rate specifies the amount of constant current multiplied by the duration (which is 5, 10, or 20 hours) when the battery can continuously supply for this current. It is nominally determined in manufacturers' datasheets as C_5, C_{10}, or C_{20}. The battery cell terminal voltage (V_{cell}) strongly depends on the *C* rate which the battery is sized for. Designing of a BESS for a typical microgrid is begun with characterization of battery cell which is the smallest unit in a battery bank.

Open-circuit terminal voltage of the cell in 100% state of charge (SOC) is considered as the float or nominal open-circuit voltage (V_{oc}).

Final voltage at the completion zone of discharge is symbolized by V_{final} for each cell. Keeping the V_{cell} above the V_{final} retains the operating point in the linear zone. Therefore, V_{final} should be chosen as high as possible and normally 80% to 90% of V_{oc} is a reasonable value. V_{final} is specified in the manufacturers' datasheets for high rate of discharge applications (e.g. 5 minutes in this work). The nearest value of voltage available in the datasheet to the calculated V_{final} can be selected as the final voltage and used to size BESS (see Figure 3.9).

Let V_{BESS} to be the BESS terminal voltage after discharge. BESS is supposed to contain N_s battery cells in series to meet the required voltage level at DC bus. The minimum DC bus voltage of VSC, in which the VSC can operate normally, is considered as V_{BESS} and can be formulated as:

$$V_{BESS} = \frac{2\sqrt{2}V_{LL}}{m\sqrt{3}} \tag{3.9}$$

where m is the PWM switching modulation index and V_{LL} is RMS value of line-to-line VSC voltage at the grid side (transformer primary side). Thus, the number of cells in series in each string is given by:

$$N_s = \frac{V_{BESS}}{V_{final}} \tag{3.10}$$

If the calculated N_s is not an integer, the subsequent higher value would be selected as N_s.

BESS should be able to absorb or supply the maximum power in a short duration and at the same rate. To design it for maximum operating ramp rate, it is enough to find the maximum difference between reference waveform estimated by moving average

processing unit and estimated solar plant output power added to difference between estimated load profile and average load (smoothing index). The maximum ramp rate can be handled by BESS is found through:

$$P_{BESS}^{max} = \left[\left(P_L - P_{Lavg}\right) + \left(P_{set} - P_{PV}\right)\right]R(t) \tag{3.11}$$

where P_L is the instantaneous load active power (in MW), P_{Lavg} is the average load active power (in MW), P_{set} is smoothed solar PV plant output active power waveform generated by moving average filtering (MAF) in MW, and P_{PV} is the real-time solar PV plant output power (in MW). $R(t)$ is the exponential or ramp function and reaches to its final unity value in $T(sec)$ and thus the maximum energy which can be absorbed or supplied by BESS is determined by:

$$\begin{aligned} E_{BESS}^{max} &= \int_0^T P_{BESS}^{max}(t)\, dt \\ &= \left[\left(P_L - P_{Lavg}\right) + \left(P_{set} - P_{PV}\right)\right].K.T \end{aligned} \tag{3.12}$$

where

$$K = \frac{\int_0^T R(t)dt}{T} \tag{3.13}$$

K is equal to 0.5 and 0.2 where $R(t)$ is either ramp or exponential function (this value can vary between 0.2 and 0.45), respectively.

Taking into account active power capability of BESS the maximum energy can be written as:

$$E_{BESS}^{max} = \frac{K.S_{VSC}.\cos\varphi\,.T}{\eta} \tag{3.14}$$

where S_{VSC} is VSC rated apparent power in VA and η is VSC efficiency which is between 0.8 to 0.9.

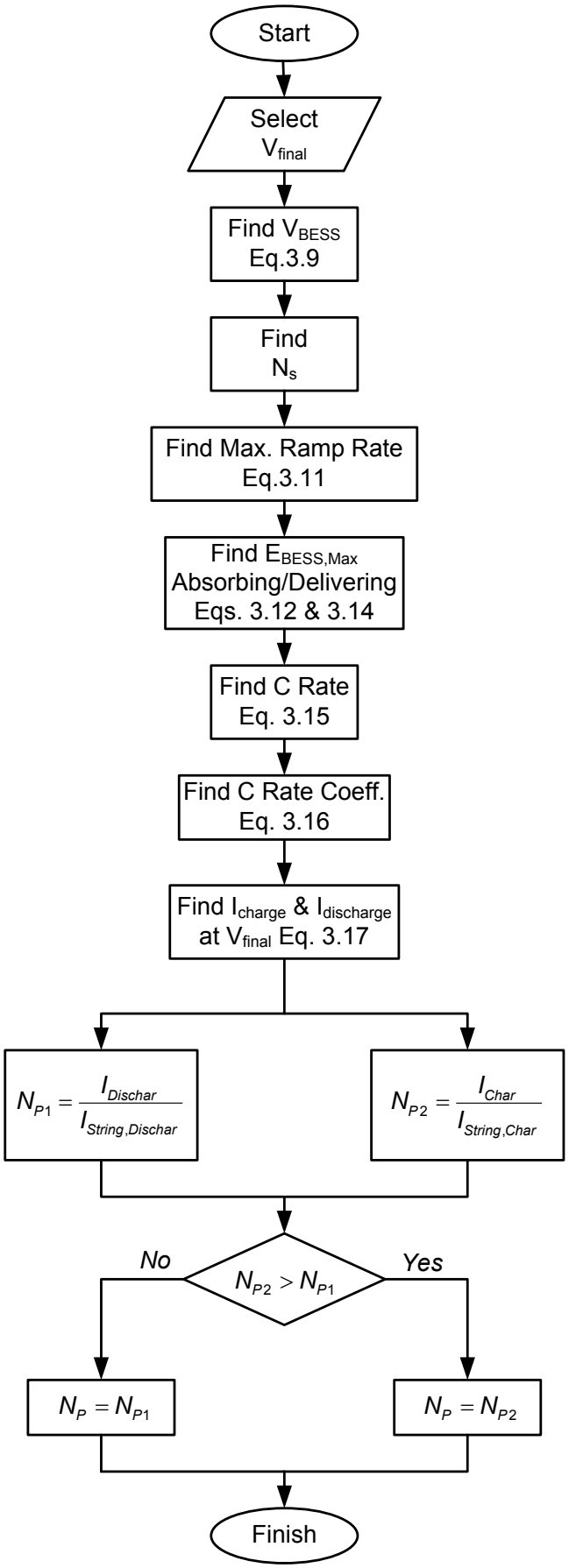

Figure 3. 9: Proposed battery house sizing and designing algorithm.

To find the charge and discharge rate of battery energy storage system (BESS), the *C* rate (Ah) of battery plant have to be obtained which is equal to:

$$C_{Ah} = \frac{E_{BESS}^{max}}{V_{BESS}.3600} \tag{3.15}$$

and thus the charge/discharge rate of BESS is denoted as a *C* rate coefficient given by:

$$D = \frac{3600}{T} \tag{3.16}$$

so the charging/discharging current in ampere(s) is written as:

$$I = D.C_{Ah} \tag{3.17}$$

3.2.8.2. Proposed Battery Charging/Discharging Controller

In the proposed microgrid (MG), battery energy storage bank is directly connected to the DC link of VSC. To prevent battery electrolyte decomposition, battery bank state of charge (*SOC*) is considered as the operating control variable in the power management system (PMS). To control the charging/discharging current PMS limits the dispatching reference (P_{ref}) through the proposed algorithm shown in Figure 3.10.

This current control strategy is embedded in BESS unit agent and confines dispatching reference (smoothing power index) of BESS to make sure that the level of charging/discharging current is allowable. Since the MG operates in grid-connected mode, any mismatch between the active power smoothing index (APSI) and BESS power limits would be supplied or absorbed by the grid. In this algorithm, PVDG unit and load forecasting modules release their estimated waveforms and then smoothing index is calculated by the main agent accordingly. It sends the dispatching signal to BESS through the generation agent. Once the unit agent receives the dispatching commands from the generation agent, the current control algorithm is activated and

determines whether the charging/discharging current is within the allowed boundary or not.

In another method, the storage unit is connected to DC link via DC-DC converter. DC-DC converter is a bidirectional buck-boost converter that has two duties. Firstly, it boosts up battery terminal voltage to that level is required at DC bus. Secondly, it contributes in charging/discharging process of battery in constant current (CC) or constant voltage (CV) modes. To control DC-DC converter elaborated control mechanisms together with filtering and switching elements have to be added to the system.

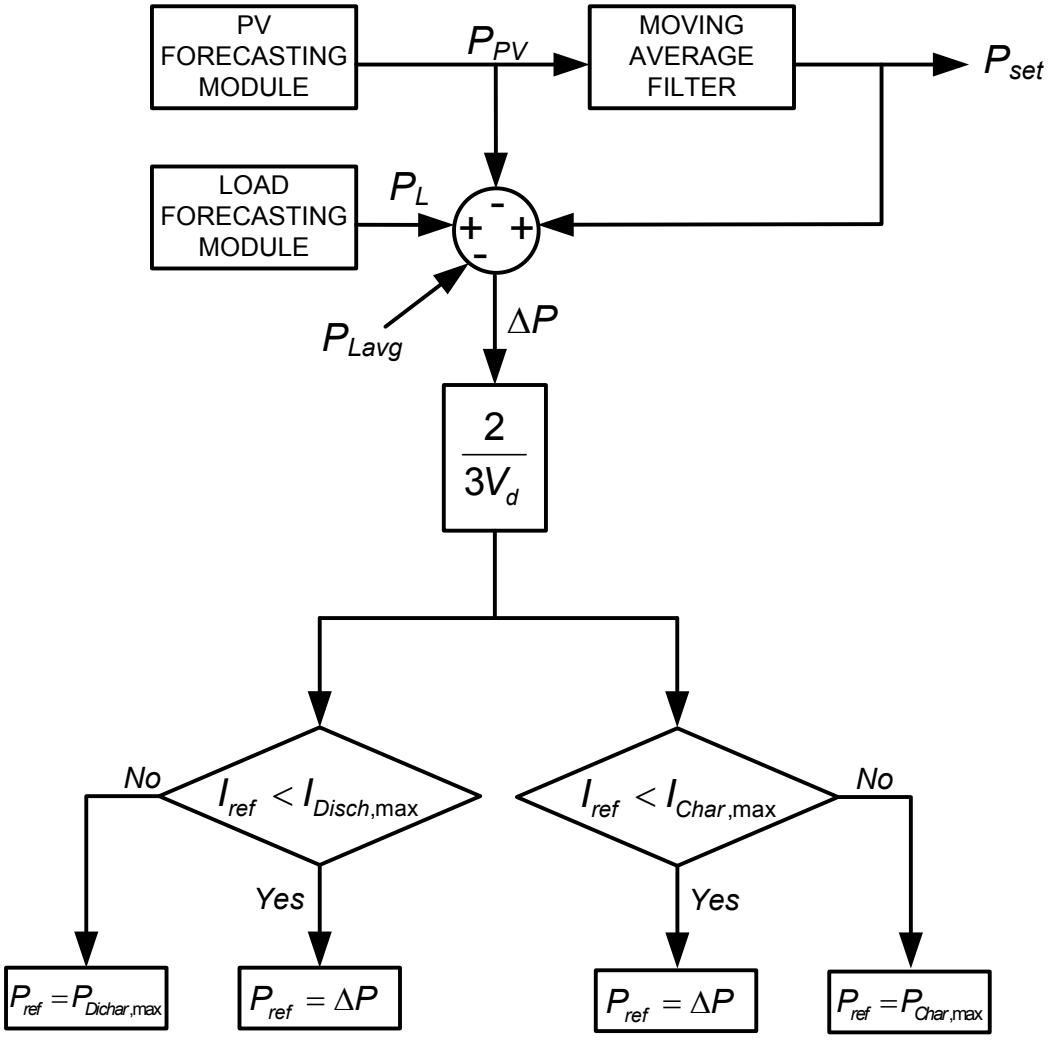

Figure 3. 10: Proposed battery charging/discharging current controller.

3.2.8.3. Proposed Battery Dynamic Model

Shepherd model (Moore & Eshani, 1996; Rekioua Pr, 2012) of lead-acid battery is used in this thesis. To improve this model, the initial state of charge (SOC_i) is substituted in the corresponding equations to accurately consider how the battery level of charge affects other parameters. The electrochemical behavior of battery is described in terms of current and voltage. This empirical model is often used incorporating with Peukert equation in order to obtain battery voltage and SOC as follow:

$$V_T = V_{oc} - R.i - K_i \frac{1}{SOC_i - DOD} \tag{3.18}$$

where V_T is the battery terminal voltage (in V), V_{oc} is the battery open-circuit voltage, R is the internal resistance (in ohm) given by:

$$R = R' + K_R \frac{1}{SOC_i - DOD} \tag{3.19}$$

where R' is residual resistance (ohm) calculated through:

$$R' = R_0 + K_R \tag{3.20}$$

K_R is electrolyte resistance at full charge and R_0 is initial battery resistance at full charge (both in ohm). i is the instantaneous battery current (in A). K_i is polarization coefficient, and DOD is depth of discharge given by:

$$DOD = \frac{1}{Q_{max}} \int idt \tag{3.21}$$

where Q_{max} is the maximum available capacity of the battery. SOC_i is initial state of charge which can vary between 0.3 and 0.9 while the simulation starts running. Instantaneous battery state of charge is formulated as:

$$SOC = \frac{Q_{ini} - Q_{used}}{Q_{max}} = SOC_i - DOD \tag{3.22}$$

where Q_{ini} is the initial available capacity of the battery and,

$$Q_{used} = \int idt \tag{3.23}$$

As shown in Figure 3.11, the equivalent circuit of battery has been implemented in PSCAD/EMTDC by a variable DC voltage source in series with a variable resistor. The amplitude of voltage source and resistor are determined through Eqs. (3.18) to (3.23).

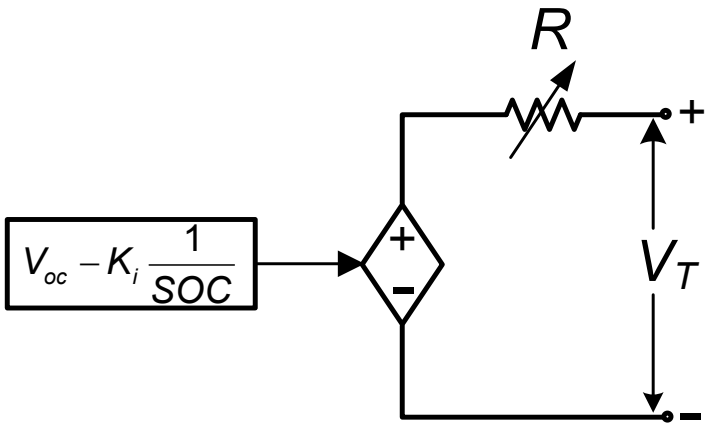

Figure 3. 11: Equivalent dynamic model of battery module.

Technical specifications of lead-acid battery module utilized to arrange the battery bank are given in Table 3.3. The lowest final voltage value for 5 minutes discharge is 9.6 V. To provide the voltage level of 912 V at the VSC DC link, 95 battery modules are estimated to be connected in series in each string (according to proposed battery sizing algorithm).

The maximum ramp rate considered for PVDG together with the load are supposed to be $\in [-300,350]\, kW/min$. Each battery string can supply up to 75Ah which means that the current can be drawn within 5 minutes would be 265.3 A and hence to supply 350 kW (384 A) power, two battery strings are adequate in discharge mode. On the other hand, the maximum allowed charge current is 22.5 A for each string and the BESS should be able to absorb 300 kW (329 A) in the matter of minutes.

To ensure that the charging current is within the boundary, 15 battery strings are allocated for this purpose. If the charge current is above 329 A, the proposed current control algorithm (see Figure 3.10) limits the smoothing reference to this value.

Table 3. 3: Technical specifications of 12 V battery module (RM12-75DC) (Remco Ltd., 2012).

Nominal Voltage	V_{oc}	12 V					
Nominal Capacity	C_{20} (Q_{max})	75 AH (20 Hours)					
Internal Resistance	R_0	≤4.8 mΩ (Fully charged battery)					
Polarization Coef	K_i	0.003					
Electrolyte Resistance	K_R	0.7 mΩ					
Units in series	N_s	1.0					
Units in parallel	N_p	1.0					
Max. Charge Current	$I_{ch,max}$	22.5 A					
Time (Mins) / Final Voltage		5	10	15	30	45	60
9.6 V	Ampere	265.3	188.2	148.5	92.6	67.9	53.3
	Watt	2501.6	1880.3	1518.7	925.2	698.6	579
10.02 V	Ampere	235.9	176.5	141.5	90	66.7	53
	Watt	2416.7	1822.3	1473.9	896.3	687.4	572.3
10.2 V	Ampere	216.6	167.4	137.3	88.2	66.1	52.4
	Watt	2271	1756.4	1426.3	881.5	675.9	564.5
10.5 V	Ampere	193.1	152	128.1	84	64	51.3
	Watt	2066.5	1620.4	1347.3	863.9	665.6	558
10.8 V	Ampere	174.9	136.4	116.6	77.9	61.6	49.7
	Watt	1820	1491.5	1242.3	836	647	547.8

3.2.8.4. BESS Control Mechanism

BESS controller is designed to operate in grid-connected mode. *P-Q* control mechanism is adopted which is a variety of current control of VSC. The references are generated by main agent in order to schedule the dispatchable DGs (BESS and diesel plant). BESS is responsible for smoothing out power oscillations due to the changes in solar irradiation and load.

A new dispatching index is formulated in this work which would be investigated in section 3.2. To employ the storage system efficiently, BESS must quickly respond within an acceptable duration. In this case, undesirable operation of load tap changers (LTCs) and capacitor banks, which can be due to the power fluctuations of PVDG and the load, is minimized and hence the AC network would not undergo the stress.

To ensure that the power is delivered into the microgrid with acceptable ramp rate, from the system operator view, BESS must quickly counteract to sudden changes in load demand and solar PV plant generation. Allowed ramp rate is normally mentioned in kilowatt per minute (kW/min) and is the common feature of solar power purchase agreement between the utility companies and power producers (Hill, Such, Dongmei, Gonzalez, & Grady, 2012).

Active and reactive power reference values for VSC of battery plant are determined by proposed power management system (PMS). These values are passed through the droop mechanism as P_0 and Q_0 which are droop active and reactive powers base points, respectively. Since the AC network is robust, the frequency and voltage are fixed in grid-connected (G.C) mode and thus PMS dispatching values (base points) are used to directly dispatch BESS. Other types of droop control scheme have been reported in the literature where all DGs are electronically dispatchable units (Hassan & Abido, 2011; Pogaku et al., 2007). Each distributed generation (DG) unit also generates its own frequency clock by itself through measuring the frequency and voltage at DG system point of connection (POC).

In power grids with high *X/R* ratio, the flow of active power predominantly depends on power angle and thus the frequency (De Brabandere et al., 2004). The flow of reactive power can be regulated by changing the voltage magnitude at POC.

Therefore, P and Q are controlled independently through frequency and voltage droop mechanisms, respectively, as:

$$P_{ref} = M_P(\omega_{POC} - \omega_0) + P_0 \tag{3.24}$$

where ω_0 is nominal grid angular frequency in p.u, ω_{POC} is the momentary angular frequency of voltage at POC in p.u, and M_P is active power droop coefficient as:

$$M_P = \frac{P_{max} - P_{min}}{\omega_{min} - \omega_{max}} \tag{3.25}$$

and P_0 (i.e. active power base point in p.u) is determined directly by system operator (main agent) or given by:

$$P_0 = \frac{P_{max} + P_{min}}{2} \tag{3.26}$$

In steady-state ($V_{err} = 0$), and thus:

$$Q_{ref} = M_Q(V_{POC} - V_0) + Q_0 \tag{3.27}$$

where V_0 is nominal grid voltage in p.u, V_{POC} is the instantaneous voltage sourced converter (VSC) voltage at point of connection (POC) in p.u, and M_Q is reactive power droop coefficient given by:

$$M_Q = \frac{Q_{max} - Q_{min}}{V_{min} - V_{max}} \tag{3.28}$$

and Q_0 is set-point (base point) for reactive power in p.u which is determined by power management system (PMS) or calculated as:

$$Q_0 = \frac{Q_{max} + Q_{min}}{2} \tag{3.29}$$

As shown in Figure 3.12 and 3.13, output of droop mechanisms sets the active and reactive power references for VSC outer power loops. The outer power loops would set current references for the inner current loops.

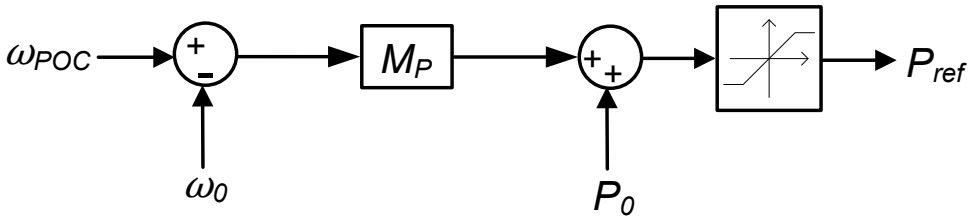

Figure 3. 12: BESS active power droop control module.

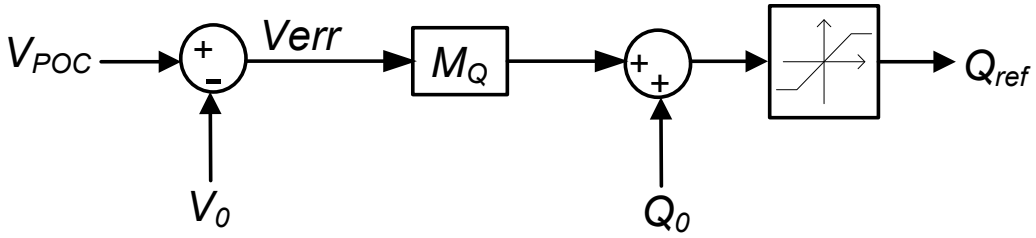

Figure 3. 13: BESS reactive power droop control module.

3.2.9. Diesel Generator Power Plant

3.2.9.1. Synchronous Generator Dynamic Model

Some typical models of diesel generator plant have been presented in (Bo, Youyi, & Yoke-Lin, 2000; Roy, Malik, & Hope, 1991a, 1991b). Diesel generator power plant is supposed to perform three tasks in the proposed microgrid. Firstly, it generates constant active power to shift down/up the grid active power profile or it shares the instantaneous load active power with the utility. Secondly, in the case that the grid is not able to charge the battery, diesel plant must do this task. Thirdly, the local load reactive power is assumed to be shared between BESS and diesel plant proportional to their ratings.

The diesel generator plant includes an internal combustion (IC) engine which drives a synchronous generator. Diesel prime mover should respond quickly to any changes in demand and thus reject the disturbances. In diesel power station, a 1.2 MW diesel IC engine, which is mechanically coupled with a 1.28 MVA ($\cos\varphi = 0.8$) synchronous generator, operates as the prime mover.

The model of IC engine which is available in PSCAD library is utilized for the simulation purpose. The IC engine model takes the mechanical speed of generator and the fuel intake as the inputs and gives the mechanical torque as the output. Input parameters of IC engine are set as given in Table 3.4.

Table 3. 4: IC engine model parameters ("ALTERNATORS LSA 50.1- 4 Pole Electrical and mechanical data," 2007).

Parameter	Value	Unit
Engine rating	1024	kW
Machine rating	1280	kVA
Engine rotating speed	1500	rpm
Number of cylinders	6	-
Number of engine cycles	Four strokes	-
Misfired cylinder	No	-

As shown in Figure 3.14, the output torque in any specific cranking angle is defined for the software as a torque map lookup table. Diesel engine is rated to be 17% larger than the synchronous generator capacity to keep the microgrid stable during the overload condition. Synchronous generator and IC engine are supposed to spin at the same speed of 1500 rpm and hence there is no need to exploit gear box.

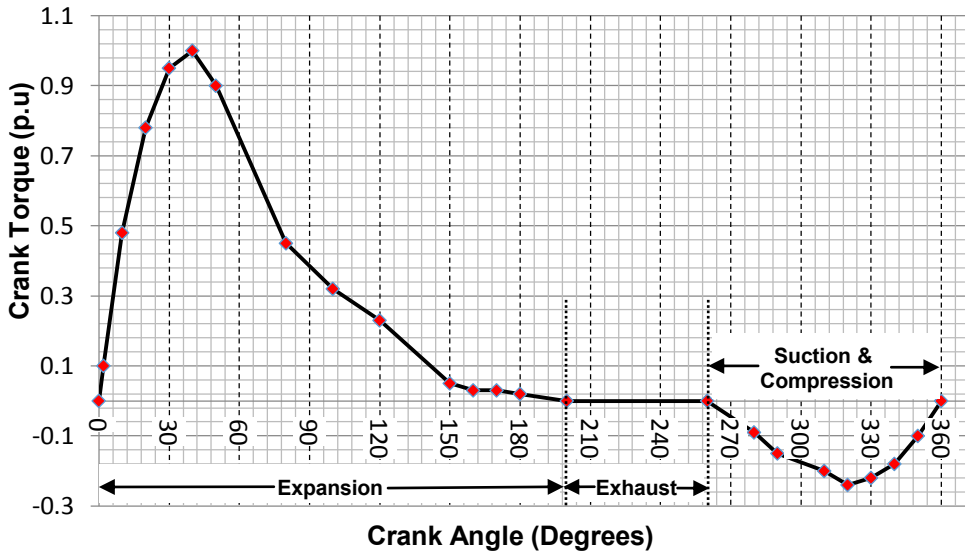

Figure 3. 14: Torque map diagram of IC engine.

The synchronous generator has 4 poles and produces 50 Hz sinusoidal voltage waveform. There is a direct and quadrature axes model for this component in PSCAD library (Stavrakakis & Kariniotakis, 1995) which is used to simulate the diesel plant. The generator parameters (see Table 3.5) are imported into the PSCAD software according to the manufacturer's datasheet.

Table 3. 5: Synchronous generator (LSA 50.1- 4P) model parameters.

Parameter	Value	Unit	Description
V_b	0.40	kV	Rated RMS line-to-line voltage
I_b	1.85	kA	Rated RMS line current
ω_b	314.16	rad/s	Base electrical angular frequency
H	1.0	s	Inertia constant (including flywheel and engine inertias)
T_a	0.041	s	Armature time constant
X_d	3.53	$p.u$	d-axis synchronous reactance
$X_d^{'}$	0.246	$p.u$	d-axis transient reactance
$X_d^{''}$	0.135	$p.u$	d-axis sub-transient reactance
X_q	2.12	$p.u$	q-axis synchronous reactance
$X_q^{''}$	0.169	$p.u$	q-axis sub-transient reactance
X_2	0.152	$p.u$	Negative sequence reactance
$T_d^{'}$	0.222	s	d-axis short-circuit transient time constant
$T_d^{''}$	0.02	s	d-axis sub-transient time constant
$T_{do}^{'}$	2.72	s	d-axis open-circuit time constant
$T_{do}^{''}$	0.043	s	d-axis sub-transient open-circuit time constant
$T_{qo}^{''}$	0.25	s	q-axis sub-transient open-circuit time constant

Some parameters of generator are not provided by the manufacturer and thus can be approximated as (Kundur, 1994; Sarma, 1997):

$$X_d \approx X_q \tag{3.30}$$

since the rotor of generator is non-salient,

$$T_{do}^{''} = \frac{X_d . T_d^{'} . T_d^{''}}{X_d^{''} . T_{do}^{'}} \tag{3.31}$$

$$X_q'' = 2X_2 - X_d'' \tag{3.32}$$

where X_2 is the negative sequence reactance, and

$$T_q'' \approx T_d'' \tag{3.33}$$

$$T_{qo}'' = \frac{X_q}{X_q''} \cdot T_q'' \tag{3.34}$$

The manufacturer datasheet provides the moment of inertia J in (kgm^2), however, the PSCAD needs inertia constant H in second(s) as a data entry given by:

$$H = \frac{\frac{1}{2} \cdot J \cdot \omega_m^2}{S_G} \tag{3.35}$$

where S_G is the generator rating base in MVA and,

$$\omega_m = \frac{2}{P} \cdot \omega_s \tag{3.36}$$

where P is the number of poles and ω_s is the synchronous angular frequency in *rad/sec.*

3.2.9.2. Proposed Controller for IC Engine Governor

A governor control mechanism is proposed in this work which enables the diesel generator to be dispatched by main agent through the droop mechanism set-point (or base point). Main agent calculates for the coefficient of power sharing with AC network and considers the diesel plant capability for this purpose. If the power sharing is not the issue, diesel plant is dispatched in fixed values.

The governor of IC engine is to regulate for the fuel intake and thus the engine rotating torque. As shown in Figure 3.15, there are two time constants in the proposed governor model. The first one (T_1) is the time required for the actuator to move and replace in a new position and is modeled by a first-order lag compensator. Another time constant is the dead-time (T_2) taken for all the cylinders to receive the fuel since they are not in a

similar position at a moment. A hard limiter is also added to ensure that the fuel intake is not negative and there is an upper limit for the fuel intake that corresponds to the maximum generation capacity. The values set for the parameters of IC engine governor model are given in Table 3.6.

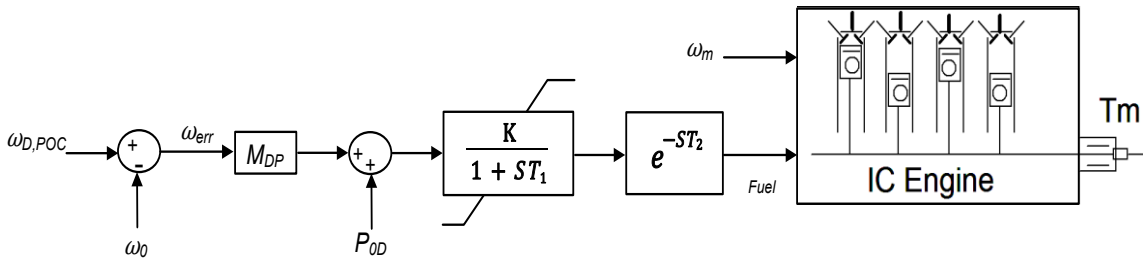

Figure 3. 15: Diesel plant governor model and suggested active power droop controller.

Table 3. 6: IC engine governor controller parameters (Bo, Youyi, & Yoke Lin, 2000).

Parameter	Value	Unit	Description
T_1	0.05	s	Time constant of actuator
T_2	0.02	s	Engine dead-time
K	1.0	p.u	Actuator gain

Active power droop coefficient (M_{PD}) of IC engine governor is given by:

$$M_{DP} = \frac{P_{max,D} - P_{min,D}}{\omega_{min} - \omega_{max}} \tag{3.37}$$

where $P_{max,D}$ and $P_{min,D}$ are the maximum and minimum of active power generation capability of diesel generator plant in p.u, respectively. In steady-state mode, when the frequency is restored to its nominal value, the momentary angular frequency of diesel generator ($\omega_{D,POC}$), measured at POC in p.u, would be equal to synchronous angular frequency (ω_s) and thus ω_{err} becomes zero.

Active power set-point of plant (P_{0D}) in p.u can be set by main agent in grid-connected (G.C) mode or obtained through:

$$P_{0D} = \frac{P_{max,D} + P_{min,D}}{2} \tag{3.38}$$

3.2.9.3. Proposed Generator Field Current Controller

Excitation system is composed of a voltage compensator together with a field exciter. The operational characteristics of excitation system have been described in (ANDERSON & FOUAD, 2002; Kundur, 1994) in detail.

IEEE has developed standard mathematical transfer functions for available commercial excitation systems for software modeling purposes ("IEEE Recommended Practice for Excitation System Models for Power System Stability Studies," 2006). The exciter AC5A model is utilized in this work and its transfer function is illustrated in Figure 3.16. All the variables definitions together with their values are given in Table 3.7. AC5A model has been already implemented in PSCAD library. Parametric default values, which are chosen in this work, confirm the proper response of exciter.

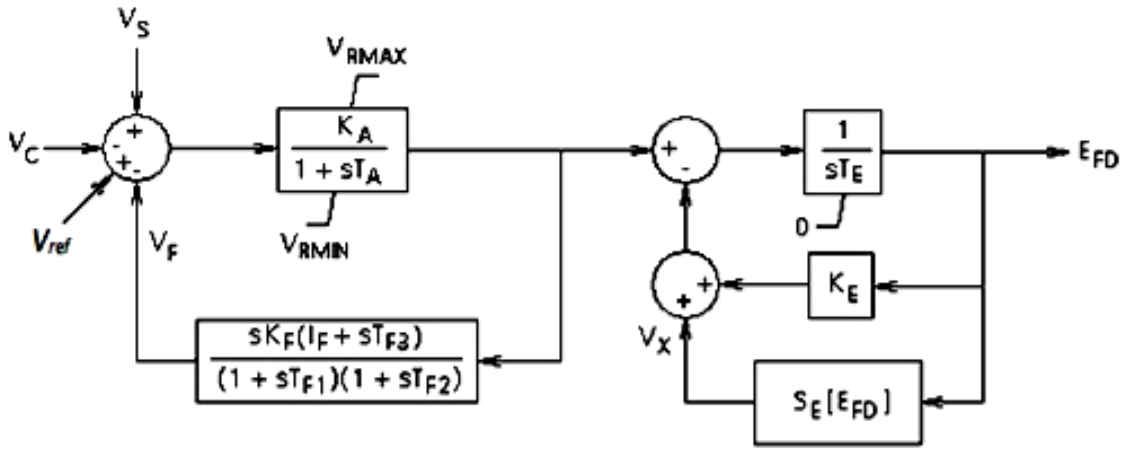

Figure 3. 16: AC5A excitation controller transfer function ("IEEE Recommended Practice for Excitation System Models for Power System Stability Studies," 2006).

Table 3. 7: Synchronous generator excitation controller parameters.

Parameter	Value	Unit	Description
T_E	0.8	s	Exciter time constant
T_A	0.02	s	Regulator amplifier time constant
T_{F1}, T_{F2}, T_{F3}	1.0, 0, 0	s	Regulator stabilizing circuit time constant
K_A	400	p.u	Regulator gain
K_E	1.0	p.u	Exciter constant related to self-excited field
K_F	0.03	p.u	Regulator stabilizing circuit gain
$S_E(E_{FD1})$	0.86	p.u	Saturation at E_{FD1}
$S_E(E_{FD2})$	0.5	p.u	Saturation at E_{FD2}
E_{FD1}	5.6	p.u	Excitation voltage for S_{E1}
E_{FD2}	4.2	p.u	Excitation voltage for S_{E2}
V_{RMIN}	-7.3	p.u	Minimum regulator output
V_{RMAX}	7.3	p.u	Maximum regulator output

To set for V_{ref} and prevent the circulation of reactive current between the DGs, a reactive power versus V_{ref} droop mechanism is proposed to be added to the excitation controller. This control loop is also responsible for sharing the load reactive power between the BESS and diesel plant. As shown in Figure 3.17, the V_{ref} can be set for grid-connected mode and operator commands the reactive power set-point (to share the local reactive power demand).

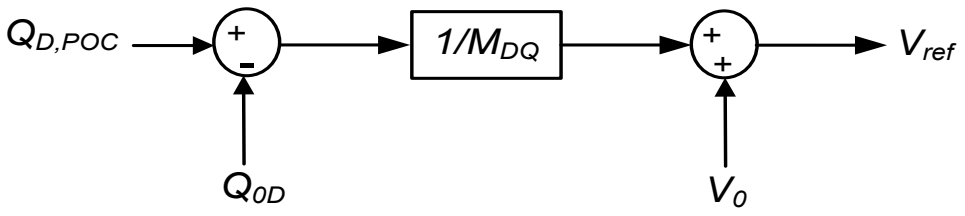

Figure 3. 17: Proposed reactive power droop controller for synchronous generator.

where $Q_{D,POC}$ is the instantaneous reactive power output of synchronous generator in p.u, Q_{0D} is the reactive power set-point (base point) in p.u given by:

$$Q_{0D} = \frac{Q_{max,D} + Q_{min,D}}{2} \tag{3.39}$$

where $Q_{max,D}$ and $Q_{min,D}$ are the maximum and minimum of reactive power generation capability of diesel generator plant, respectively. M_{DQ} is the reactive power droop coefficient and is given by:

$$M_{DQ} = \frac{Q_{max,D} - Q_{min,D}}{V_{min} - V_{max}} \tag{3.40}$$

where V_{min} and V_{max} are the allowed boundary of variation (±5%) for V_{ref} in p.u.

3.2.10. Designed Variable Load Model

To ensure the stability of a power network, the generation of power should be closely matched with its consumption. In this case, the load dynamic behavior is very important and has to be considered in power grid modeling and evaluating stages. Several kinds of load model have been introduced by (Kundur, 1994) e.g. constant power (P), constant current (I), and constant impedance (Z) loads. Modeling of load is not a straightforward task because so many factors are involved such as time, meteorological constrains, and economy status. For example, in tropical countries with humid and hot climate, the people mostly use air cooling systems and thus the load nature differs from those countries where there exist four season in a year.

The load demand pattern can also vary season by season. In countries with four seasons the load nature also changes from one season to another (seasonal load). People use heating apparatuses in the winter (resistive load) whereas they use cooling system in the summer (motor load). Time of use (ToU) is also another important factor which can affect the load profile in a country. For instance, in the morning the power demand peaks for some hours because the people wake up and do their routines. Then, people go to work and the demand drops. In evening when they back home, the load demand peaks again.

There exist two load categories, in this work, i.e. industrial and residential loads. As shown in Figure 3.18, each consists of three similar feeders and hence there are totally six load feeders. The load model contains two portions. The first portion includes the base load and the second part represents as the alternating load. This microgrid totally supplies 260 kVA domestic base load ($\cos\varphi = 0.963$) and 357 kVA industrial base load ($\cos\varphi = 0.98$), respectively. Second portion of domestic load varies between 85 and 260 kVA ($0.9 \leq \cos\varphi \leq 0.96$). Variable part of industrial load varies between 95 and 175 kVA ($0.8 \leq \cos\varphi \leq 0.9$). Base load has been implemented by static load model and the variable load modeled using the dynamic definition suggested in section 3.2.10.2.

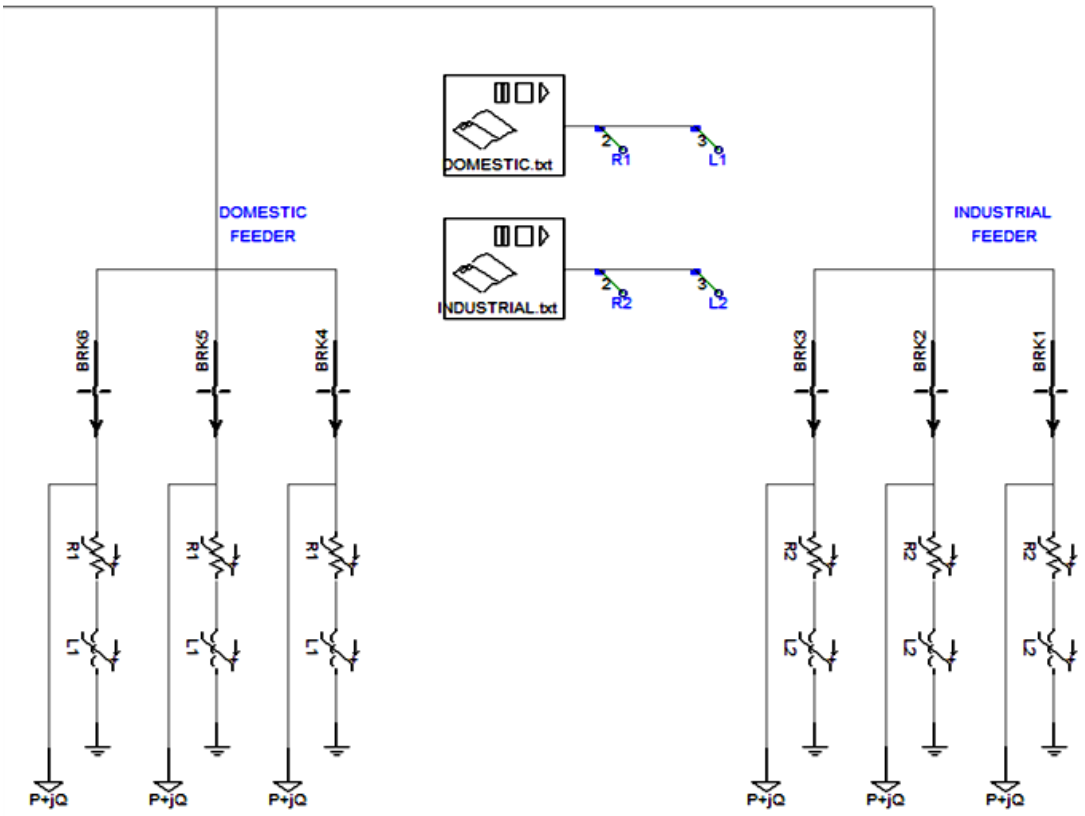

Figure 3. 18: Designed load model which is simulated in PSCAD/EMTDC software.

3.2.10.1. Static Load Portion

Base load is modeled by algebraic functions in which the instantaneous voltage and frequency are independent variables as:

$$P = P_0 \cdot \left(\frac{V}{V_0}\right)^a \cdot (1 + K_{PF} \cdot df) \tag{3.41}$$

$$Q = Q_0 \cdot \left(\frac{V}{V_0}\right)^b \cdot \left(1 + K_{QF} \cdot df\right) \tag{3.42}$$

where a and b are equal to the voltage indices for active and reactive powers, respectively. These two parameters are set to be zero. K_{PF} and K_{QF} are the frequency indices for active and reactive powers, respectively, and are considered to be zero.

The zero value of parameters assures that the base load is constant power load and thus is independent from voltage and frequency variations.

3.2.10.2. Dynamic Load Portion

This portion is simulated through the variable inductance *L* in series with variable resistance *R* and this branch is connected to the ground in parallel with the base load. *R* and *L* values have to be altered during (considering forecasted load profiles) the simulation to represent the variable portion of the load. Since the actual load profile is available, by deducting the base load whatever remains would be the dynamic portion. Given the values of load active (P) and reactive (Q) powers, *R* and *L* values can be calculated as:

$$G(Mho) = \frac{P}{V^2} \tag{3.43}$$

$$B(Siemens) = \frac{Q}{V^2} \tag{3.44}$$

where G and B are the load conductance and susceptance, respectively. V is the nominal RMS line voltage and thus,

$$R(\Omega) = \frac{G}{Y^2} \tag{3.45}$$

$$L(H) = \frac{B}{Y^2 \cdot \omega_s} \tag{3.46}$$

where ω_s is synchronous angular frequency and Y is the load admittance given by:

$$Y^2(ohm^{-2}) = \sqrt{G^2 + B^2} \tag{3.47}$$

3.3. Data Inputs

Power system behavior is inherently unpredictable. Generation, transmission, and load demand all have a degree of uncertainty. To keep power system stable and cost effective, grid codes and regulations have been mandated by the utilities and regulatory authorities over the last decades ("IEEE Application Guide for IEEE Std 1547, IEEE Standard for Interconnecting Distributed Resources with Electric Power Systems," 2009; "IEEE Recommended Practice for Utility Interface of Photovoltaic (PV) Systems," 2000). From the system planning and operation perspectives, load scheduling, forecasting, and economic dispatching are those kinds of remedies to cope with the variable nature of power system. In this case, planners and operators attain a prior knowledge, from their databases, about the system uncertainties. Hence, they can propose their most efficient and cheapest solutions for this purpose.

Load and generation forecasting are both beyond the scope of this research. However, to examine the impacts of load and generation variations on dynamics of system, it is necessary to collect the real load, solar PV irradiation, and temperature data. In here, the solar irradiation and the daily load profiles are assumed to be forecasted by a data centre

or a forecasting module (embedded in unit and load agents) one day in advance. This information, after some logical manipulation, is used as inputs for PSCAD software.

3.3.1. Solar Irradiation Profile

A typical location in Malaysia in the city of Kuala Lumpur with latitude of $3^{\circ}, 7'N$ and longitude of $101^{\circ}, 39'E$ is chosen (Kamali & Mekhilef, 2009; KoohiKamali et al., 2010) as the sampling point. The solar radiation pattern is extracted through the HOMER software which is a Micropower optimization model developed and supported by Homer Energy LLC. This software is able to estimate the average hourly irradiation profile using the method suggested by (Graham & Hollands, 1990). HOMER creates a set of 8,760 solar radiation values for each hour of the year.

On the other hand, to study the dynamic behavior of microgrid in presence of PVDG plant, solar irradiation profile is needed with higher precision than the hourly data (F. Katiraei et al., 2011). For example, to see the power flow changes, in the system, followed by PVDG unit output power variation (ramp rate) within 5 minutes, the solar irradiation profile should be sampled in every 5 minutes during a day. In this case, the BESS is sized so that it can absorb or supply the power difference between P_{set} and P_{pv} (together with that part of smoothing index related to the load) during the period PVDG ramps up or down, respectively.

Solar PV plant generates power in an unpredictable manner. This fact can be considered as the result of cloudy sky, in worst condition, or rising and setting of the sun during the day which causes 10% to 13% variation in PV plant output power.

The abrupt changes in generated power are the main concerns for the system planners and operators. A passing cloud can lead to more than 60% change in PVDG output in a matter of seconds (Mills et al., 2011). Figure 3.19 shows the average solar irradiation (G) profile for a typical day on May approximated at the coordinates of sampling. To

prevent the curves against overlapping the noise minus is shown in this figure. Twenty four hourly irradiation values are interpolated to obtain 288 values and redraw the solar pattern for every 5 minutes during a day.

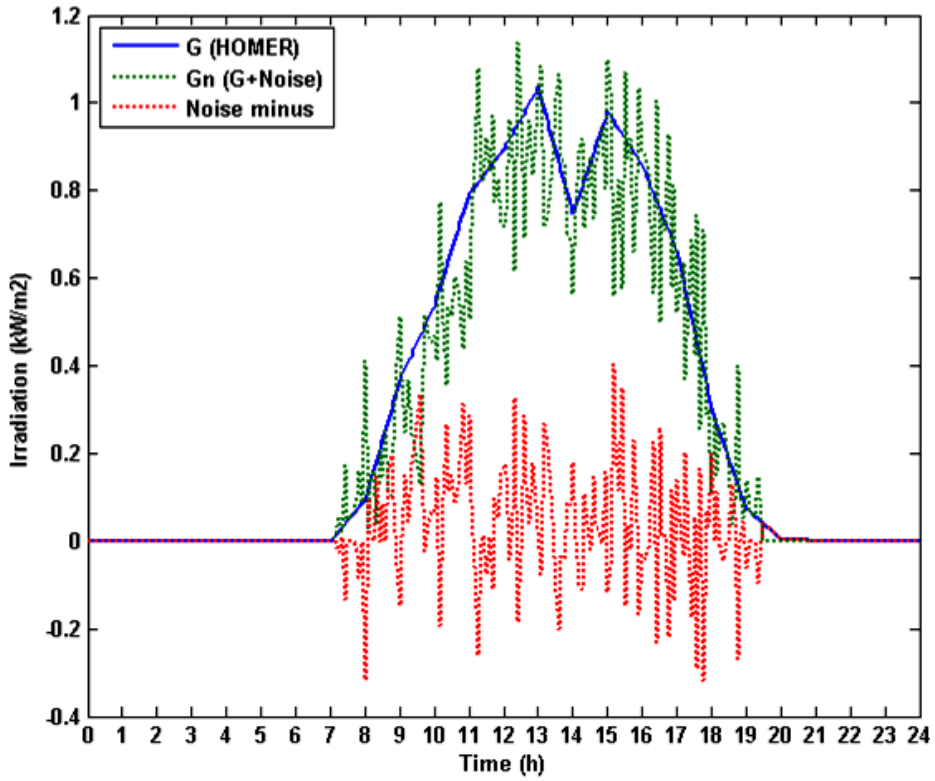

Figure 3. 19: Forecasted solar irradiation profile by HOMER in sampling location in Peninsular Malaysia on May and the noise applied on.

To investigate the ramp rate effects on the network, a normal distributed random noise with 0 mean and standard deviation 1 is applied on the averaged solar profile. Hence, the noisy signal G_n which is finally estimated through the MATLAB module is utilized as the input of PV plant model given by:

$$G_n = G + \left[randn\big(size(G)\big) - 0.5\right] \times 0.15 \tag{3.48}$$

where G is a $(m \times n)$ array in which $m = 288$ and $n = 1$, respectively.

3.3.2. Operating Temperature Profile

To study the impacts of variation in temperature on photovoltaic distributed generation (PVDG) plant output power, the temperature profile of sampling location is collected from Malaysia Meteorological Department (MMD). The input of PV generator accepts the cell operating temperature given by (Tsai, 2010):

$$T_{cell} = T_{Amb} + \left(\frac{T_{NOCT} - 20}{0.8}\right) \cdot G_n \tag{3.49}$$

where T_{Amb} is the ambient temperature shown in Figure 3.20 and T_{NOCT} is nominal cell operating temperature available in manufacturer's datasheet (46˚C). T_{cell} profile was estimated (in Celsius) during the day of sampling and exploited as solar PV generator model data input in PSCAD/EMTDC software.

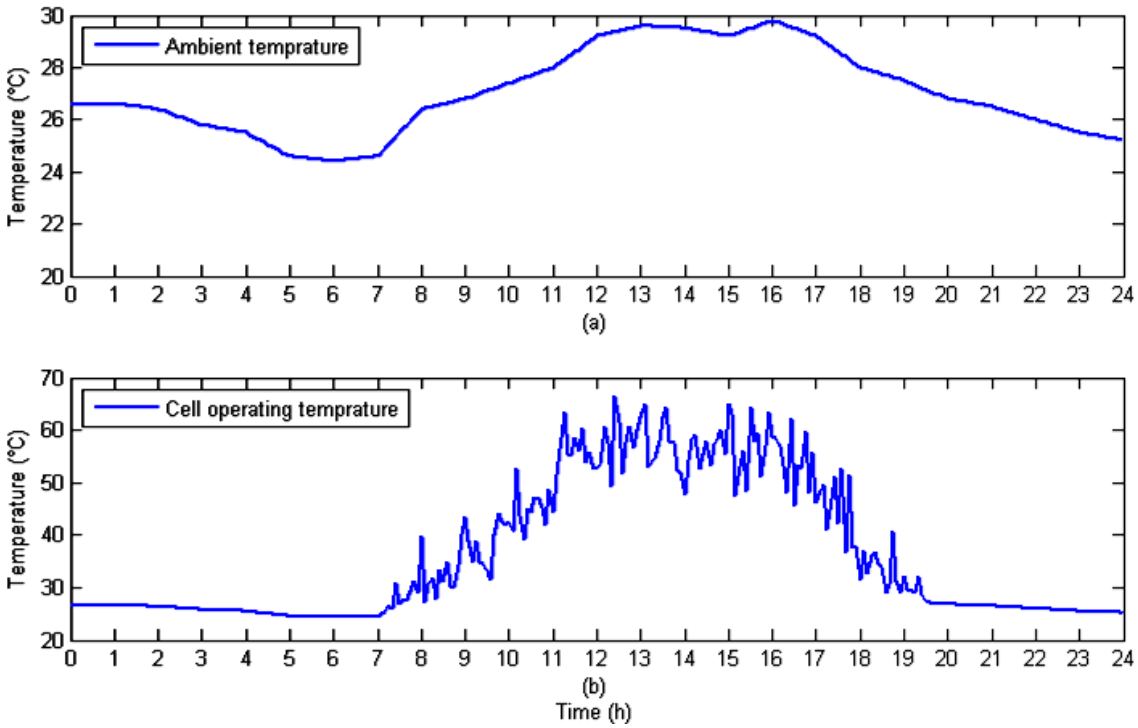

Figure 3. 20: Temperature profiles (a) Malaysia ambient temperature. (b) Cell operating temperature.

3.3.3. Load Data

The load characteristic is one of the main factors in power system modeling for dynamic stability and transient studies. Similar to the stochastic generation, load also varies during the day. In some hours in a day the load profile is in its maximum value when the utility charges the customer for highest prices. The changes of load also generate power mismatch between the generation and consumption.

System power quality can be highly affected if distributed energy resources (DERs) also generate intermittent power and the main grid is weak. In this case, the flow of power in the system undergoes too many undesirable oscillations. In this thesis, two kinds of customer i.e. the residential and industrial are investigated. The former is considered to be non-vital load. The industrial processes are classified as vital loads since any power disruption is not acceptable in terms of economic and safety issues. The load profile associated with each category was collected from Tenaga National Berhad (TNB) office of sampling distribution in Malaysia. As shown in Figure 3.21, the industrial load profile is almost constant since the industrial processes are often consistent while the domestic load varies during the day.

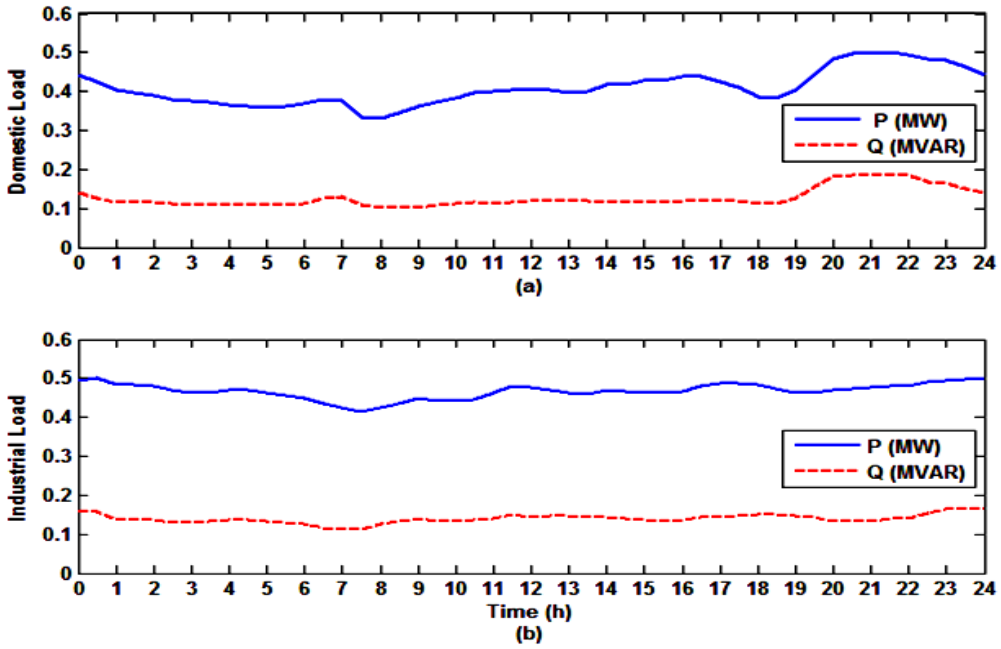

Figure 3. 21: Distribution network load profile in Malaysia.

3.4. Proposed Power Management System (PMS)

A coordinated power management algorithm (PMA) is proposed in this work (see APPENDIX A). Network operator as the highest level of hierarchy in PMS decides to run PMA and schedules the dispatchable distributed energy resources (DERs). PMA only considers technical issues (i.e. battery state of charge, power capabilities of plant, and ramp rate limits) to schedule DERs and economic issues are not taken into account. The most important PMA objective is to minimize the stresses on the AC network due to solar PV plant ramp ups/downs and load fluctuations.

In addition, BESS and diesel plant are supposed to share the local reactive power demand proportional to their ratings. Diesel can also share the local active power demand with AC network as in Eq. 3.50 or it can supply a constant active power to shift up/down the grid active power profile.

$$P'_{0D} = \begin{cases} \beta P_L & P_{D,min} \le P'_{0D} \le P_{D,max} \\ P_{0D} & otherwise \end{cases} \tag{3.50}$$

where P'_{0D} is dispatching reference of diesel plant. β is the active power sharing coefficient determined by the system operator provided that the share allocated to diesel in within its power capability boundary. P_{0D} is the droop controller (or characteristic) set-point (base point) at nominal frequency (50 Hz). $P_{D,min}$ and $P_{D,max}$ denote the minimum and maximum power capabilities of diesel plant, respectively. The instantaneous power mismatch between the local generation and load would be compensated by the grid.

Main agent receives all the field information from lower stream agents (generation and load agents) and saves them in the PMS database. Data pointed out in here can be battery *SOC*, photovoltaic plant power production status, breakers states, DERs apparent power outputs, DERs power capabilities, and forecasting signals.

The integration of DER should not put stress on the main grid components. In this microgrid, since the demand and generation are both variable, efficient smoothing indices are proposed to smooth out the active and reactive power oscillations caused by solar PV plant generation and load demand together. Photovoltaic distributed generation (PVDG) unit is supposed to operate in unity power factor and hence it only contributes in the active power ramp ups/downs. In the case of load, both active and reactive powers change according to load profiles. To smooth out the active power oscillation during the time when the PVDG generation is down (night time), diesel and grid contribute to supply the load demand. *SOC* of battery plant is controlled instantaneously to ensure that BESS operates within its power capability limits as:

$$SOC_{min} \leq SOC \leq SOC_{max} \tag{3.51}$$

Diesel can operate in its capacity at nominal frequency which can be determined by the PMS unit (P_{0D}) or dispatched up to its maximum generation capacity by operator (βP_L). It can be used to charge the battery up to SOC_{ref} which is 60% in here. The reference *SOC* is determined by the operator which has the previous knowledge about the load and PV active power profiles. If SOC_{ref} is properly selected, by end of the day, the battery can be recharged up to SOC_{ref} (if needed) by diesel or grid depending on the operator's decision.

3.4.1. Active Power Smoothing Index (APSI)

During the daytime, as long as the *SOC* battery is within the operational boundary, battery energy storage system (BESS) is controlled in *P*-*Q* mode and thus active power reference is equal to smoothing index calculated by the main agent as:

$$\Delta P = \left(P_L - P_{Lavg}\right) + \left(P_{set} - P_{PV}\right) \tag{3.52}$$

where ΔP is smoothing index in MW, P_L is the instantaneous load estimated by the load agent in MW, P_{Lavg} is the active power load profile mean value in MW given by:

$$P_{Lavg} = \frac{P_{L,max} + P_{L,min}}{2} \tag{3.53}$$

where

$$P_{L,min} = P_{inds,min} + P_{doms,min} \tag{3.54}$$

$$P_{L,max} = P_{inds,max} + P_{doms,max} \tag{3.55}$$

where $P_{inds,min}$ and $P_{doms,max}$ denote the minimum industrial active load and maximum domestic active load, respectively. P_{PV} is PVDG output active power which is calculated by solar PV plant unit agent and is sent to main agent through generation agent. P_{set} is the moving average value of PVDG output power in MW. Embedded moving average module in main agent receives the noisy P_{PV} profile one day ahead and thus P_{set} is generated through this module. Taking into account that P_{Lavg} is $872\ kW$ and $P_L \in [787,1000]\ kW$ and thus first term in (3.52) would be member of $[85,128]\ kW$. If the boundary of changes for second term in (3.52) is between 215 and $222\ kW$ (see Figure 3.22), the smoothing index would be member of $[-300,350]\ kW$.

3.4.2. Reactive Power Smoothing Index (RPSI)

To supply the microgrid reactive power, Q_{0D} of synchronous generator excitation controller, and Q_{ref} of BESS are both set through the commands issued by network operator through the main agent. A constant smoothed share of reactive power (Q_{Lavg}) is supposed to be supplied by the power grid. In this case, the load reactive power fluctuations about Q_{Lavg} is minimized by BESS and diesel plant as:

$$Q_{Lavg} = \frac{Q_{L,max} + Q_{L,min}}{2} \tag{3.56}$$

where

$$Q_{L,min} = Q_{inds,min} + Q_{doms,min} \tag{3.57}$$

$$Q_{L,max} = Q_{inds,max} + Q_{doms,max} \tag{3.58}$$

where $Q_{inds,min}$ and $Q_{doms,max}$ denote the minimum industrial reactive load and maximum domestic reactive load, respectively. In another case, if the operator decides to supply the whole reactive power locally, Q_{Lavg} is set to zero and hence BESS together with diesel plant share the local load demand.

Reactive power smoothing difference (ΔQ) should be shared between BESS and diesel generator proportional to their ratings. In this case, the set-point (base point) reference values can be calculated as:

$$[Q_{0B} \quad Q_{0D}]^T = [\Delta Q]\begin{bmatrix} \dfrac{1}{1 + 1/\alpha} \\ \dfrac{1}{1+\alpha} \end{bmatrix} \tag{3.59}$$

where α is droop coefficient given by:

$$\alpha = \frac{S_{BESS}}{S_{Diesel}} \tag{3.60}$$

and,

$$\Delta Q = Q_L - Q_{Lavg} \tag{3.61}$$

where S_{BESS}, S_{Diesel} are the MVA ratings of BESS and diesel plant, respectively.

3.4.3. Application of Moving Average Filtering (MAF)

Moving average method is often used to remove the random noise content of a signal and is the best offer for time domain encoded signals. Principle of operation is to get average from a number of input signal points and hence to reproduce each point in the output signal as (Steven, 1997):

$$Y[i] = F_k \sum_{j=-(n_p-1)/2}^{(n_p-1)/2} X[i+j] \tag{3.62}$$

where X and Y are the input (P_{PV}) and output (P_{set}) vectors, respectively. n_p is the number of points used in the moving average filter. Eq. 3.62 represents double-sided averaging which is so-called "symmetrical averaging". Symmetrical averaging requires n_p as an odd number. Moving average is a convolution of input signal with a rectangular unity area pulse which exploits filter kernel (F_k) given by:

$$F_k = \frac{1}{n_p} \tag{3.63}$$

As shown in Figure 3.22, along with the increase in number of points in moving average filter, the level of noise decreases. If 5-point or 11-point moving average filters are used, the average waveform (in blue color) after filtering is still noisy that imposes power oscillations on AC network. The number of points has to be increased until the average waveform becomes quite smoothed. In this work, 21-point moving average filter is exploited to smooth out the noisy signal (P_{PV}) and generate P_{set} because the level of smoothness in average waveform is satisfactory.

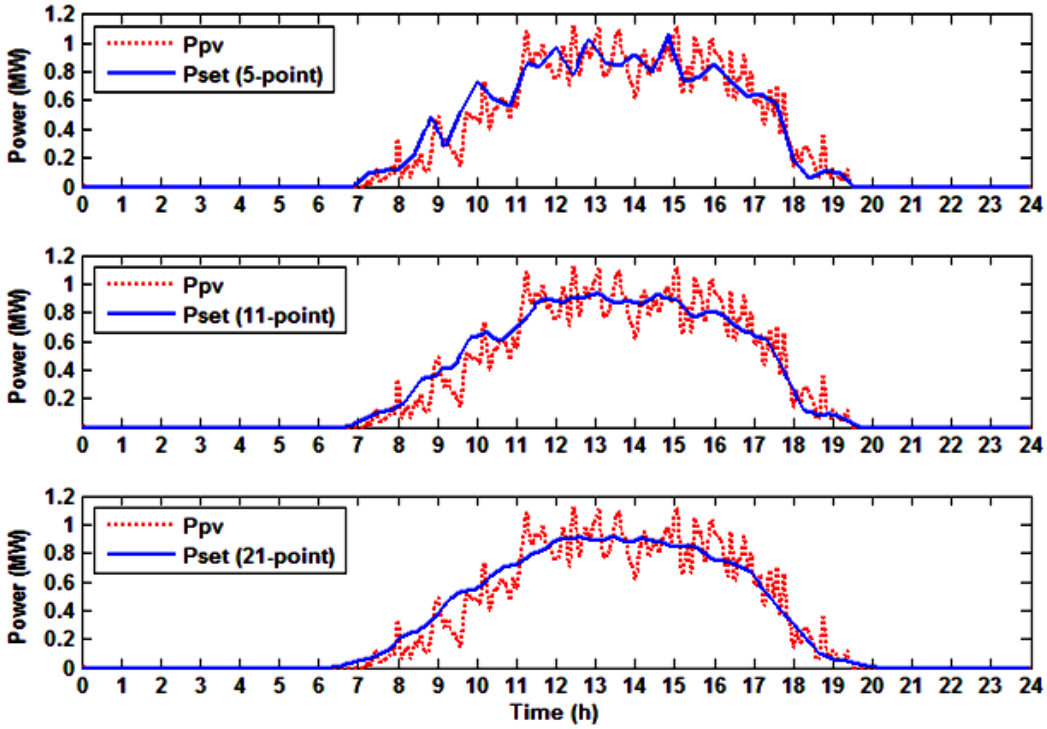

Figure 3. 22: Generation of PV average reference using moving average filter.

3.4.4. Battery Energy Storage System (BESS) Operating Zones

Battery storage plant can be either source or sink of active and reactive powers. The smoothing indices which were formulated in previous sections (3.4.1 and 3.4.2) are exploited to schedule BESS and diesel generator plant. Positivity of active power smoothing index (APSI) reflects the lack of active power that should be supplied by BESS to fill up the dip of AC network active power profile. Negativity of APSI ($\Delta P < 0$) reflects the surplus active power (ΔP) that should be absorbed by BESS to shave the peaks of AC network active power profile. Likewise, positivity of reactive power smoothing index (RPSI) indicates that there is a peak (with respect to Q_{Lavg}) in reactive power profile of AC network (Q_{Lavg}). This peak should be shaved by BESS and diesel plant (through reactive power supplying) as discussed in 3.4.2. Negativity of RPSI ($\Delta Q < 0$) confirms the presence of a dip in reactive power profile of AC network that have to be filled up by BESS and diesel plant through reactive power absorbing or generating.

In this case, five operating zones are defined for BESS as follows:

(a) $\Delta P > 0$ and $\Delta Q < 0$ thus BESS delivers active power (discharge mode) and absorbs reactive power;

(b) $\Delta P < 0$ and $\Delta Q < 0$ thus BESS absorbs both active (charge mode) and reactive powers;

(c) $\Delta P > 0$ and $\Delta Q > 0$ thus BESS delivers both active (discharge mode) and reactive powers;

(d) $\Delta P < 0$ and $\Delta Q > 0$ thus BESS absorbs active power (charge mode) and delivers reactive power;

(e) Standby (idle) mode in which no active power is supplied or received but reactive power still can be exchanged.

3.4.5. Proposed Power Management Algorithm (PMA)

Power management system (PMS) is able to handle the smart microgrid based on the solar radiation level together with BESS and diesel plant technical constrains. Battery storage plant can be safely charged or discharge when needed as well as it can share reactive power with diesel plant at the same time.

PMS also makes it possible for the network operator to determine the active and reactive power portions supplied by each generation unit. The flowchart of proposed power management algorithm is shown in Figure 3.23. In this case, the stepwise operation of power management system to run PMA (including three modules) is described in the next sections.

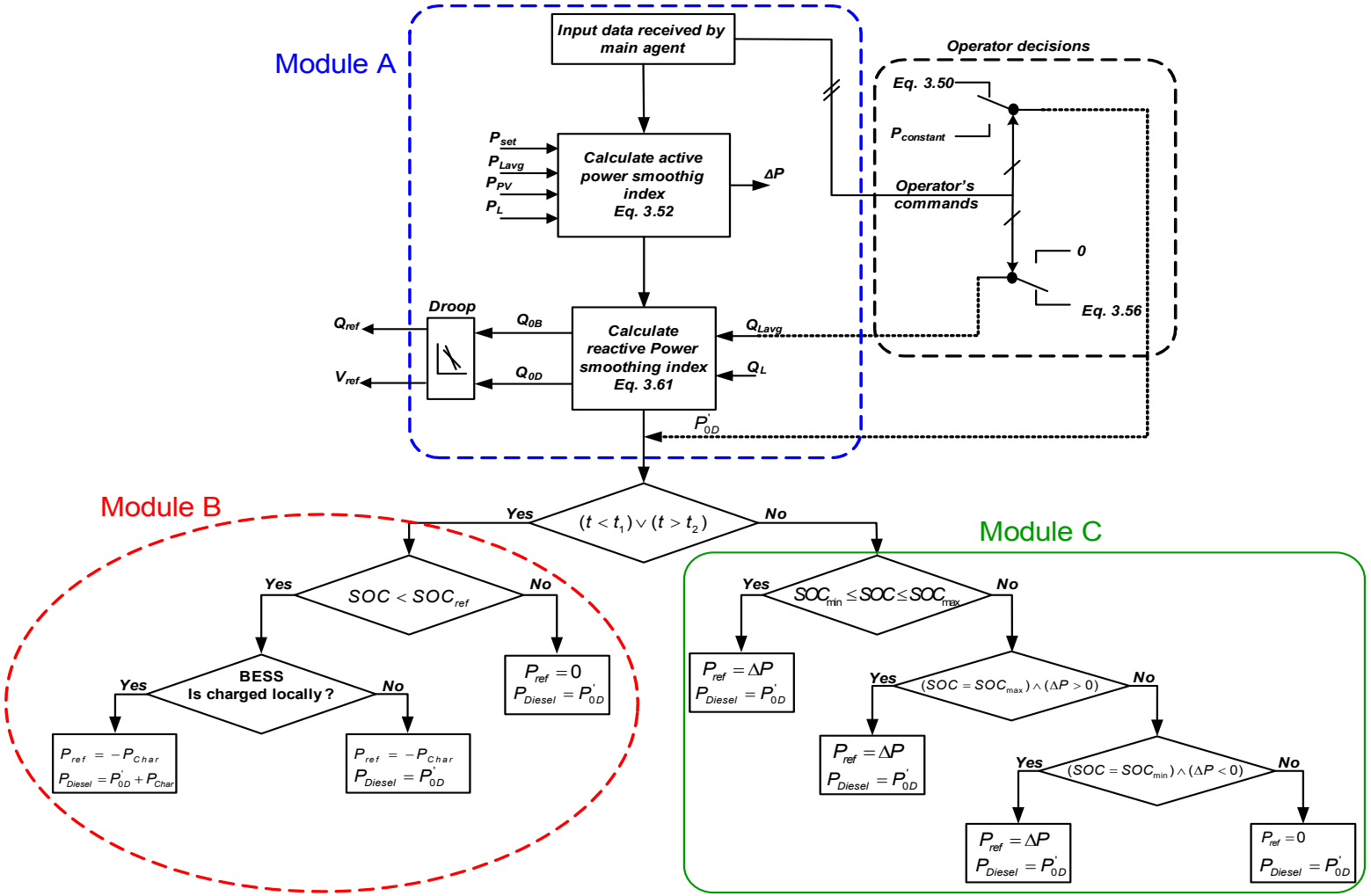

Figure 3. 23: Proposed power management algorithm for smart microgrid.

3.4.5.1. Module A

This module can be so-called operator decision making module. Data collected from the generation agent, load agent, and unit agent is recorded in the main agent. Main agent processes the signals which are listed in the following as:

(a) P_{PV} received from generation forecasting module;

(b) P_{Lavg} calculated by system operator through Eq. 3.53;

(c) P_{set} obtained using moving average filter (section 3.4.3);

(d) P_L received from load agent;

(e) Q_{Lavg} calculated by system operator through Eq. 3.56;

(f) SOC received from battery plant unit agent;

(g) Positions of load and DG units breakers.

Main agent calculates for active and reactive powers smoothing indices (ΔP and ΔQ) according to equations 3.62 and 3.61, respectively. Network operator can also decide to supply the load locally (by diesel and AC network) or remotely (by AC network).

To supply the load locally, P_{0D} and Q_{Lavg} are set (by network operator) through Eq. 3.50 and to zero, respectively. Thus, the net active power difference ($P_L - \beta P_L - P_{set}$) between the smoothed active power generated by solar plant and remaining load active power ($P_L - \beta P_L$) is compensated by AC network.

To supply the load remotely, diesel plant can be scheduled to supply a constant amount of active power which is normally minimum generation assigned to a power plant ($P'_{0D} = P_{constant}$). The AC network supplies or absorbs the remaining real-time difference between the load active power and smoothed active power generated by solar plant. In the case of reactive power, AC network supplies a constant amount of reactive power (Q_{Lavg}) and the reactive power smoothing index (ΔQ) is shared between battery and diesel plant proportionally.

At all times, operator sets the values of $Q_{0B}$and Q_{0D} through Eq. 3.59 and hence the reactive power references are set for BESS and diesel through Q_{ref} and V_{ref}, respectively.

3.4.5.2. Module B

From evening to morning when the solar radiation is low, the local load is supplied by the grid and diesel plant. If battery SOC is less than SOC_{ref}, depending on operator decision, it has to be charged up to the level of SOC_{ref} by diesel plant (locally) as:

$$P_{Diesel} = P'_{0D} - P_{ref} \tag{3.64}$$

where P'_{0D} is obtained through Eq. 3.50 in Module A. P_{ref} is the dispatching reference of battery storage plant in MW given by:

$$P_{ref} = -P_{Char} \tag{3.65}$$

where P_{Char} is dispatching reference of battery plant in charging mode in MW during the darkness when it does not smooth out the power fluctuations.

In the next scenario, to charge the battery plant remotely by AC network, diesel plant dispatching reference is given by:

$$P_{Diesel} = P'_{0D} \tag{3.66}$$

and P_{ref} remains unchanged (as given by Eq. 3.65).

On the other hand, if SOC is not less than SOC_{ref}, the battery continues to operate in standby mode and hence P_{ref} is set to zero.

3.4.5.3. Module C

During the daytime, battery energy storage plant smoothing function is activated if:

- SOC of BESS is between 30-90% when time is between t_1 and t_2;
- BESS is fully-charged and smoothing index is positive;
- BESS is fully-discharged and smoothing index is negative;

In these cases, the diesel plant dispatching reference is given by Eq. 3.64 and battery plant is dispatched as:

$$P_{ref} = \Delta P \tag{3.67}$$

where ΔP is the real-time active power smoothing index (APSI) and is obtained through Eq. 3.52.

Otherwise, battery keeps on operating in idle (standby) mode ($P_{ref} = 0$).

3.5. Summary

The stepwise modeling of proposed microgrid components (i.e. DERs and loads) and the power management system are described in this chapter. In this case, the mathematical model of prime movers (i.e. diesel, battery, and solar plats) and their associated controllers developed in PSCAD/EMTDC software are discussed in detail. Proposed power management algorithm consists of three modules and each module has to perform some certain tasks that are explained in this chapter. Input data preparations for the components modeled in PSCAD/EMTDC are investigated as well. This chapter also introduces the proposed battery sizing and charge controlling algorithms.

CHAPTER 4: RESULTS & DISCUSSIONS

4.1. Introduction

Four test cases are conducted to assess the operation of proposed power management algorithm (PMA) in this microgrid (see Figure 3.1) when the system works in grid-connected mode. Microgrid with the agents and communication channels are simulated in PSCAD/EMTDC software. Solar irradiation, cell operating temperature, and load are not constant and hence they change during the day. Power management system (PMS) should be able to manage distributed energy resources (DERs) and hence relief the stresses imposed on the AC network. The network operator concern is about the active power ramp ups/downs caused by PVDG plant since integration of DERs must not negatively affect the equipments of AC network. For each test case, the proposed active power smoothing index is evaluated as well. The ability of BESS, diesel plant, and grid to share the local active and reactive power demand is also evaluated along with battery plant smoothing capability. The role of operator's decision is taken into account as well.

4.2. Test System and Study Cases

The one-line diagram of test system used in this work is shown in Figure 4.1 and the simulated test system in PSCAD/EMTDC is shown in Figure 4.2. The complementary description about this test system is brought in section 3.2.1. Values of LC filter inductive and capacitive reactances are given (see Table 4.1) in per unit based on corresponding unit nominal generation capacity. Value of each DER transformer positive sequence reactance is also given in per unit based on corresponding transformer nominal rating (see Table 4.1).

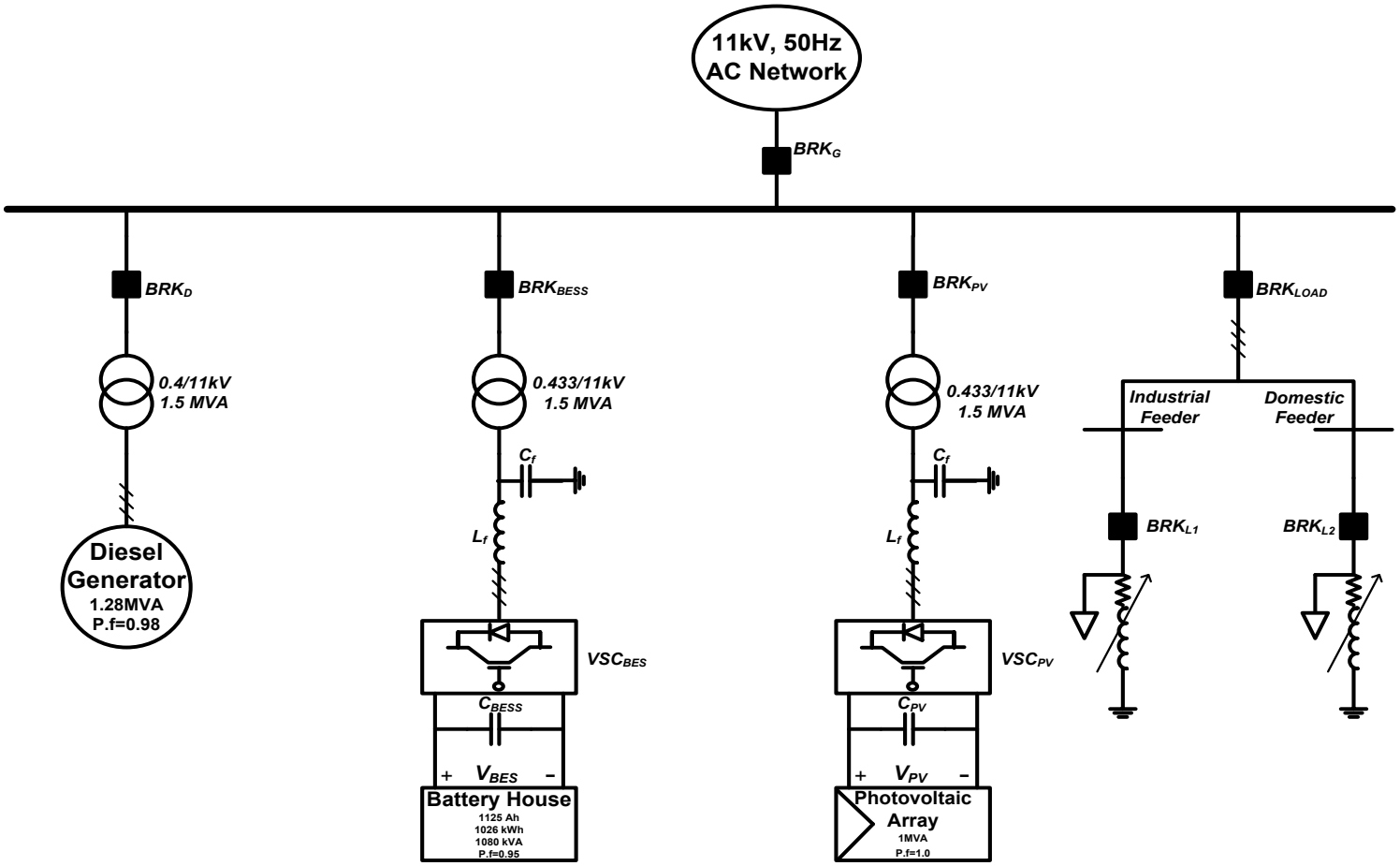

Figure 4. 1: The one-line diagram of test System.

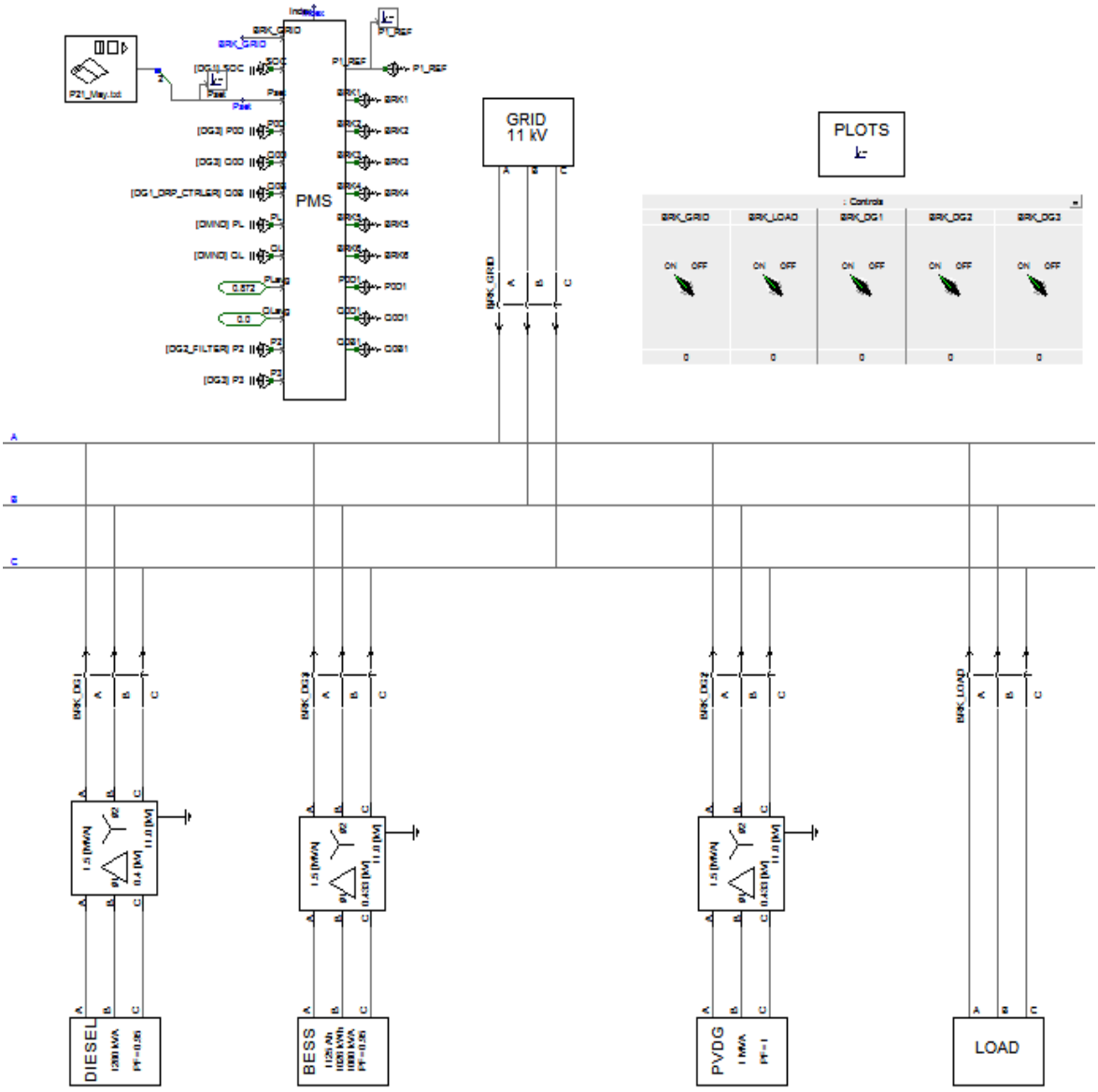

Figure 4. 2: Simulated test system in PSCAD/EMTDC software.

Table 4. 1: Test system information.

DER	X_{Lf} $(p.u)$	X_{Cf} $(p.u)$	X_{Trans} $(p.u)$	*Transformer vector group*
Battery Plant	3.62×10^{-1}	3.67	6×10^{-2}	$YNd11$
Solar PV Plant	3.36×10^{-1}	3.40	6×10^{-2}	$YNd11$
Diesel Plant	-	-	5.8×10^{-2}	$YNd11$

In this chapter, four test cases are studied to validate effectiveness of proposed algorithms and controllers. The information about how to conduct each test case is given in Table 4.2. In the first test case, two scenarios are conducted. In the first scenario, the power smoothing function of battery plant is disabled to see how the original grid active power profile fluctuates. In the second scenario, battery plant actively smoothes out active power fluctuations. In this test case, power smoothing index is also evaluated and the ability of diesel and battery plants to share the load reactive power proportionally is assessed.

In the second test case, the capability of power management system (PMS) to dispatch the diesel plant and to shift up or down the AC network active power profile is examined. Battery storage plant is supposed to smooth out active power fluctuations and reactive power is shared between diesel and battery plants.

In the third test case, the ability of diesel plant to charge the battery is tested while smoothing function of battery plant is acting and grid is supplying average local reactive demand.

In the last test case, active and reactive powers are supposed to be supplied locally. Battery plant is supposed to be charged locally by the diesel plant.

Table 4. 2: Information about the test cases.

	Test case 1		Test case 2	Test case 3	Test case 4
	Scenario 1	Scenario 2			
Diesel Plant Status	On	On	On	On	On
Battery Plant Status	On	On	On	On	On
Solar PV Plant Status	On	On	On	On	On
Power Smoothing Function	Disabled	Enabled	Enabled	Enabled	Enabled
Load Active Power Supplied Locally/Remotely	Locally	Locally	Remotely	Remotely	Locally
Load Reactive Power Supplied Locally/Remotely	Locally	Locally	Locally	Remotely	Locally
Battery is charged Locally/Remotely	-	Remotely	Locally	Locally	Locally

4.3. Analysis of Results

4.3.1. Test Case 1

In this test case, diesel plant is supposed to supply 50% of load active power (P_L) and hence operator decides to dispatch this unit (Eq. 3.50) with $\beta = 0.5$. The net active power between the load, diesel plant generation, and PVDG smoothed output power ($P_L - \beta P_L - P_{set}$) is compensated by the AC network. Battery storage plant also smoothes out the power fluctuation caused by load and solar PV plant. This test case is also designed to evaluate diesel plant governor and excitation controllers when BESS smoothing function is enabled and disabled. The effectiveness of BESS controllers to respond the set-points issued by the system operator is examined as well. The operator, who has received the forecasted waveforms, sets SOC_{ref} to be 60% at the day beginning and battery should be recharged (if any) up to this level by the grid at the end of day. The parameters set for this test case is brought in Table 4.3.

Table 4. 3: Parameter settings for test case 1.

Parameter	Value	Unit
P_{Lavg}	0.872	MW
Q_{Lavg}	0.0	MW
SOC_{ref}	60	Percent
SOC_{min}	30	Percent
SOC_{max}	90	Percent
t_1	6.5	Hours
t_2	19.5	Hours
β	0.5	-
α	0.84375	-

Operator also sets $P_{Lavg} = 0.872\ (MW)$ and thus the load fluctuations about this value are compensated by battery energy storage system (BESS). Operator also assigns the diesel plant and BESS to share the load reactive power (Q_L) locally between themselves and sets $Q_{Lavg} = 0$.

The term of "locally" is used because the diesel plant set-point follows the load active power pattern. Power management algorithm (PMA) is activated between t_1 and t_2 for the purpose of smoothing. In here, t_1 and t_2 are supposed to be at 6:30 a.m and 7:30 p.m, respectively. There are two scenarios which are implemented in this test case. Microgrid operates while BESS smoothing function is disabled in the former scenario and is enabled in the latter scenario. In both scenarios, load reactive power still can be shared properly between two distributed energy resources (i.e. battery and diesel plants). As shown in Figure 4.3 through 4.11, between 12:00 a.m and 6:30 a.m the diesel plant and the grid supply the load together. From 6:30 a.m to 7:30 p.m, as shown in Figure 4.3a, AC grid encounters with too many fluctuations as the PVDG unit output starts increasing, however, these oscillations are mitigated in the second scenario (see Figure 4.3b). Diesel plant active power output in the first scenario is similar to the second one since the dispatching strategy is also similar in both scenarios (see Figure 4.4).

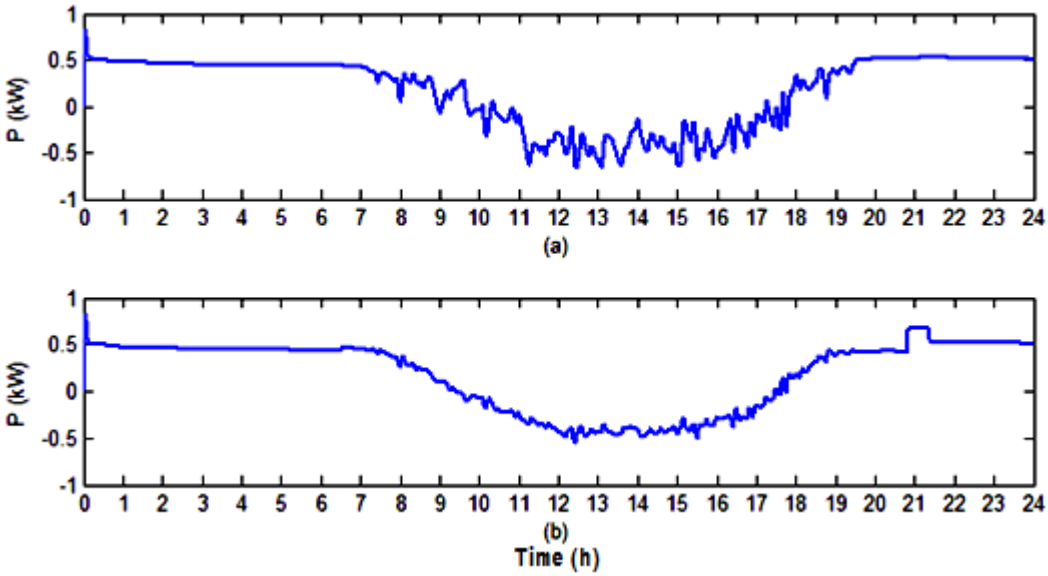

Figure 4. 3: Grid active power profile. (a) Without battery plant. (b) With battery plant.

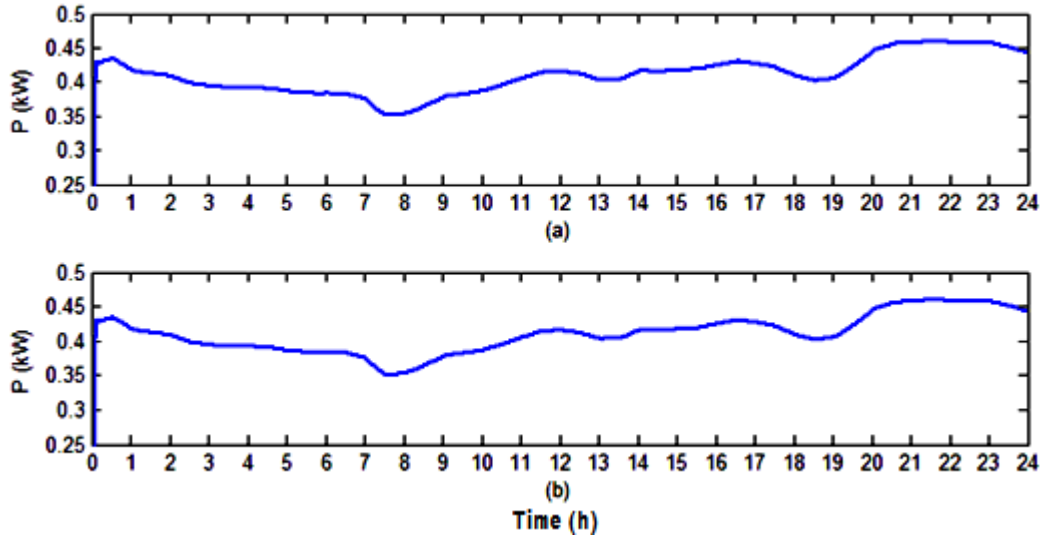

Figure 4. 4: Diesel plant output active power. (a) Without battery plant. (b) With battery plant.

In the first scenario, *SOC* of battery keeps unchanged (see Figure 4.5a) since BESS is in idle (standby) mode (see Figure 4.6a) but in the second scenario battery *SOC* varies (see Figure 4.5b) which confirms that BESS compensates the active power oscillations (see Figure 4.6b). In the first scenario, grid experiences too many ramp ups/downs. In second scenario, all the active power fluctuations are suppressed by BESS and hence the grid active power profile becomes smoothed.

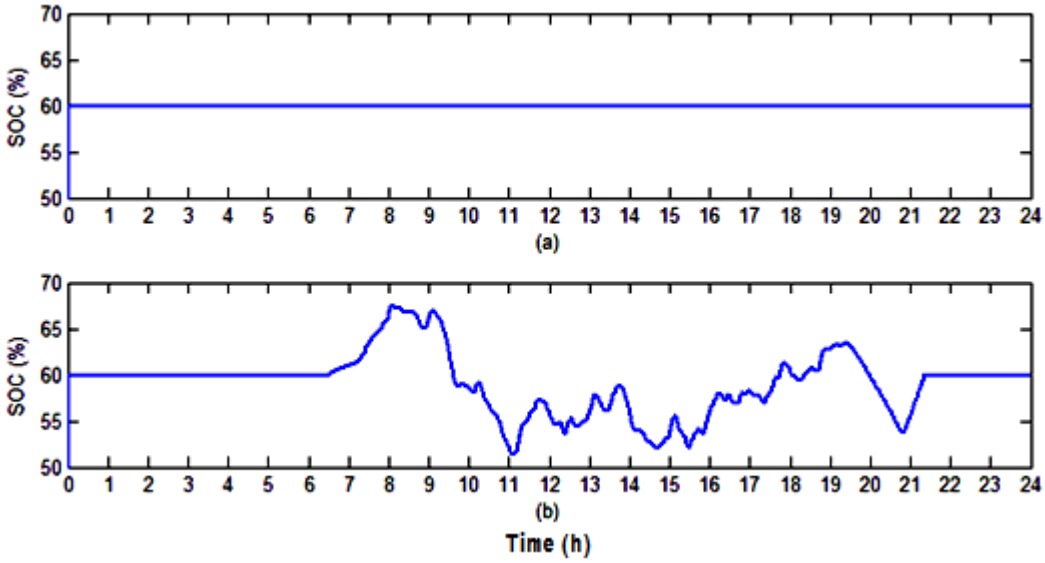

Figure 4. 5: Battery energy storage plant state of charge. (a) When its smoothing function is disabled. (b) When its smoothing function is enabled.

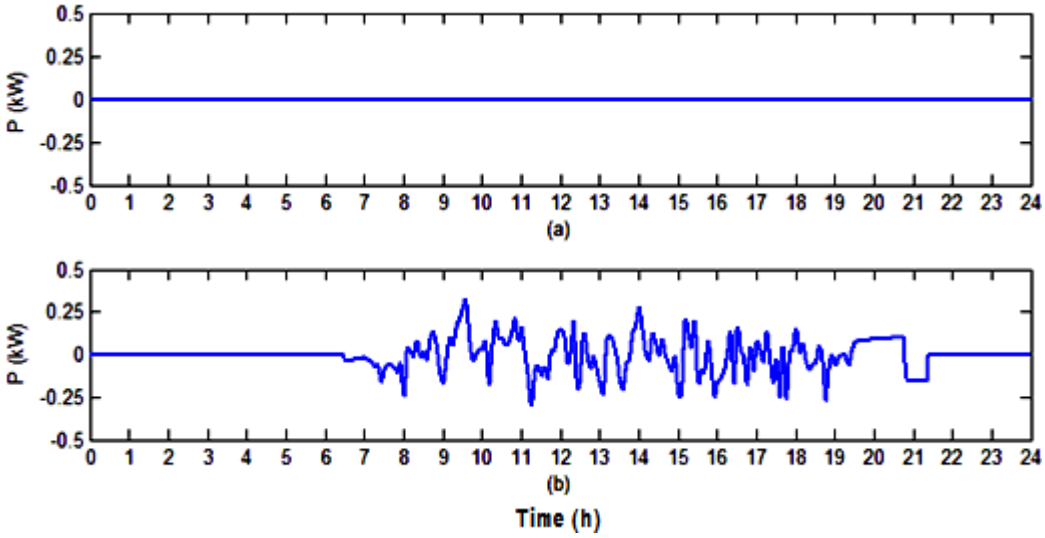

Figure 4. 6: Battery energy storage plant output active power. (a) When its smoothing function is disabled. (b) When its smoothing function is enabled.

The grid reactive power profiles for both scenarios are shown in Figures 4.7a and 4.7b. As expected, these two figures are similar which confirms the whole reactive power is supplied locally. As depicted in Figures 4.8a and 4.9a, the load reactive power is shared between diesel and battery plants proportional to their ratings in the first scenario. In the second scenario, reactive power is also shared proportionally (see Figures 4.8b and 4.9b). The grid supplies zero reactive power in both cases because Q_L is supplied locally.

The reactive power outputs of both DERs and the grid reactive power profile for both scenarios are similar which confirms that the control of active and reactive powers is independent.

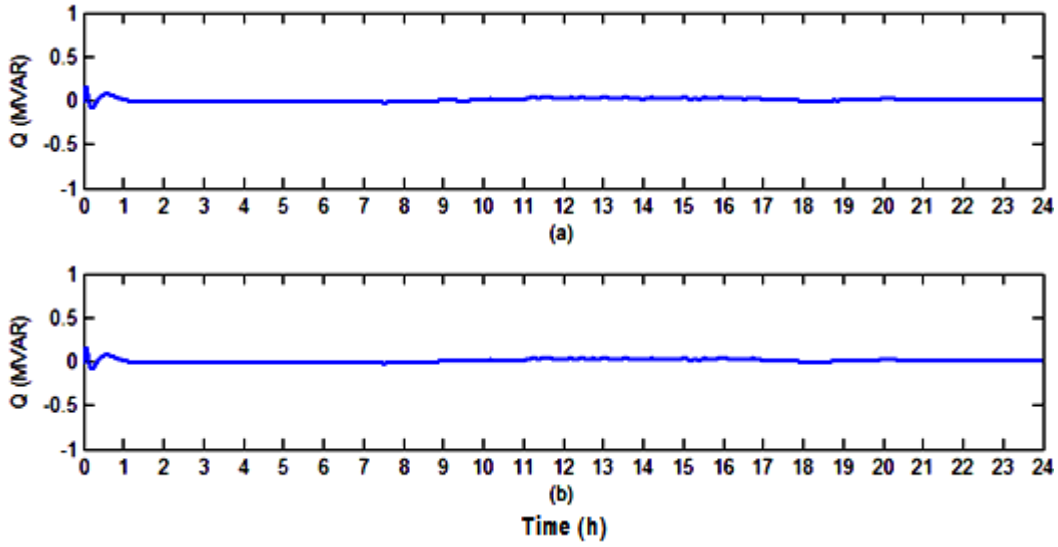

Figure 4. 7: Grid reactive power profile. (a) Without battery plant. (b) With battery plant.

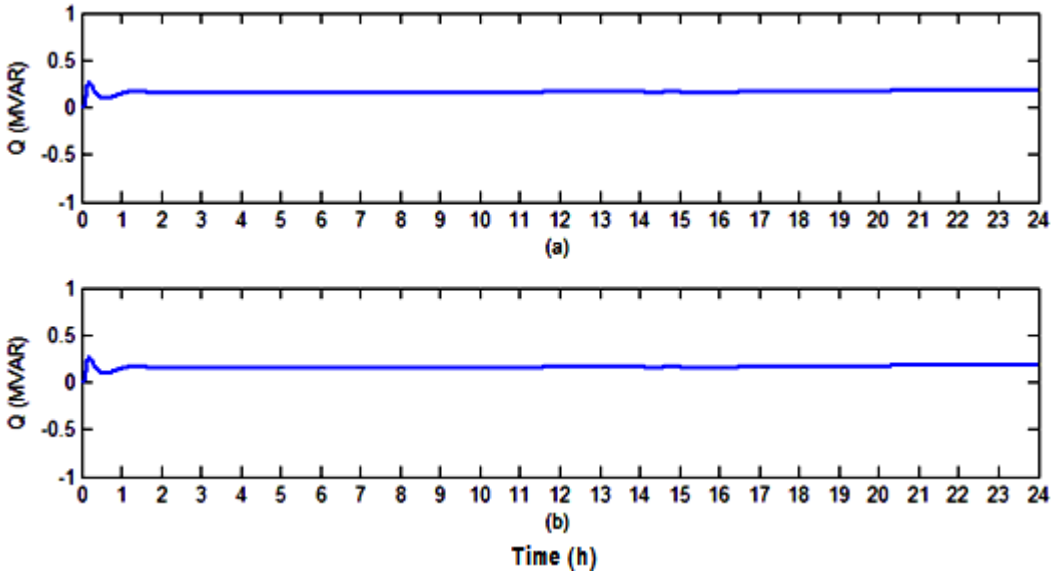

Figure 4. 8: Diesel plant output reactive power. (a) Without battery plant. (b) With battery plant.

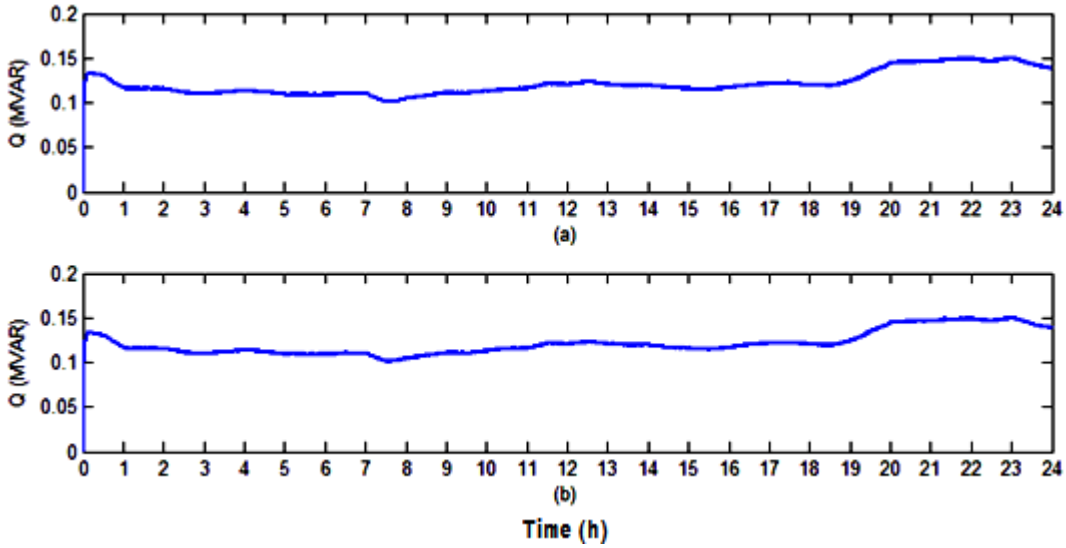

Figure 4. 9: Battery energy storage plant output reactive power. (a) When its smoothing function is disabled. (b) When its smoothing function is enabled.

Battery bank output voltage and output current keep unchanged in the first scenario (see Figures 4.10a and 4.11a) because BESS smoothing function is disabled. The battery house terminal voltage changes stably around the final voltage value in the second scenario (see Figure 4.10b) and the output current also varies within allowable boundary (see Figure 4.11b). At the end of day when the *SOC* becomes less than 60%, the grid starts charging the battery (see the grid active power profile which peaks between 08:30 p.m and 09:30 p.m in Figure 4.3b).

BESS current control unit checks for the value of charging power set-point which is sent by the network operator. If this value is within the allowable boundary, battery keeps on charging until the *SOC* reaches to 60% (see BESS active power which is absorbed between 08:30 p.m and 09:30 p.m in Figure 4.6b) and the system gets ready for the next day. If the amount of charging current is above the limit specified in current control algorithm (see Figure 3.6), algorithm limits charging active power reference value to maximum allowed value (i.e. 300 kW).

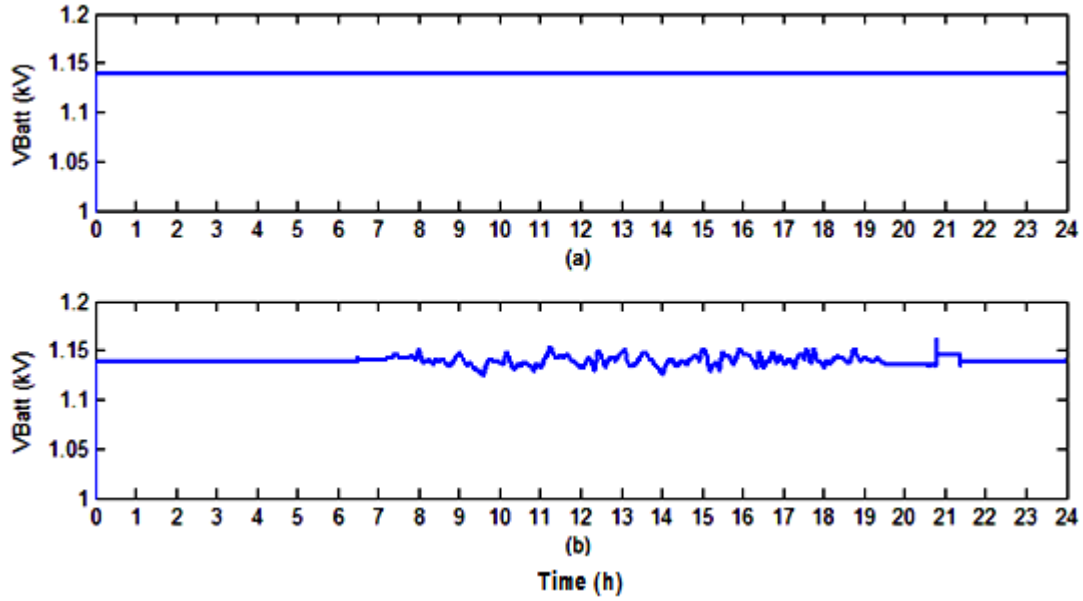

Figure 4. 10: Battery energy storage bank terminal voltage. (a) When its smoothing function is disabled. (b) When its smoothing function is enabled.

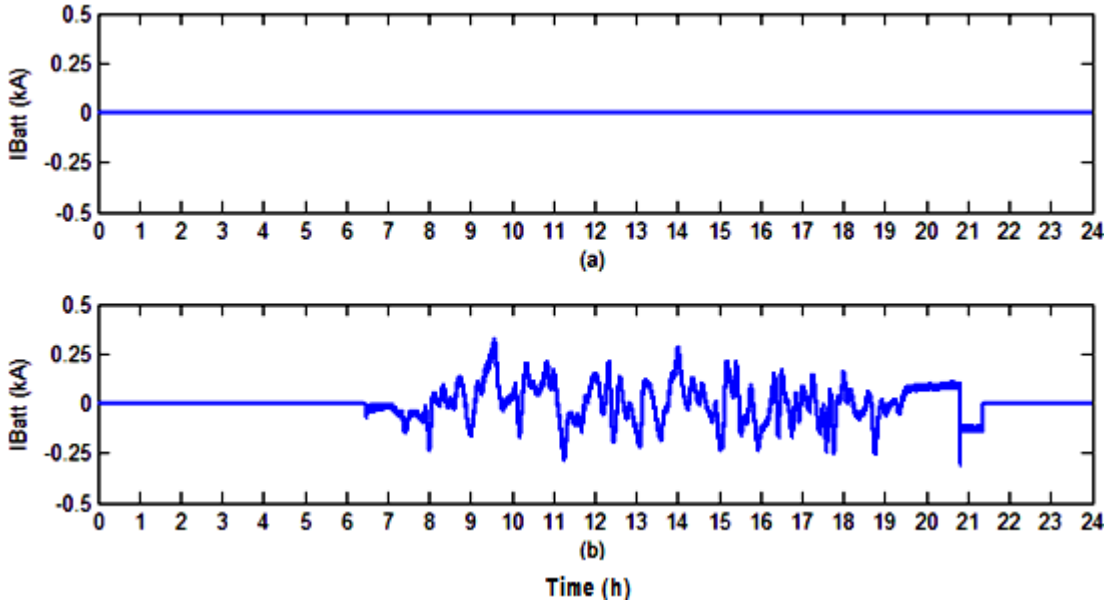

Figure 4. 11: Battery energy storage bank output current. (a) When its smoothing function is disabled. (b) When its smoothing function is enabled.

4.3.2. Test Case 2

In this test case, operator decides to dispatch the diesel plant by a fixed active power set point. The aim is to shift down/up the grid active power profile while BESS smoothing function is enabled throughout the day. As shown in Figure 4.12 through 4.14, from 12 a.m to 2 a.m the diesel plant active power output is 200 kW (reference set by operator is 200 kW). Between 2 a.m and 4 a.m active power reference increases to 400 kW by the operator and then declines to 300 kW from 4 a.m until end of the day. BESS smoothes out the power fluctuations (i.e. similar to test case 1, scenario 2) and the changes in diesel plant output power has no effect on the operation of battery plant.

At the end of the day, diesel plant receives the command from the distribution network operator in order to increase its active power generation and charge the battery. Battery bank whose *SOC* has fallen to less than 60% is recharged up to the level of reference *SOC* (by setting $P_{0D} = 350kW$ and $P_{ref} = -150\ kW$) and then system gets ready for the next day (see Figure 4.13a).

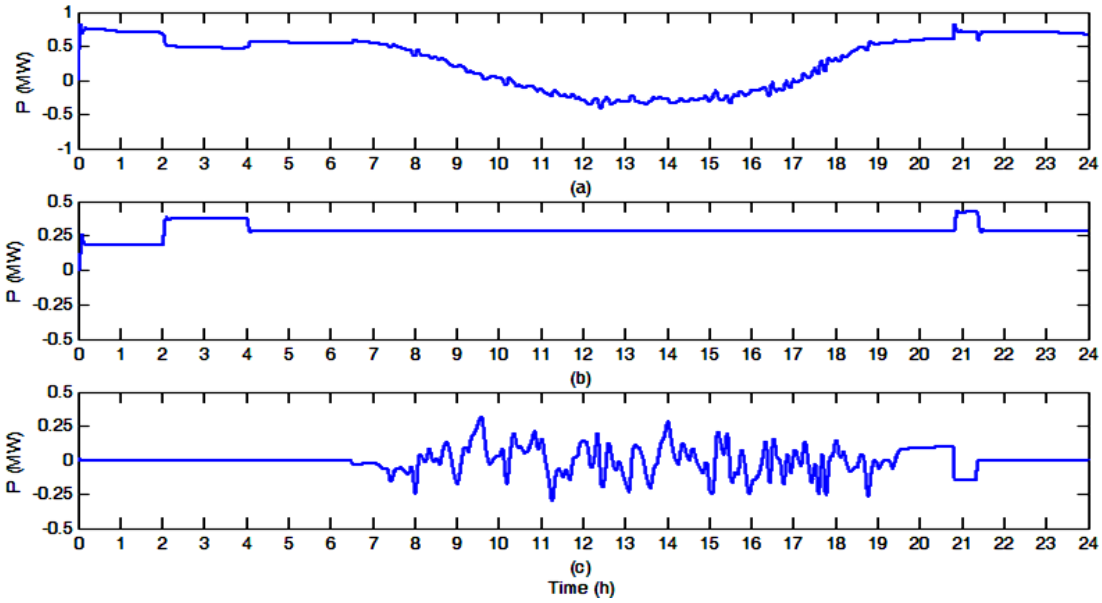

Figure 4. 12: (a) Grid active power profile. (b) Diesel plant output active power. (c) BESS output active power.

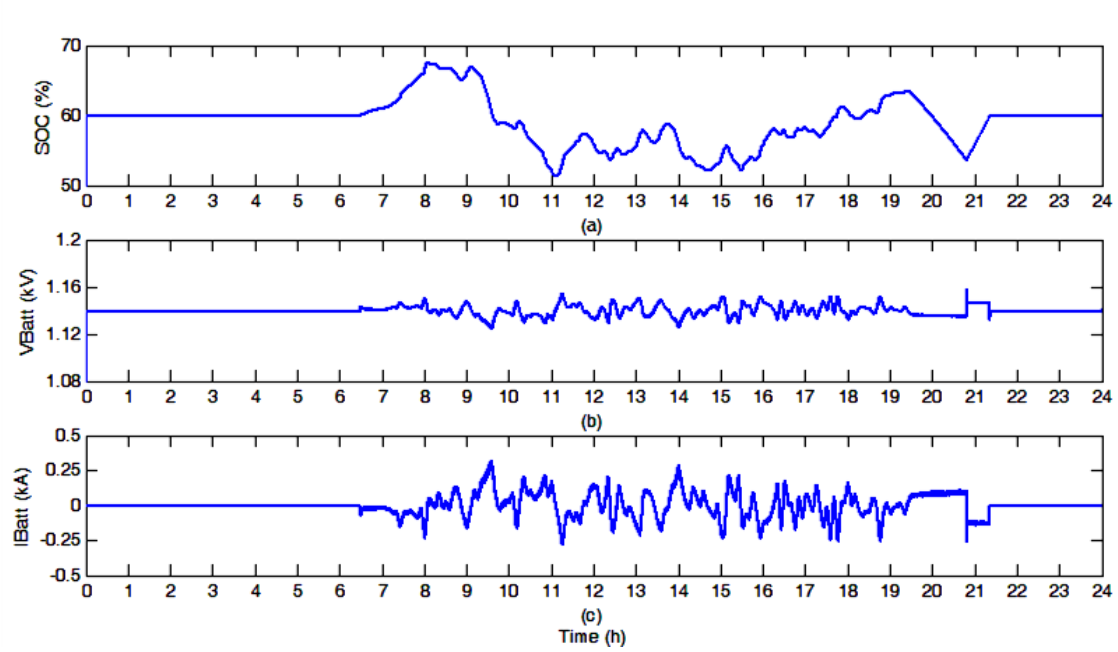

Figure 4. 13: (a) Battery house *SOC*. (b) Battery house terminal voltage. (c) Battery house output current.

Battery bank terminal voltage (see Figure 4.13b) and output current (see Figure 4.13c) vary within the allowable boundary. As shown in Figure 4.14, grid is supposed to supply zero reactive power (see Figure 4.14a) and hence the load reactive power is shared between diesel plant and BESS proportionally (see Figures 4.14b and 4.14c). In this case, whenever the diesel output power changes (see Figure 4.12b) to charge the battery (see Figure 4.12c), its output reactive power slightly oscillates. This matter happens because in rotary based distributed generation (DG) plants control of active and reactive power to some extent is dependent to each other. To deliver as much active power as possible by synchronous generator, diesel engine must rotate as much as faster and hence power angle increases accordingly. Along with sudden increase in power angle, the amount of reactive power delivered by diesel plant shortly grows. Then, the excitation acts against this phenomenon and reduces the reference voltage until the operating point returns to its original value in a short while.

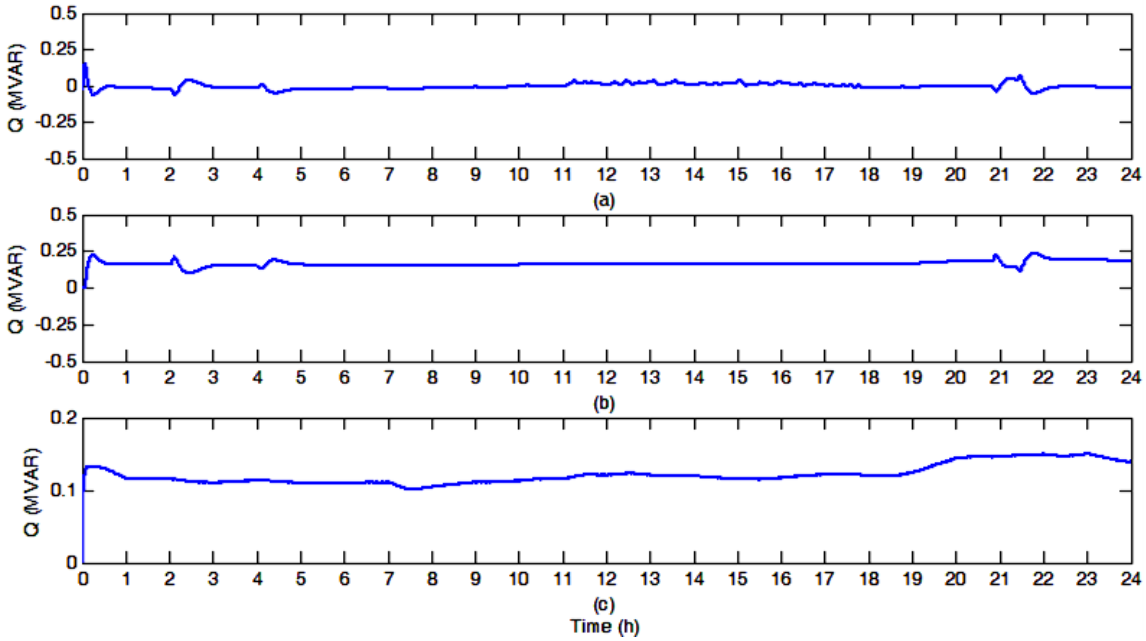

Figure 4. 14: (a) Grid reactive power profile. (b) Diesel plant output reactive power. (c) BESS output reactive power.

4.3.3. Test Case 3

This test case is to confirm the effectiveness of proposed reactive power smoothing index (ΔQ). Between 12 a.m and 6:30 a.m BESS is idle (standby) and diesel plant generates constant active power. The grid compensates for the net difference between the diesel plant active power output, smoothed solar PV plant generated active power, and the active load (see Figure 4.15).

As shown in Figure 4.15, BESS follows the active power index closely and the ramp ups/downs are completely compensated by this unit. The voltage at the battery house terminal fluctuates due to the battery output current oscillations. Since the final voltage value is chosen properly and battery is sized precisely, these variations have no undesirable effect on the operation of BESS (see Figure 4.16b). The current controller module in BESS unit agent instantaneously controls the current of battery to make sure that its value is allowable (see Figure 4.16c).

At 4 a.m operator issues a command to supply the average load reactive power by the grid (see Figure 4.17a) and hence the load reactive power fluctuations about this value are shared proportionally between diesel plant (see Figure 4.17b) and BESS (see Figure 4.17c). Once the operator command is received by the generation agent, this agent informs unit agent associated with BESS and diesel plant. These units adjust their reactive power generation accordingly (see Figures 4.17a and 4.17c). Q_{Lavg} can be calculated through Eq. 3.56 and it is also possible to be considered as constant offset value provided that the remaining reactive load above this offset complies with BESS and diesel plant power capabilities as being shared between them. At end of the day, battery is charged by diesel plant (by setting for $P_{0D} = 350\ kW$ and $P_{ref} = -150\ kW$) up to the reference *SOC* and system gets prepared for the next day.

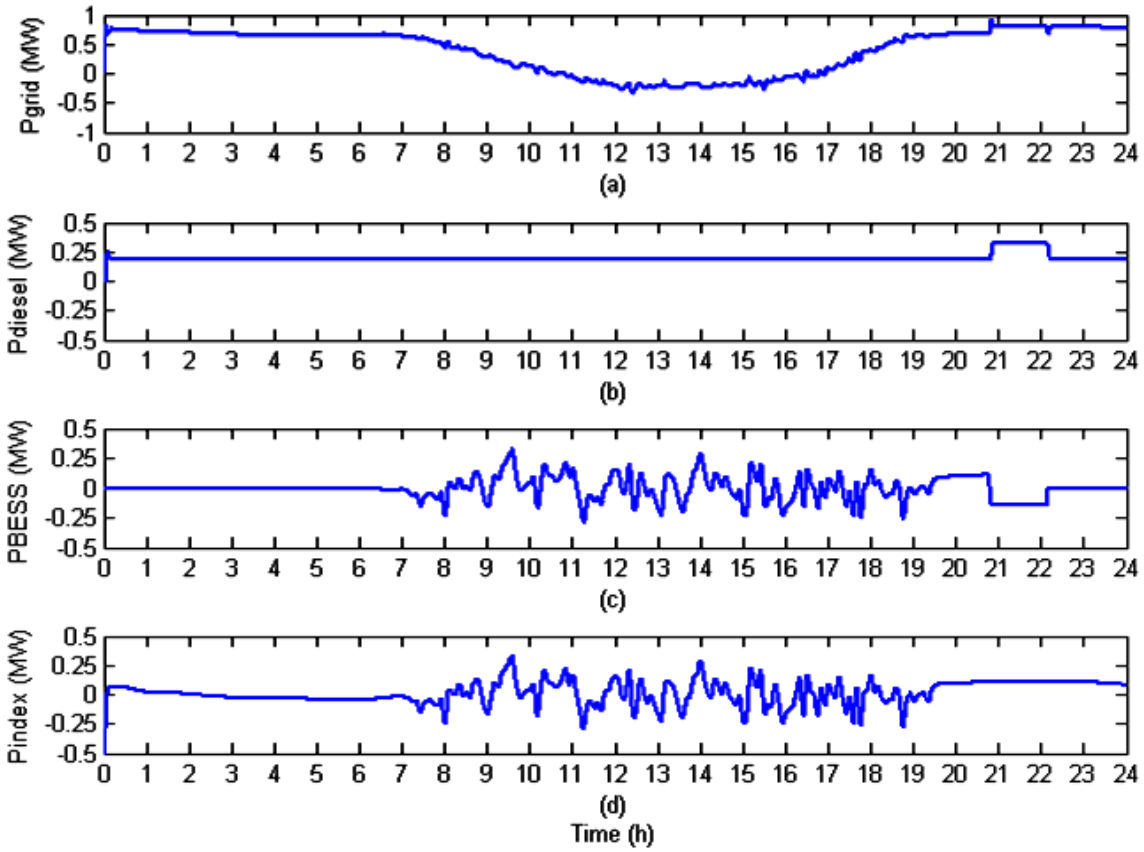

Figure 4. 15: (a) Grid active power profile. (b) Diesel plant output active power. (c) BESS output active power. (d) Active power smoothing index profile (ΔP).

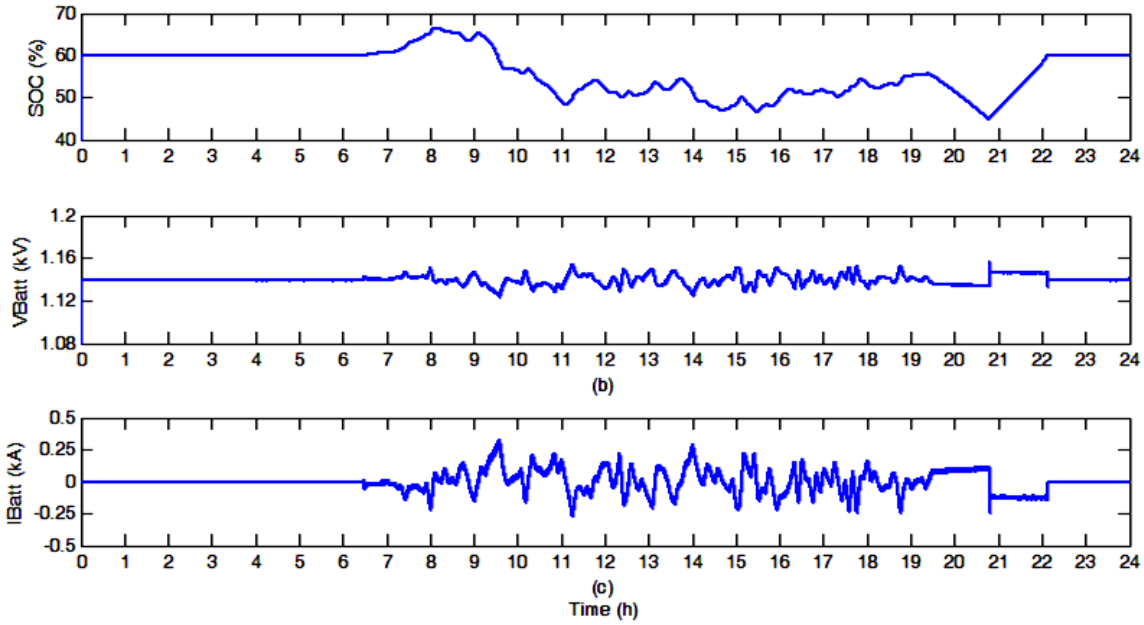

Figure 4. 16: (a) Battery house SOC. (b) Battery house terminal voltage. (c) Battery house current.

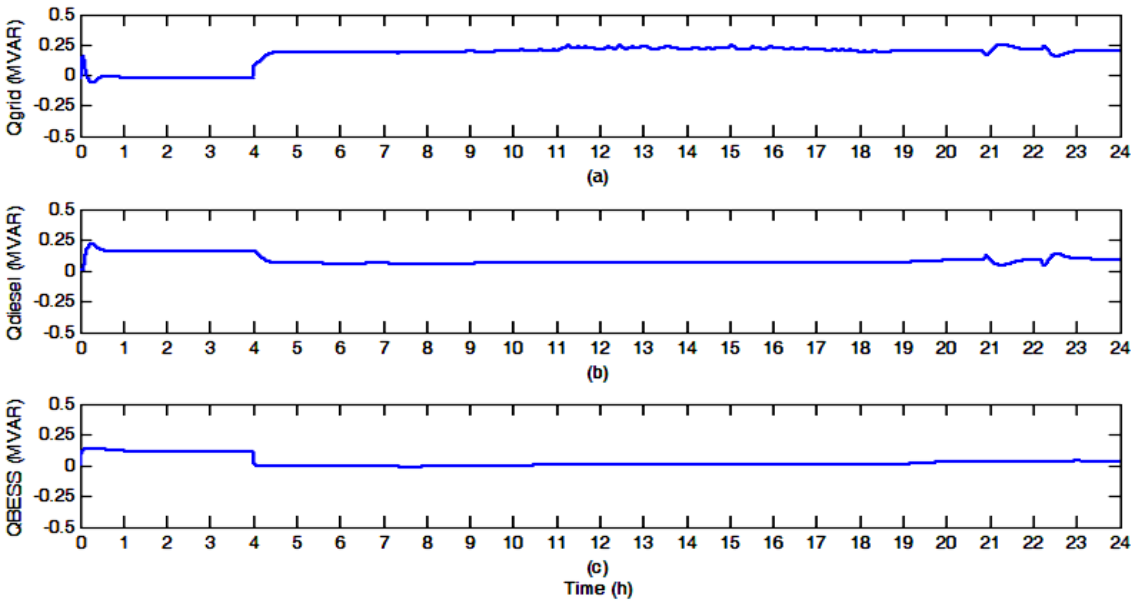

Figure 4. 17: (a) Grid reactive power profile. (b) Diesel output plant reactive power. (c) BESS output reactive power.

4.3.4. Test Case 4

In this test case, the grid active power profile is smoothed (see Figure 4.18a) because the battery plant compensate power fluctuations (see Figure 4.18c) caused by load and solar PV plant (see Figure 4.18d).

As shown in Figure 4.18b, diesel plant is dispatched ($P_{0D} = \beta P_L$) to supply the load locally and hence it follows the load pattern. At the end of the day, diesel plant receives the command from the distribution network operator in order to increase its active power generation and charge the battery (local charging). Battery (with *SOC* less than 60%) is recharged up to the level of reference *SOC* (by setting $P_{0D} = \beta P_L + 150$ and $P_{ref} = -150\,kW$) and then system gets ready for the next day (see Figure 4.19a). Battery terminal voltage (see Figure 4.19b) and output current (see Figure 4.19c) both vary within their allowable boundaries. This matter indicates that both battery sizing and charge controlling algorithms act properly and as expected.

As shown in Figure 4.20, grid is supposed to supply zero reactive power (see Figure 4.20a) and hence the load reactive power is shared between diesel and battery plants proportional to their ratings (see Figures 4.20b and 4.20c). In this case, whenever the diesel output power changes (see Figure 4.18b) to charge the battery (see Figure 4.18c), its output reactive power slightly oscillates. Excitation controller act against this phenomenon and thus the reactive power output of diesel plant settles at its original value after a short while.

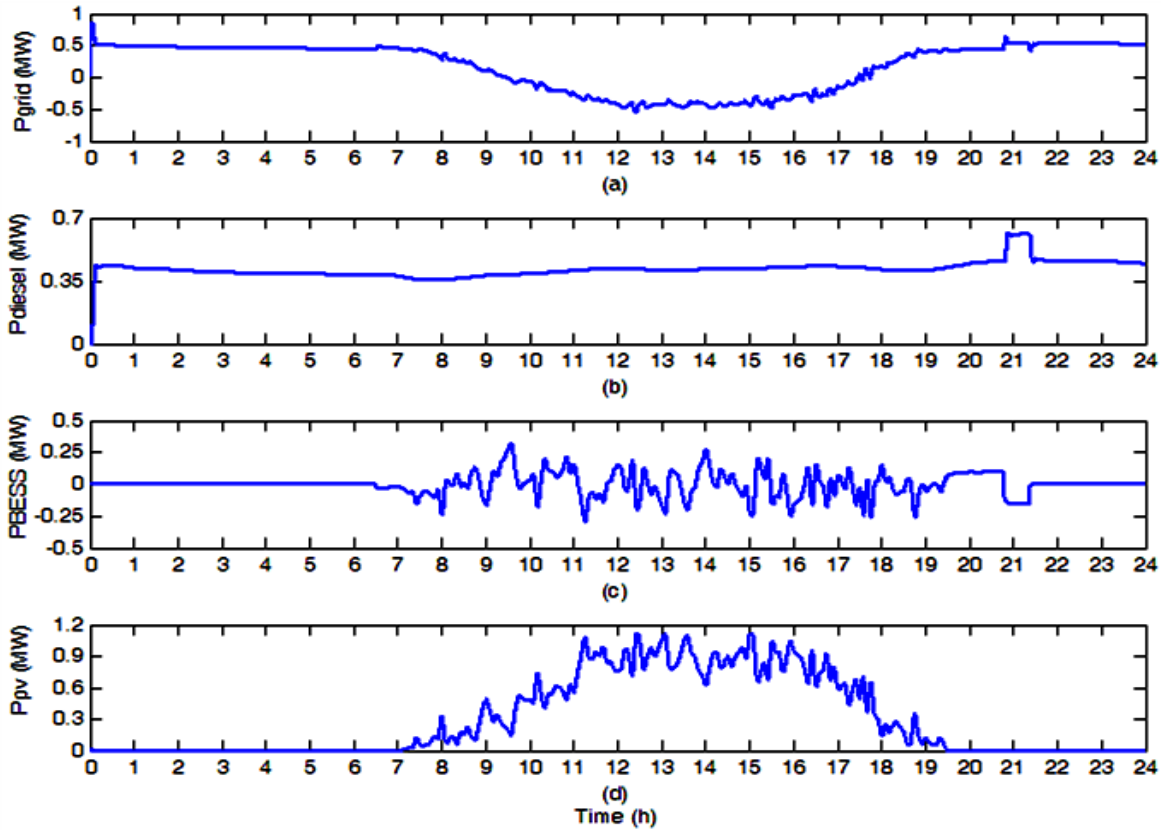

Figure 4. 18: (a) Grid active power profile. (b) Diesel plant output active power. (c) BESS output active power. (d) Solar PV plant output active power.

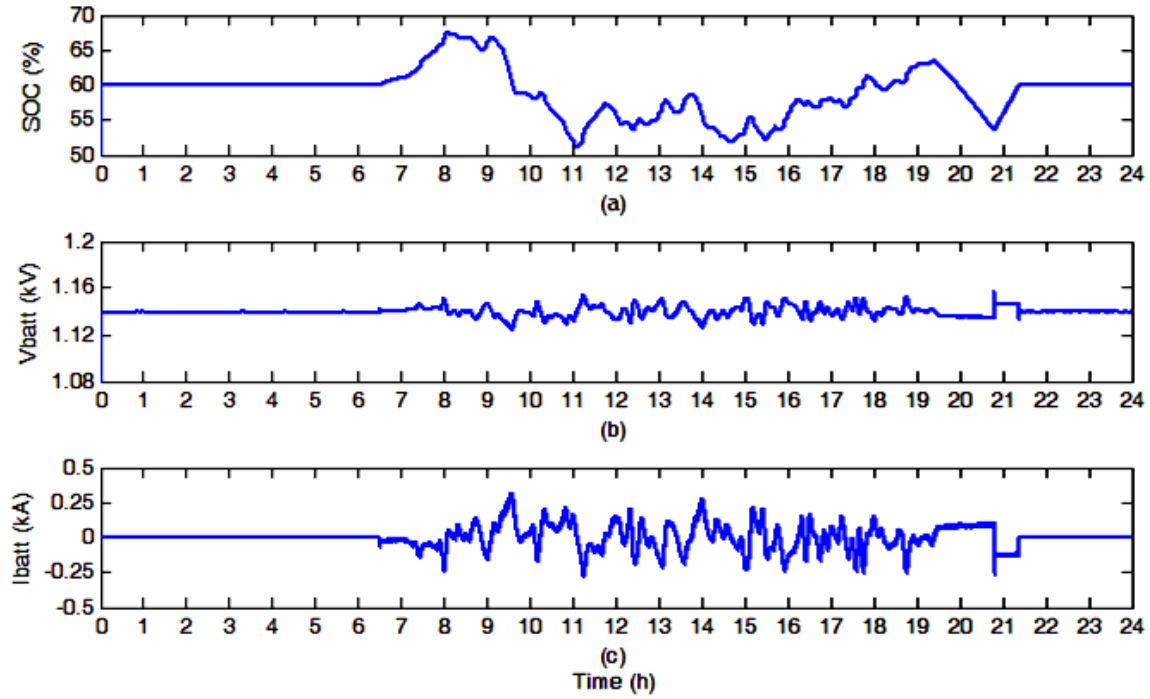

Figure 4. 19: (a) Battery house *SOC*. (b) Battery house terminal voltage. (c) Battery house output current.

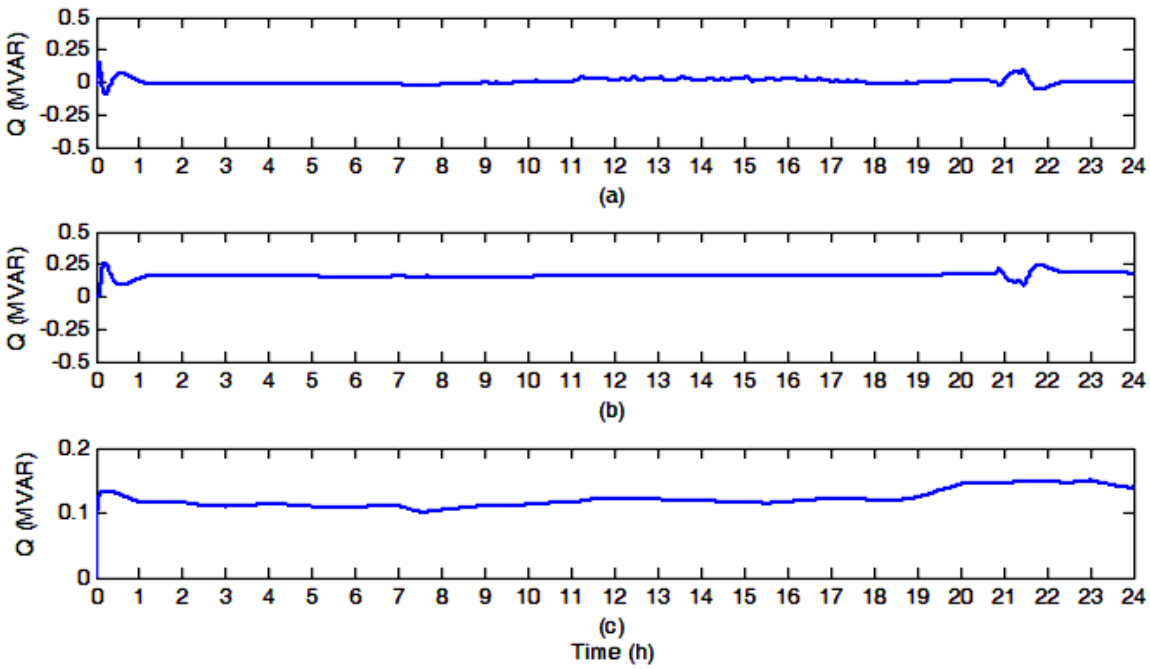

Figure 4. 20: (a) Grid reactive power profile. (b) Diesel plant output reactive power. (c) BESS output reactive power.

4.4. Summary

There are four test cases implemented to evaluate the operations of the power management system (PMS), distributed energy resources (DERs), and the controllers in grid-connected mode. PMS is supposed to manage DERs and hence to limit the ramp rates imposed on the main grid. For each test case (except the first scenario of the first test case), the proposed active power smoothing index is assessed as well. The ability of battery and diesel plants to share the local active and reactive power demand is also evaluated. The role of operator's decision is taken into account as well.

In the first test case, two scenarios are conducted. In the first scenario, the power smoothing function of battery plant is disabled to see how the original system experiences the active power oscillations.

In the second scenario, battery plant actively smoothes out active power fluctuations. In this scenario, power smoothing index is also evaluated and the ability of diesel and

battery plants to share the load reactive power locally is verified. Diesel plant also charges the battery plant and supplies the local active power demand as expected.

In the second test case, the capability of power management system (PMS) to dispatch the diesel plant and to shift up or down the main grid active power profile is examined. Battery storage plant smoothes out active power oscillations and reactive power is shared between diesel and battery plants properly.

In the third test case, the ability of diesel plant to charge the battery is tested while smoothing function of battery plant is acting and grid is supplying average local reactive power demand.

In the fourth test case, all the DERs are connected and smoothing function is active. The only difference between this test case and the previous one is that the load reactive power is supplied locally.

CHAPTER 5: CONCLUSIONS & FUTURE WORKS

5.1. Conclusions

This work proposes a novel power management system (PMS) which utilizes the battery and diesel plants efficiently inside of a smart microgrid. Microgrid is subject to operate in grid-connected mode. Microgrid consists of both rotary and electronically interfaced distributed energy resources (DERs). This thesis also investigates the role of battery energy storage system in order to alleviate power oscillations caused by the solar PV plant and load demand in the microgrid.

Proposed power management system integrates moving average filtering method into the scheduled dispatching of battery plant in order to smooth out the grid active power profile and minimize the undesirable effects on grid equipments. Moving average filter also lessens the computational burden and helps the operator to determine the degree of smoothness. Results show that if one day ahead forecasting information about the load demand and solar irradiation is available (considering a ramp rate of -50% to +10% for solar plant together with load), a 21-point symmetrical filter produces an acceptable smoothed reference waveform.

A practical algorithm is also suggested to design and size the battery plant accurately based on data available through forecasting modules together with network constraints. Size of the battery plant obtained through this algorithm is closely matched to suppress solar plant power fluctuations along with the variable load.

A current control algorithm is also proposed to limit the battery charging and discharging currents. The results show that the magnitude of active power dispatching reference does not go beyond the specified limits (i.e. $\in [-300,350]\, kW/min$) determined for the proposed charge controlling algorithm. This confirms that the operation of proposed charge controlling algorithm satisfies the technical requirements of battery plant and hence the battery bank current varies within the allowed boundary (i.e. $\in [-329,384]\, A$).

Algorithm of PMS is implemented in an agent oriented communicating platform with four hierarchical levels. This communicating environment helps the network operator to interfere in the operation of power management algorithm (PMA) and hence schedule dispatchable DERs based on the real-time system requirements.

Ability of the proposed diesel plant governor and excitation controllers are also verified through shifting up/down the grid active power profile and sharing reactive power with battery plant, respectively. Proposed governor controller makes it possible for the system operator to decide about the locally or remotely (by the grid) supplying the load active power. The results also indicate that the proposed droop mechanism as the outer loop for excitation controller ensures the accurate reactive power sharing between the battery and diesel plants.

A load model is also designed which is suitable for power system real-time simulation and results prove the effectiveness of this model. The overall operation of microgrid to limit ramp rates imposed on AC network and to meet generation as well as consumption requirements and to bring ancillary services for the AC network is quite satisfactory.

5.2. Future Works

The topics that are proposed for a future work are presented in the next sections.

a) Extending PMS for Off-grid Applications

The proposed power management system (PMS) is subject to control the microgrid in grid-connected mode. However, during the period of disconnection from the grid (islanded mode) the microgrid needs a different power management algorithm in order to sustain its stability. In islanded mode, voltage magnitude and its frequency drift away from their nominal values and hence the stability of microgrid highly depends on the balance between generation and consumption. In this case, role of droop control mechanisms is very important to keep the frequency and voltage in microgrid at a certain level.

At the same time, there exist power fluctuations due to non-linearity of load and the stochastic behavior of solar PV plant. This matter exacerbates the situation and pushes the microgrid forward to become unstable. Therefore, a sophisticated power management approach must be adopted to keep microgrid stable during the islanded operating mode.

b) Adding Load and Generation Forecasting Modules to PMS

In the proposed power management system (PMS), the solar PV generation and load demand are assumed to be forecasted one day ahead and the related data are used as inputs for the PMS. As a future work, load and generation forecasting modules can be added to the existing PMS in this work. In this case, PMS is able to forecast the generation and load profile by itself and hence it does not need any external source of data.

c) Considering Supplementary Factors in PMS

The issues such as economic dispatch, demand response (DR), and demand side management (DSM) are not considered in the proposed PMS. Each concept can also be added as a function to the proposed power management system in this work.

REFERENCES

A. Huggins, R. (2010). Energy Storage. New York: Springer.

Abbey, C., Wei, L., & Joos, G. (2010). An Online Control Algorithm for Application of a Hybrid ESS to a Wind-Diesel System. IEEE Transactions on Industrial Electronics, 57(12), 3896-3904. doi: 10.1109/TIE.2010.2051392

Acharjee, P. (2012, 14-17 Oct. 2012). Investigation of the power scenario in India for the implementation of smart grid. Paper presented at the Innovative Smart Grid Technologies (ISGT Europe), 2012 3rd IEEE PES International Conference and Exhibition on.

Acharjee, P. (2013). Strategy and implementation of Smart Grids in India. Energy Strategy Reviews, 1(3), 193-204. doi: http://dx.doi.org/10.1016/j.esr.2012.05.003

Agalgaonkar, A. P., Kulkarni, S. V., & Khaparde, S. A. (2006). Evaluation of configuration plans for DGs in developing countries using advanced planning techniques. IEEE Transactions on Power Systems, 21(2), 973-981. doi: 10.1109/tpwrs.2006.873420

Ahmed, N. A., Miyatake, M., & Al-Othman, A. K. (2008). Power fluctuations suppression of stand-alone hybrid generation combining solar photovoltaic/wind turbine and fuel cell systems. Energy Conversion and Management, 49(10), 2711-2719. doi: http://dx.doi.org/10.1016/j.enconman.2008.04.005

Al-Nasseri, H., Redfern, M. A., & O'Gorman, R. (2005, 18-18 Nov. 2005). Protecting micro-grid systems containing solid-state converter generation. Paper presented at the Future Power Systems, 2005 International Conference on.

Al-Smairan, M. (2012). Application of photovoltaic array for pumping water as an alternative to diesel engines in Jordan Badia, Tall Hassan station: Case study. Renewable and Sustainable Energy Reviews, 16(7), 4500-4507. doi: http://dx.doi.org/10.1016/j.rser.2012.04.033

Albuquerque, F. L., Moraes, A. J., Guimarães, G. C., Sanhueza, S. M. R., & Vaz, A. R. (2010). Photovoltaic solar system connected to the electric power grid operating as active power generator and reactive power compensator. Solar Energy, 84(7), 1310-1317. doi: http://dx.doi.org/10.1016/j.solener.2010.04.011

Alegria, E., Brown, T., Minear, E., & Lasseter, R. H. (2014). CERTS Microgrid Demonstration With Large-Scale Energy Storage and Renewable Generation. IEEE Transactions on Smart Grid, 5(2), 937-943. doi: 10.1109/TSG.2013.2286575

. ALTERNATORS LSA 50.1- 4 Pole

Electrical and mechanical data. (2007). In L. SOMER (Ed.).

Amin, Bambang, R. T., Rohman, A. S., Dronkers, C. J., Ortega, R., & Sasongko, A. (2014). Energy Management of Fuel Cell/Battery/Supercapacitor Hybrid Power Sources Using Model Predictive Control. IEEE Transactions on Industrial Informatics,, 10(4), 1992-2002. doi: 10.1109/TII.2014.2333873

ANDERSON, P., & FOUAD, A. (2002). Power system control and stability.

Ault, G. W., McDonald, J. R., & Burt, G. M. (2003). Strategic analysis framework for evaluating distributed generation and utility strategies. IEE Proceedings-Generation, Transmission and Distribution, 150(4), 475-481. doi: 10.1049/ip-gtd:20030374

Bae, I.-S., & Kim, J.-O. (2007). Reliability evaluation of distributed generation based on operation mode. IEEE Transactions on Power Systems, 22(2), 785-790.

Balakrishnan, J. (2006, 8-11 Aug. 2006). Renewable Energy and Distributed Generation in Rural Villages. Paper presented at the Industrial and Information Systems, First International Conference on.

Barklund, E., Pogaku, N., Prodanovic, M., Hernandez-Aramburo, C., & Green, T. C. (2008). Energy Management in Autonomous Microgrid Using Stability-Constrained Droop Control of Inverters. IEEE Transactions on Power Electronics, 23(5), 2346-2352. doi: 10.1109/tpel.2008.2001910

Barton, J. P., & Infield, D. G. (2004). Energy storage and its use with intermittent renewable energy. IEEE Transactions on Energy Conversion, 19(2), 441-448. doi: 10.1109/tec.2003.822305

Batista, N. C., Melício, R., Matias, J. C. O., & Catalão, J. P. S. (2013). Photovoltaic and wind energy systems monitoring and building/home energy management using ZigBee devices within a smart grid. Energy, 49(0), 306-315. doi: http://dx.doi.org/10.1016/j.energy.2012.11.002

Beaudin, M., Zareipour, H., Schellenberglabe, A., & Rosehart, W. (2010). Energy storage for mitigating the variability of renewable electricity sources: An updated review. Energy for Sustainable Development, 14(4), 302-314. doi: 10.1016/j.esd.2010.09.007

Bhatnagar, P., & Nema, R. K. (2013). Maximum power point tracking control techniques: State-of-the-art in photovoltaic applications. Renewable and Sustainable Energy Reviews, 23(0), 224-241. doi: http://dx.doi.org/10.1016/j.rser.2013.02.011

Bhowmik, A., Maitra, A., Halpin, S. M., & Schatz, J. E. (2003). Determination of allowable penetration levels of distributed generation resources based on harmonic limit considerations. IEEE Transactions on Power Delivery, 18(2), 619-624. doi: 10.1109/tpwrd.2003.810494

Blyden, B. K., & Wei-Jen, L. (2006). Modified microgrid concept for rural electrification in Africa. Paper presented at the Power Engineering Society General Meeting, 2006. IEEE.

Bo, K., Youyi, W., & Yoke-Lin, T. (2000, 2000). An H_∞ controller design for diesel engine systems. Paper presented at the Power System Technology, 2000. Proceedings. PowerCon 2000. International Conference on.

Bo, K., Youyi, W., & Yoke Lin, T. (2000, 2000). An H∞ controller design for diesel engine systems. Paper presented at the International Conference on Power System Technology.

Brahma, S. M., & Girgis, A. A. (2004). Development of adaptive protection scheme for distribution systems with high penetration of distributed generation. IEEE Transactions on Power Delivery, 19(1), 56-63. doi: 10.1109/tpwrd.2003.820204

Brinkman, G., Denholm, P., Drury, E., Margolis, R., & Mowers, M. (2011). Toward a Solar-Powered Grid. IEEE Power and Energy Magazine, 9(3), 24-32. doi: 10.1109/MPE.2011.940574

Brown, P. D., Peas Lopes, J. A., & Matos, M. A. (2008). Optimization of Pumped Storage Capacity in an Isolated Power System With Large Renewable Penetration. IEEE Transactions on Power Systems, 23(2), 523-531. doi: 10.1109/tpwrs.2008.919419

Carbone, R. (Ed.). (2011). Energy Storage in the Emerging Era of Smart Grids. Croatia: InTech.

Carrero, C., Amador, J., & Arnaltes, S. (2007). A single procedure for helping PV designers to select silicon PV modules and evaluate the loss resistances. Renewable Energy, 32(15), 2579-2589. doi: http://dx.doi.org/10.1016/j.renene.2007.01.001

Chandorkar, M. C., Divan, D. M., & Adapa, R. (1993). Control of parallel connected inverters in standalone AC supply systems. IEEE Transactions on Industry Applications, 29(1), 136-143. doi: 10.1109/28.195899

Chang, Y., Mao, X., Zhao, Y., Feng, S., Chen, H., & Finlow, D. (2009). Lead-acid battery use in the development of renewable energy systems in China. Journal of Power Sources, 191(1), 176-183. doi: 10.1016/j.jpowsour.2009.02.030

Chow, S. K. H., Lee, E. W. M., & Li, D. H. W. (2012). Short-term prediction of photovoltaic energy generation by intelligent approach. Energy and Buildings, 55(0), 660-667. doi: http://dx.doi.org/10.1016/j.enbuild.2012.08.011

Chowdhury, S., & Crossley, P. (2009). Microgrids and active distribution networks The Institution of Engineering and Technology.

Colson, C. M., & Nehrir, M. H. (2011, 24-29 July 2011). Algorithms for distributed decision-making for multi-agent microgrid power management. Paper presented at the Power and Energy Society General Meeting, 2011 IEEE.

Cornforth, D. (2011). Role of Microgrids in the Smart Grid. Journal of Electronic Science and Technology, 9(1), 9-16.

Datta, M., Senjyu, T., Yona, A., Funabashi, T., & Chul-Hwan, K. (2011). A Frequency-Control Approach by Photovoltaic Generator in a PV-Diesel Hybrid Power System. IEEE Transactions on Energy Conversion, 26(2), 559-571. doi: 10.1109/TEC.2010.2089688

Daud, M. Z., Mohamed, A., & Hannan, M. A. (2013). An improved control method of battery energy storage system for hourly dispatch of photovoltaic power sources. Energy Conversion and Management, 73(0), 256-270. doi: http://dx.doi.org/10.1016/j.enconman.2013.04.013

De Brabandere, K., Bolsens, B., Van den Keybus, J., Woyte, A., Driesen, J., & Belmans, R. (2007). A Voltage and Frequency Droop Control Method for

Parallel Inverters. IEEE Transactions on Power Electronics, 22(4), 1107-1115. doi: 10.1109/tpel.2007.900456

De Brabandere, K., Bolsens, B., Van Den Keybus, J., Woyte, A., Driesen, J., Belmans, R., & Leuven, K. U. (2004, 2004). A voltage and frequency droop control method for parallel inverters. Paper presented at the Power Electronics Specialists Conference, 2004. PESC 04. 2004 IEEE 35th Annual.

De Doncker, R., Pulle, D. W., & Veltman, A. (2010). Advanced Electrical Drives: Analysis, Modeling, Control: Springer.

Díaz-González, F., Sumper, A., Gomis-Bellmunt, O., & Villafáfila-Robles, R. (2012). A review of energy storage technologies for wind power applications. Renewable and Sustainable Energy Reviews, 16(4), 2154-2171. doi: 10.1016/j.rser.2012.01.029

Divya, K. C., & Østergaard, J. (2009). Battery energy storage technology for power systems—An overview. Electric Power Systems Research, 79(4), 511-520. doi: 10.1016/j.epsr.2008.09.017

Downer, D. (2001). Rural electrification scheme in Uganda. Power Engineering Journal, 15(4), 185-192. doi: 10.1049/pe:20010403

Droste-Franke, B., P. Paal, B., Rehtanz, C., Uwe Sauer, D., Schneider, J. P., Schreurs, M., . . . Noll, T. (2012). Balancing Renewable Electricity - Energy Storage, Demand Side Management, and Network Extension from an Interdisciplinary Perspective. Heidelberg: Springer.

Eckroad, S., & Gyuk, I. (2003). EPRI-DOE handbook of energy storage for transmission & distribution applications. Electric Power Research Institute, Inc.

Eftekharnejad, S., Vittal, V., Heydt, G. T., Keel, B., & Loehr, J. (2013). Impact of Increased Penetration of Photovoltaic Generation on Power Systems. IEEE Transactions on Power Systems, 28(2), 893-901. doi: 10.1109/TPWRS.2012.2216294

El-Khattam, W., Hegazy, Y. G., & Salama, M. M. A. (2005). An integrated distributed generation optimization model for distribution system planning. IEEE Transactions on Power Systems, 20(2), 1158-1165. doi: 10.1109/tpwrs.2005.846114

El Moursi, M. S., Weidong, X., & Kirtley, J. L. (2013). Fault ride through capability for grid interfacing large scale PV power plants. IET Generation, Transmission & Distribution, 7(9), 1027-1036. doi: 10.1049/iet-gtd.2013.0154

Ellis, A., Behnke, M., & Keller, J. (2011). Model Makers. IEEE Power and Energy Magazine, 9(3), 55-61. doi: 10.1109/MPE.2011.940577

Elmitwally, A., & Rashed, M. (2011). Flexible Operation Strategy for an Isolated PV-Diesel Microgrid Without Energy Storage. IEEE Transactions on Energy Conversion, 26(1), 235-244. doi: 10.1109/TEC.2010.2082090

Eltawil, M. A., & Zhao, Z. (2013). MPPT techniques for photovoltaic applications. Renewable and Sustainable Energy Reviews, 25(0), 793-813. doi: http://dx.doi.org/10.1016/j.rser.2013.05.022

Fernandez-Jimenez, L. A., Muñoz-Jimenez, A., Falces, A., Mendoza-Villena, M., Garcia-Garrido, E., Lara-Santillan, P. M., . . . Zorzano-Santamaria, P. J. (2012). Short-term power forecasting system for photovoltaic plants. Renewable Energy, 44(0), 311-317. doi: http://dx.doi.org/10.1016/j.renene.2012.01.108

Ghoddami, H., Delghavi, M. B., & Yazdani, A. (2012). An integrated wind-photovoltaic-battery system with reduced power-electronic interface and fast control for grid-tied and off-grid applications. Renewable Energy, 45(0), 128-137. doi: http://dx.doi.org/10.1016/j.renene.2012.02.016

Ghosn, S. B., Ranganathan, P., Salem, S., Jingpeng, T., Loegering, D., & Nygard, K. E. (2010, 4-6 Oct. 2010). Agent-Oriented Designs for a Self Healing Smart Grid. Paper presented at the Smart Grid Communications (SmartGridComm), 2010 First IEEE International Conference on.

Gil, H. A., & Joos, G. (2008). Models for quantifying the economic benefits of distributed generation. IEEE Transactions on Power Systems, 23(2), 327-335.

Golshan, M. E. H., & Arefifar, S. A. (2006). Distributed generation, reactive sources and network-configuration planning for power and energy-loss reduction. IEE Proceedings-Generation, Transmission and Distribution, 153(2), 127-136. doi: 10.1049/ip-gtd:20050170

Graham, V. A., & Hollands, K. G. T. (1990). A method to generate synthetic hourly solar radiation globally. Solar Energy, 44(6), 333-341. doi: http://dx.doi.org/10.1016/0038-092X(90)90137-2

Guerrero, J. M., Matas, J., de Vicuna, L. G., Castilla, M., & Miret, J. (2006). Wireless-Control Strategy for Parallel Operation of Distributed-Generation Inverters. IEEE Transactions on Industrial Electronics, 53(5), 1461-1470. doi: 10.1109/tie.2006.882015

Guerrero, J. M., Matas, J., Luis Garcia de, V., Castilla, M., & Miret, J. (2007). Decentralized Control for Parallel Operation of Distributed Generation Inverters Using Resistive Output Impedance. IEEE Transactions on Industrial Electronics, 54(2), 994-1004. doi: 10.1109/tie.2007.892621

Guerrero, J. M., Vasquez, J. C., Matas, J., de Vicuna, L. G., & Castilla, M. (2011). Hierarchical Control of Droop-Controlled AC and DC Microgrids; A General Approach Toward Standardization. IEEE Transactions on Industrial Electronics, 58(1), 158-172.

Haffner, S., Pereira, L. F. A., Pereira, L. A., & Barreto, L. S. (2008). Multistage model for distribution expansion planning with distributed generation—Part I: Problem formulation. IEEE Transactions on Power Delivery, 23(2), 915-923.

Hankins, M. (2010). Stand-alone Solar Electric Systems: The Earthscan Expert Handbook for Planning, Design and Installation: Earthscan.

Haruna, H., Itoh, S., Horiba, T., Seki, E., & Kohno, K. (2011). Large-format lithium-ion batteries for electric power storage. Journal of Power Sources, 196(16), 7002-7005. doi: 10.1016/j.jpowsour.2010.10.045

Hassan, M. A., & Abido, M. A. (2011). Optimal Design of Microgrids in Autonomous and Grid-Connected Modes Using Particle Swarm Optimization. IEEE Transactions on Power Electronics, 26(3), 755-769. doi: 10.1109/TPEL.2010.2100101

Hernández, J. C., Ruiz-Rodriguez, F. J., & Jurado, F. (2013). Technical impact of photovoltaic-distributed generation on radial distribution systems: Stochastic simulations for a feeder in Spain. International Journal of Electrical Power & Energy Systems, 50(0), 25-32. doi: http://dx.doi.org/10.1016/j.ijepes.2013.02.010

Hernandez, R. R., Easter, S. B., Murphy-Mariscal, M. L., Maestre, F. T., Tavassoli, M., Allen, E. B., . . . Allen, M. F. (2014). Environmental impacts of utility-scale

solar energy. Renewable and Sustainable Energy Reviews, 29(0), 766-779. doi: http://dx.doi.org/10.1016/j.rser.2013.08.041

Hill, C. A., Such, M. C., Dongmei, C., Gonzalez, J., & Grady, W. M. (2012). Battery Energy Storage for Enabling Integration of Distributed Solar Power Generation. IEEE Transactions on Smart Grid, 3(2), 850-857. doi: 10.1109/TSG.2012.2190113

Hoke, A., Butler, R., Hambrick, J., & Kroposki, B. (2013). Steady-State Analysis of Maximum Photovoltaic Penetration Levels on Typical Distribution Feeders. IEEE Transactions on Sustainable Energy, 4(2), 350-357. doi: 10.1109/TSTE.2012.2225115

IEEE Application Guide for IEEE Std 1547, IEEE Standard for Interconnecting Distributed Resources with Electric Power Systems. (2009). IEEE Std 1547.2-2008, 1-207. doi: 10.1109/IEEESTD.2008.4816078

IEEE Recommended Practice for Excitation System Models for Power System Stability Studies. (2006). IEEE Std 421.5-2005 (Revision of IEEE Std 421.5-1992), 0_1-85. doi: 10.1109/IEEESTD.2006.99499

IEEE Recommended Practice for Utility Interface of Photovoltaic (PV) Systems. (2000). IEEE Std 929-2000, i. doi: 10.1109/IEEESTD.2000.91304

IEEE Standard for Interconnecting Distributed Resources With Electric Power Systems. (2003). IEEE Std 1547-2003, 0_1-16. doi: 10.1109/ieeestd.2003.94285

Inman, R. H., Pedro, H. T. C., & Coimbra, C. F. M. (2013). Solar forecasting methods for renewable energy integration. Progress in Energy and Combustion Science, 39(6), 535-576. doi: http://dx.doi.org/10.1016/j.pecs.2013.06.002

International Energy Agency. (2014). PVPS Trends in Photovoltaic Applications, . Sweden: IEA.

Ishaque, K., & Salam, Z. (2013). A review of maximum power point tracking techniques of PV system for uniform insolation and partial shading condition. Renewable and Sustainable Energy Reviews, 19(0), 475-488. doi: http://dx.doi.org/10.1016/j.rser.2012.11.032

Jiayi, H., Chuanwen, J., & Rong, X. (2008). A review on distributed energy resources and MicroGrid. Renewable and Sustainable Energy Reviews, 12(9), 2472-2483. doi: 10.1016/j.rser.2007.06.004

Kakigano, H., Miura, Y., Ise, T., & Uchida, R. (2006, 18-22 June 2006). DC Micro-grid for Super High Quality Distribution - System Configuration and Control of Distributed Generations and Energy Storage Devices. Paper presented at the Power Electronics Specialists Conference, 2006. PESC '06. 37th IEEE.

Kamali, S. K., & Mekhilef, S. (2009, 14-15 Dec. 2009). Evaluation study on grid-connected PV system at University of Malaya. Paper presented at the IEEE International Conference for Technical Postgraduates (TECHPOS).

Katiraei, F., Abbey, C., Tang, S., & Gauthier, M. (2008, 20-24 July 2008). Planned islanding on rural feeders-utility perspective. Paper presented at the Power and Energy Society General Meeting - Conversion and Delivery of Electrical Energy in the 21st Century, 2008 IEEE.

Katiraei, F., Agu, x, & ero, J. R. (2011). Solar PV Integration Challenges. IEEE Power and Energy Magazine, 9(3), 62-71. doi: 10.1109/MPE.2011.940579

Katiraei, F., Iravani, R., Hatziargyriou, N., & Dimeas, A. (2008). Microgrids management. IEEE Power and Energy Magazine, 6(3), 54-65.

Kauhaniemi, K., & Kumpulainen, L. (2004, 5-8 April 2004). Impact of distributed generation on the protection of distribution networks. Paper presented at the Developments in Power System Protection, 2004. Eighth IEE International Conference on.

Khodr, H. M., Vale, Z. A., & Ramos, C. (2009). A Benders Decomposition and Fuzzy Multicriteria Approach for Distribution Networks Remuneration Considering DG. IEEE Transactions on Power Systems, 24(2), 1091-1101. doi: 10.1109/tpwrs.2009.2016526

Koohi-Kamali, S., Rahim, N. A., & Mokhlis, H. (2014). Smart power management algorithm in microgrid consisting of photovoltaic, diesel, and battery storage plants considering variations in sunlight, temperature, and load. Energy Conversion and Management, 84(0), 562-582. doi: http://dx.doi.org/10.1016/j.enconman.2014.04.072

Koohi-Kamali, S., Tyagi, V. V., Rahim, N. A., Panwar, N. L., & Mokhlis, H. (2013). Emergence of energy storage technologies as the solution for reliable operation of smart power systems: A review. Renewable and Sustainable Energy Reviews, 25(0), 135-165. doi: http://dx.doi.org/10.1016/j.rser.2013.03.056

KoohiKamali, S., Yusof, S., Selvaraj, J., & Esa, M. N. B. (2010, Nov. 29 2010-Dec. 1 2010). Impacts of grid-connected PV system on the steady-state operation of a Malaysian grid. Paper presented at the IEEE International Conference on Power and Energy (PECon).

Kroposki, B., Basso, T., & DeBlasio, R. (2008, 20-24 July 2008). Microgrid standards and technologies. Paper presented at the Power and Energy Society General Meeting - Conversion and Delivery of Electrical Energy in the 21st Century, 2008 IEEE.

Kroposki, B., Lasseter, R., Ise, T., Morozumi, S., Papatlianassiou, S., & Hatziargyriou, N. (2008). Making microgrids work. IEEE Power and Energy Magazine, 6(3), 40-53.

Kundur, P. (1994). Power System Stability and Control. New York: McGraw-Hill Inc.,.

Lasseter, R. H. (2002). Microgrids. Paper presented at the Power Engineering Society Winter Meeting, 2002. IEEE.

Lee, K.-J., Shin, D., Yoo, D.-W., Choi, H.-K., & Kim, H.-J. (2013). Hybrid photovoltaic/diesel green ship operating in standalone and grid-connected mode – Experimental investigation. Energy, 49(0), 475-483. doi: http://dx.doi.org/10.1016/j.energy.2012.11.004

Lewis, P. (1997). Rural electrification in Nicaragua. IEEE Technology and Society Magazine, 16(2), 6-13, 32. doi: 10.1109/44.592251

Li, Y. W., & Kao, C.-N. (2009). An accurate power control strategy for power-electronics-interfaced distributed generation units operating in a low-voltage multibus microgrid. IEEE Transactions on Power Electronics, 24(12), 2977-2988.

Lidula, N., & Rajapakse, A. (2011). Microgrids research: A review of experimental microgrids and test systems. Renewable and Sustainable Energy Reviews, 15(1), 186-202.

Lin, X., Xinbo, R., Chengxiong, M., Buhan, Z., & Yi, L. (2013). An Improved Optimal Sizing Method for Wind-Solar-Battery Hybrid Power System. IEEE Transactions on Sustainable Energy, 4(3), 774-785. doi: 10.1109/TSTE.2012.2228509

Lopez, M., de Vicuna, L. G., Castilla, M., Matas, J., & Lopez, O. (2000, 2000). Control loop design of parallel connected converters using sliding mode and linear control techniques. Paper presented at the Power Electronics Specialists Conference, 2000. PESC 00. 2000 IEEE 31st Annual.

Mackay, L. (1990). Rural electrification in Nepal: new techniques for affordable power. Power Engineering Journal, 4(5), 223-231.

Majumder, R., Ghosh, A., Ledwich, G., & Zare, F. (2009a, 26-30 July 2009). Angle droop versus frequency droop in a voltage source converter based autonomous microgrid. Paper presented at the Power & Energy Society General Meeting, 2009. PES '09. IEEE.

Majumder, R., Ghosh, A., Ledwich, G., & Zare, F. (2009b). Load sharing and power quality enhanced operation of a distributed microgrid. IET Renewable Power Generation, 3(2), 109-119. doi: 10.1049/iet-rpg:20080001

Mandal, P., Madhira, S. T. S., haque, A. U., Meng, J., & Pineda, R. L. (2012). Forecasting Power Output of Solar Photovoltaic System Using Wavelet Transform and Artificial Intelligence Techniques. Procedia Computer Science, 12(0), 332-337. doi: http://dx.doi.org/10.1016/j.procs.2012.09.080

Marra, F., Yang, G. Y., Fawzy, Y. T., Traeholt, C., Larsen, E., Garcia-Valle, R., & Jensen, M. M. (2013). Improvement of Local Voltage in Feeders With Photovoltaic Using Electric Vehicles. IEEE Transactions on Power Systems, PP(99), 1-2. doi: 10.1109/TPWRS.2013.2248959

Marwali, M. N., Jin-Woo, J., & Keyhani, A. (2004). Control of distributed generation systems - Part II: Load sharing control. IEEE Transactions on Power Electronics, 19(6), 1551-1561. doi: 10.1109/tpel.2004.836634

Marwali, M. N., Jin-Woo, J., & Keyhani, A. (2007). Stability Analysis of Load Sharing Control for Distributed Generation Systems. IEEE Transactions on Energy Conversion, 22(3), 737-745. doi: 10.1109/tec.2006.881397

Marwali, M. N., & Keyhani, A. (2004). Control of distributed generation systems-Part I: Voltages and currents control. IEEE Transactions on Power Electronics, 19(6), 1541-1550. doi: 10.1109/tpel.2004.836685

Marwali, M. N., Min, D., & Keyhani, A. (2006). Robust stability analysis of voltage and current control for distributed generation systems. IEEE Transactions on Energy Conversion, 21(2), 516-526. doi: 10.1109/tec.2005.860406

Matallanas, E., Castillo-Cagigal, M., Gutiérrez, A., Monasterio-Huelin, F., Caamaño-Martín, E., Masa, D., & Jiménez-Leube, J. (2012). Neural network controller for Active Demand-Side Management with PV energy in the residential sector. Applied Energy, 91(1), 90-97. doi: http://dx.doi.org/10.1016/j.apenergy.2011.09.004

Mellit, A., Massi Pavan, A., & Lughi, V. (2014). Short-term forecasting of power production in a large-scale photovoltaic plant. Solar Energy, 105(0), 401-413. doi: http://dx.doi.org/10.1016/j.solener.2014.03.018

Menti, A., Zacharias, T., & Milias-Argitis, J. (2011). Harmonic distortion assessment for a single-phase grid-connected photovoltaic system. Renewable Energy, 36(1), 360-368. doi: http://dx.doi.org/10.1016/j.renene.2010.07.001

Mercier, P., Cherkaoui, R., & Oudalov, A. (2009). Optimizing a Battery Energy Storage System for Frequency Control Application in an Isolated Power System. IEEE Transactions on Power Systems, 24(3), 1469-1477. doi: 10.1109/tpwrs.2009.2022997

Mills, A., Ahlstrom, M., Brower, M., Ellis, A., George, R., Hoff, T., . . . Yih-Huei, W. (2011). Dark Shadows. IEEE Power and Energy Magazine, 9(3), 33-41. doi: 10.1109/MPE.2011.940575

Milosevic, M., Rosa, P., Portmann, M., & Andersson, G. (2007). Generation Control with Modified Maximum Power Point Tracking in Small Isolated Power Network with Photovoltaic Source. Paper presented at the Power Engineering Society General Meeting, 2007. IEEE.

Mipoung, O. D., Lopes, L. A. C., & Pillay, P. (2014). Frequency Support From a Fixed-Pitch Type-2 Wind Turbine in a Diesel Hybrid Mini-Grid. IEEE Transactions on Sustainable Energy, 5(1), 110-118. doi: 10.1109/TSTE.2013.2273944

Miret, J., Castilla, M., Camacho, A., Garci, x, a de, V., . . . Matas, J. (2012). Control Scheme for Photovoltaic Three-Phase Inverters to Minimize Peak Currents During Unbalanced Grid-Voltage Sags. IEEE Transactions on Power Electronics, 27(10), 4262-4271. doi: 10.1109/TPEL.2012.2191306

Mishra, S., Ramasubramanian, D., & Sekhar, P. C. (2013). A Seamless Control Methodology for a Grid Connected and Isolated PV-Diesel Microgrid. IEEE Transactions on Power Systems, 28(4), 4393-4404. doi: 10.1109/TPWRS.2013.2261098

Moore, S., & Eshani, M. (1996). An empirically based electrosource horizon lead-acid battery model. SAE transactions, 105(6), 421-424.

Moslehi, K., & Kumar, R. (2010, 19-21 Jan. 2010). Smart Grid - a reliability perspective. Paper presented at the Innovative Smart Grid Technologies (ISGT), 2010.

Mukhopadhyay, S., & Singh, B. (2009, 26-30 July 2009). Distributed generation-Basic policy, perspective planning, and achievement so far in india. Paper presented at the Power & Energy Society General Meeting, 2009. PES '09. IEEE.

Munasinghe, M. (1990). Rural electrification in the Third World. Power Engineering Journal, 4(4), 189-202.

Nasiri, A. (2008, 10-13 Nov. 2008). Integrating energy storage with renewable energy systems. Paper presented at the Industrial Electronics, 2008. IECON 2008. 34th Annual Conference of IEEE.

Nayar, C. V., Ashari, M., & Keerthipala, W. W. L. (2000). A grid-interactive photovoltaic uninterruptible power supply system using battery storage and a back up diesel generator. IEEE Transactions on Energy Conversion, 15(3), 348-353. doi: 10.1109/60.875502

Nikkhajoei, H., & Lasseter, R. H. (2007, 24-28 June 2007). Microgrid Protection. Paper presented at the Power Engineering Society General Meeting, 2007. IEEE.

Nikkhajoei, H., & Lasseter, R. H. (2009). Distributed generation interface to the CERTS microgrid. IEEE Transactions on Power Delivery, 24(3), 1598-1608.

Nishioka, K., Sakitani, N., Uraoka, Y., & Fuyuki, T. (2007). Analysis of multicrystalline silicon solar cells by modified 3-diode equivalent circuit model taking leakage current through periphery into consideration. Solar Energy Materials and Solar Cells, 91(13), 1222-1227. doi: http://dx.doi.org/10.1016/j.solmat.2007.04.009

Omran, W. A., Kazerani, M., & Salama, M. M. A. (2011). Investigation of Methods for Reduction of Power Fluctuations Generated From Large Grid-Connected

Photovoltaic Systems. IEEE Transactions on Energy Conversion, 26(1), 318-327. doi: 10.1109/TEC.2010.2062515

Oudalov, A., Buehler, T., & Chartouni, D. (2008, 17-18 Nov. 2008). Utility Scale Applications of Energy Storage. Paper presented at the Energy 2030 Conference, 2008. ENERGY 2008. IEEE.

Owen, E. L. (1998). Rural electrification: the long struggle. IEEE Industry Applications Magazine, 4(3), 6, 8, 10-17. doi: 10.1109/2943.667902

Parisio, A., & Glielmo, L. (2011, 12-15 Dec. 2011). Energy efficient microgrid management using Model Predictive Control. Paper presented at the 50th IEEE Conference on Decision and Control and European Control Conference (CDC-ECC).

Parisio, A., Rikos, E., & Glielmo, L. (2014). A Model Predictive Control Approach to Microgrid Operation Optimization. IEEE Transactions on Control Systems Technology,, 22(5), 1813-1827. doi: 10.1109/TCST.2013.2295737

Pogaku, N., Prodanovic, M., & Green, T. C. (2007). Modeling, Analysis and Testing of Autonomous Operation of an Inverter-Based Microgrid. IEEE Transactions on Power Electronics, 22(2), 613-625. doi: 10.1109/TPEL.2006.890003

Poullikkas, A. (2013). A comparative overview of large-scale battery systems for electricity storage. Renewable and Sustainable Energy Reviews, 27(0), 778-788. doi: http://dx.doi.org/10.1016/j.rser.2013.07.017

Prema, V., & Rao, K. U. (2014, 23-25 Jan. 2014). Predictive models for power management of a hybrid microgrid — A review. Paper presented at the International Conference on Advances in Energy Conversion Technologies (ICAECT),.

Puttgen, H. B., MacGregor, P. R., & Lambert, F. C. (2003). Distributed generation: Semantic hype or the dawn of a new era? Power and Energy Magazine, IEEE, 1(1), 22-29. doi: 10.1109/mpae.2003.1180357

PVPS, I. (2012). Trends in photovoltaic applications. Survey report of selected IEA countries between 1992 and 2011. Report IEA-PVPS T1–21.

Rabiee, A., Khorramdel, H., & Aghaei, J. (2013). A review of energy storage systems in microgrids with wind turbines. Renewable and Sustainable Energy Reviews, 18(0), 316-326. doi: http://dx.doi.org/10.1016/j.rser.2012.09.039

Rajapakse, A. D., & Muthumuni, D. (2009, 22-23 Oct. 2009). Simulation tools for photovoltaic system grid integration studies. Paper presented at the Electrical Power & Energy Conference (EPEC), 2009 IEEE.

Ramasamy, M., & Thangavel, S. (2011). Photovoltaic Based Dynamic Voltage Restorer with Outage Handling Capability Using PI Controller. Energy Procedia, 12(0), 560-569. doi: http://dx.doi.org/10.1016/j.egypro.2011.10.076

Ramasamy, M., & Thangavel, S. (2012). Photovoltaic based dynamic voltage restorer with power saver capability using PI controller. International Journal of Electrical Power & Energy Systems, 36(1), 51-59. doi: http://dx.doi.org/10.1016/j.ijepes.2011.10.023

Rekioua Pr, D. (2012). Optimization of Photovoltaic Power Systems.

Remco Ltd. (2012). REMCO Renewable Energy Manufacturing Company. Hong Kong.

Renewable Energy Policy Network for the 21st Century. (2014). Renewables Global Status report. France: REN21.

Reza, M., Sudarmadi, D., Viawan, F. A., Kling, W. L., & Van Der Sluis, L. (2006, Oct. 29 2006-Nov. 1 2006). Dynamic Stability of Power Systems with Power Electronic Interfaced DG. Paper presented at the Power Systems Conference and Exposition, 2006. PSCE '06. 2006 IEEE PES.

Ribeiro, P. F., Johnson, B. K., Crow, M. L., Arsoy, A., & Liu, Y. (2001). Energy storage systems for advanced power applications. Proceedings of the IEEE, 89(12), 1744-1756. doi: 10.1109/5.975900

Roberts, B. P., & Sandberg, C. (2011). The Role of Energy Storage in Development of Smart Grids. Proceedings of the IEEE, 99(6), 1139-1144.

Roy, S., Malik, O. P., & Hope, G. S. (1991a). An adaptive control scheme for speed control of diesel driven power-plants. IEEE Transactions on Energy Conversion, 6(4), 605-611. doi: 10.1109/60.103632

Roy, S., Malik, O. P., & Hope, G. S. (1991b). A least-squares based model-fitting identification technique for diesel prime-movers with unknown dead-time. IEEE Transactions on Energy Conversion, 6(2), 251-256. doi: 10.1109/60.79629

S. Barnes, F., & G. Levine, J. (2011). Large Energy Storage Systems Handbook. USA: CRC Press, Taylor & Francis Group.

Sadineni, S. B., Atallah, F., & Boehm, R. F. (2012). Impact of roof integrated PV orientation on the residential electricity peak demand. Applied Energy, 92(0), 204-210. doi: http://dx.doi.org/10.1016/j.apenergy.2011.10.026

Salamah, A., Finney, S., & Williams, B. (2008). Autonomous controller for improved dynamic performance of AC grid, parallel-connected, single-phase inverters. IET Generation, Transmission & Distribution, 2(2), 209-218.

Salas, V., Olías, E., Barrado, A., & Lázaro, A. (2006). Review of the maximum power point tracking algorithms for stand-alone photovoltaic systems. Solar Energy Materials and Solar Cells, 90(11), 1555-1578. doi: http://dx.doi.org/10.1016/j.solmat.2005.10.023

Salomonsson, D., Soder, L., & Sannino, A. (2008). An Adaptive Control System for a DC Microgrid for Data Centers. IEEE Transactions on Industry Applications, 44(6), 1910-1917. doi: 10.1109/tia.2008.2006398

Samuels, M. M. (1946). Specific Engineering Problems in Rural Electrification and Electroagriculture. Transactions of the American Institute of Electrical Engineers, 65(12), 1065-1073. doi: 10.1109/t-aiee.1946.5059286

SANYO North America. (2010). HIT Photovoltaic Module Power 210A. In SANYO Energy (U.S.A.) Corp. (Ed.). the United States.

Sao, C. K., & Lehn, P. W. (2008). Control and power management of converter fed microgrids. IEEE Transactions on Power Systems, 23(3), 1088-1098.

Sarma, M. S. (1997). Electric Machines : Steady-State Theory and Dynamic Performance (2 ed.). Boston, MA: Cengage Learning,.

Sechilariu, M., Baochao, W., & Locment, F. (2013). Building Integrated Photovoltaic System With Energy Storage and Smart Grid Communication. IEEE Transactions on Industrial Electronics, 60(4), 1607-1618. doi: 10.1109/TIE.2012.2222852

Senjyu, T., Miyazato, Y., Yona, A., Urasaki, N., & Funabashi, T. (2008). Optimal Distribution Voltage Control and Coordination With Distributed Generation. IEEE Transactions on Power Delivery, 23(2), 1236-1242. doi: 10.1109/tpwrd.2007.908816

Shah, R., Mithulananthan, N., & Bansal, R. C. (2013). Oscillatory stability analysis with high penetrations of large-scale photovoltaic generation. Energy Conversion and

Management, 65(0), 420-429. doi: http://dx.doi.org/10.1016/j.enconman.2012.08.004

Shahabi, M., Haghifam, M.-R., Mohamadian, M., & Nabavi-Niaki, S. (2009). Microgrid dynamic performance improvement using a doubly fed induction wind generator. IEEE Transactions on Energy Conversion, 24(1), 137-145.

Shahnia, F., Majumder, R., Ghosh, A., Ledwich, G., & Zare, F. (2011). Voltage imbalance analysis in residential low voltage distribution networks with rooftop PVs. Electric Power Systems Research, 81(9), 1805-1814. doi: http://dx.doi.org/10.1016/j.epsr.2011.05.001

Silva, S. B., Severino, M. M., & de Oliveira, M. A. G. (2013). A stand-alone hybrid photovoltaic, fuel cell and battery system: A case study of Tocantins, Brazil. Renewable Energy, 57(0), 384-389. doi: http://dx.doi.org/10.1016/j.renene.2013.02.004

Slootweg, J. G., & Kling, W. L. (2002, 25-25 July 2002). Impacts of distributed generation on power system transient stability. Paper presented at the Power Engineering Society Summer Meeting, 2002 IEEE.

Sorensen, B., Breeze, P., Suppes, G. J., El Bassam, N., Silveira, S., Yang, S.-T., . . . Doble, M. (2008). Renewable Energy Focus Handbook: Academic Press.

Stavrakakis, G. S., & Kariniotakis, G. N. (1995). A general simulation algorithm for the accurate assessment of isolated diesel-wind turbines systems interaction. I. A general multimachine power system model. IEEE Transactions on Energy Conversion, 10(3), 577-583. doi: 10.1109/60.464885

Steffel, S., & Dinkel, A. (2013). Absorbing the Rays: Advanced Inverters Help Integrate PV into Electric Utility Distribution Systems. IEEE Power and Energy Magazine, 11(2), 45-54. doi: 10.1109/MPE.2012.2234406

Steven, W. S. (1997). The scientist and engineer's guide to digital signal processing. California Technical Pub.

Suryanarayanan, S., Mitra, J., & Biswas, S. (2010, 19-22 April 2010). A conceptual framework of a hierarchically networked agent-based microgrid architecture. Paper presented at the 2010 IEEE PES Transmission and Distribution Conference and Exposition.

Taheri, H. (2011). Accurate MATLAB simulink PV system simulator based on a two-diode model. Journal of Power Electronics, 11(2), 179-187.

Tamimi, B., Canizares, C., & Bhattacharya, K. (2013). System Stability Impact of Large-Scale and Distributed Solar Photovoltaic Generation: The Case of Ontario, Canada. IEEE Transactions on Sustainable Energy, PP(99), 1-9. doi: 10.1109/TSTE.2012.2235151

Tan, K. T., Peng, X. Y., So, P. L., Chu, Y. C., & Chen, M. Z. Q. (2012). Centralized Control for Parallel Operation of Distributed Generation Inverters in Microgrids. IEEE Transactions on Smart Grid, 3(4), 1977-1987. doi: 10.1109/TSG.2012.2205952

Tan, K. T., So, P. L., Chu, Y. C., & Chen, M. Z. Q. (2013). Coordinated Control and Energy Management of Distributed Generation Inverters in a Microgrid. IEEE Transactions on Power Delivery, 28(2), 704-713. doi: 10.1109/TPWRD.2013.2242495

Teleke, S., Baran, M. E., Bhattacharya, S., & Huang, A. Q. (2010). Rule-Based Control of Battery Energy Storage for Dispatching Intermittent Renewable Sources. IEEE Transactions on Sustainable Energy, 1(3), 117-124. doi: 10.1109/TSTE.2010.2061880

Teleke, S., Baran, M. E., Huang, A. Q., Bhattacharya, S., & Anderson, L. (2009). Control Strategies for Battery Energy Storage for Wind Farm Dispatching. IEEE Transactions on Energy Conversion, 24(3), 725-732. doi: 10.1109/TEC.2009.2016000

Tonkoski, R., & Lopes, L. A. C. (2011). Impact of active power curtailment on overvoltage prevention and energy production of PV inverters connected to low voltage residential feeders. Renewable Energy, 36(12), 3566-3574. doi: http://dx.doi.org/10.1016/j.renene.2011.05.031

Tonkoski, R., Turcotte, D., & El-Fouly, T. H. M. (2012). Impact of High PV Penetration on Voltage Profiles in Residential Neighborhoods. IEEE Transactions on Sustainable Energy, 3(3), 518-527. doi: 10.1109/TSTE.2012.2191425

Townsend, B. S. (1985). Distribution: the years of change. IEE Proceedings C Generation, Transmission and Distribution, 132(1), 1-7. doi: 10.1049/ip-c:19850001

Tsai, H.-L. (2010). Insolation-oriented model of photovoltaic module using Matlab/Simulink. Solar Energy, 84(7), 1318-1326. doi: http://dx.doi.org/10.1016/j.solener.2010.04.012

Tzung-Lin, L., & Po-Tai, C. (2007). Design of a New Cooperative Harmonic Filtering Strategy for Distributed Generation Interface Converters in an Islanding Network. IEEE Transactions on Power Electronics, 22(5), 1919-1927. doi: 10.1109/tpel.2007.904200

Tzung-Lin, L., Po-Tai, C., Akagi, H., & Fujita, H. (2008). A Dynamic Tuning Method for Distributed Active Filter Systems. IEEE Transactions on Industry Applications, 44(2), 612-623. doi: 10.1109/tia.2008.916596

Urbanetz, J., Braun, P., & Rüther, R. (2012). Power quality analysis of grid-connected solar photovoltaic generators in Brazil. Energy Conversion and Management, 64(0), 8-14. doi: http://dx.doi.org/10.1016/j.enconman.2012.05.008

Valverde, L., Bordons, C., & Rosa, F. (2012, 25-28 Oct. 2012). Power management using model predictive control in a hydrogen-based microgrid. Paper presented at the IECON 2012 - 38th Annual Conference on IEEE Industrial Electronics Society.

Varaiya, P. P., Wu, F. F., & Bialek, J. W. (2011). Smart Operation of Smart Grid: Risk-Limiting Dispatch. Proceedings of the IEEE, 99(1), 40-57. doi: 10.1109/JPROC.2010.2080250

Vazquez, S., Lukic, S. M., Galvan, E., Franquelo, L. G., & Carrasco, J. M. (2010). Energy Storage Systems for Transport and Grid Applications. IEEE Transactions on Industrial Electronics, 57(12), 3881-3895.

Vieira, J. C. M., Freitas, W., Wilsun, X., & Morelato, A. (2006). Efficient coordination of ROCOF and frequency relays for distributed generation protection by using the application region. IEEE Transactions on Power Delivery, 21(4), 1878-1884. doi: 10.1109/tpwrd.2006.881588

Vilathgamuwa, D. M., Poh Chiang, L., & Li, Y. (2006). Protection of Microgrids During Utility Voltage Sags. IEEE Transactions on Industrial Electronics, 53(5), 1427-1436. doi: 10.1109/tie.2006.882006

von Appen, J., Braun, M., Stetz, T., Diwold, K., & Geibel, D. (2013). Time in the sun: the challenge of high PV penetration in the German electric grid. IEEE Power and Energy Magazine, 11(2), 55-64. doi: 10.1109/MPE.2012.2234407

Wang, C. (2006). Modeling and control of hybrid wind/photovoltaic/fuel cell distributed generation systems. MONTANA STATE UNIVERSITY Bozeman.

Wei, Q., Jinfeng, L., Xianzhong, C., & Christofides, P. D. (2011). Supervisory Predictive Control of Standalone Wind/Solar Energy Generation Systems. IEEE Transactions on Control Systems Technology,, 19(1), 199-207. doi: 10.1109/TCST.2010.2041930

Widén, J., Wäckelgård, E., Paatero, J., & Lund, P. (2010). Impacts of distributed photovoltaics on network voltages: Stochastic simulations of three Swedish low-voltage distribution grids. Electric Power Systems Research, 80(12), 1562-1571. doi: http://dx.doi.org/10.1016/j.epsr.2010.07.007

Yazdani, A., Di Fazio, A. R., Ghoddami, H., Russo, M., Kazerani, M., Jatskevich, J., . . . Martinez, J. A. (2011). Modeling Guidelines and a Benchmark for Power System Simulation Studies of Three-Phase Single-Stage Photovoltaic Systems. IEEE Transactions on Power Delivery, 26(2), 1247-1264. doi: 10.1109/TPWRD.2010.2084599

Yazdani, A., & Iravani, R. (2010). Voltage-sourced converters in power systems: Wiley. com.

Yoshimoto, K., Nanahara, T., & Koshimizu, G. (2006, Oct. 29 2006-Nov. 1 2006). New Control Method for Regulating State-of- Charge of a Battery in Hybrid Wind Power/Battery Energy Storage System. Paper presented at the Power Systems Conference and Exposition, 2006. PSCE '06. 2006 IEEE PES.

Yu, R., Kleissl, J., & Martinez, S. (2013). Storage Size Determination for Grid-Connected Photovoltaic Systems. IEEE Transactions on Sustainable Energy, 4(1), 68-81. doi: 10.1109/TSTE.2012.2199339

Yun-Hyun, K., Soo-Hong, K., Chang-Jin, L., Sang Hyun, K., & Byeong-Ki, K. (2011, May 30 2011-June 3 2011). Control strategy of energy storage system for power

stability in a wind farm. Paper presented at the Power Electronics and ECCE Asia (ICPE & ECCE), 2011 IEEE 8th International Conference on.

Yun Wei, L., Vilathgamuwa, D. M., & Poh Chiang, L. (2007). Robust Control Scheme for a Microgrid With PFC Capacitor Connected. IEEE Transactions on Industry Applications, 43(5), 1172-1182. doi: 10.1109/tia.2007.904388

Zahedi, A. (2011). Maximizing solar PV energy penetration using energy storage technology. Renewable and Sustainable Energy Reviews, 15(1), 866-870. doi: http://dx.doi.org/10.1016/j.rser.2010.09.011

Zhang, Y., & Ooi, B. T. (2013). Stand-Alone Doubly-Fed Induction Generators (DFIGs) With Autonomous Frequency Control. IEEE Transactions on Power Delivery, 28(2), 752-760. doi: 10.1109/TPWRD.2013.2243170

Zhou, D., Zhao, Z., Eltawil, M., & Yuan, L. (2008, 24-28 Feb. 2008). Design and control of a three-phase grid-connected photovoltaic system with developed maximum power point tracking. Paper presented at the Applied Power Electronics Conference and Exposition, 2008. APEC 2008. Twenty-Third Annual IEEE.

LIST OF PUBLICATIONS AND PAPERS PRESENTED

This work has been reported through following publications:

Journal Papers

1. Sam Koohi-Kamali, N.A. Rahim, H. Mokhlis, Smart power management algorithm in microgrid consisting of photovoltaic, diesel, and battery storage plants considering variations in sunlight, temperature, and load, Energy Conversion and Management, Volume 84, August 2014, Pages 562-582.

2. Koohi-Kamali, S., et al., Emergence of energy storage technologies as the solution for reliable operation of smart power systems: A review. Renewable and Sustainable Energy Reviews, Volume 25, September 2013, Pages 135-165.

3. Koohi-Kamali, S., et al., Photovoltaic electricity generator dynamic modeling methods for smart grid applications: A review. Renewable and Sustainable Energy Reviews, 2014. (under review).

Conference and Symposium Papers

1. Koohi-Kamali S, Rahim NA, Mokhlis H. A Novel Power Smoothing Index for Dispatching of Battery Energy Storage Plant in Smart Microgrid. IEEE Conference on Clean Energy and Technology (CEAT); 2014.

2. Koohi-Kamali S, Rahim NA, Mokhlis H. New Algorithms to Size and Protect Battery Energy Storage Plant in Smart Microgrid Considering Intermittency in Load and Generation. IEEE Conference on Clean Energy and Technology (CEAT); 2014.

3. Koohi-Kamali S, Rahim NA, Mokhlis H. A Survey on Power Management Strategies for Parallel Operation of DG Units in Smart Microgrids. Power and Energy Conversion Symposium (PECS 2012): Universiti Teknikal Malaysia (UTem); 2012. p. 164-8.

APPENDIX

APPENDIX A. Power management algorithm (PMA) FORTRAN codes developed in PSCAD/EMTDC software

```
IF ($BRK_GRID==0) THEN
$Index=($Pset-$Ppv)+($PL-$PLavg)
$Q0D1=(($QL-$QLavg)/(1+$D))
$Q0B1=(($QL-$QLavg)/(1+(1/$D)))
IF (Time<$t1 .OR. Time>$t2) THEN
IF ($SOC<$SOCref) THEN
$P1_REF=-0.15
$P0D1=($PL*beta)
ELSE
$P1_REF=0
$P0D1=($PL*beta)
ENDIF
ENDIF
IF (Time>=$t1 .AND. Time<=$t2) THEN
IF ($SOC>$SOCmin .AND. $SOC<$SOCmax) THEN
$P1_REF=$Index
$P0D1=($PL*beta)
ELSEIF ($Index>0 .AND. $SOC>=SOCmax) THEN
$P1_REF=$Index
$P0D1=($PL*beta)
ELSEIF ($Index<0 .AND. $SOC<=$SOCmin) THEN
$P1_REF=$Index
$P0D1=($PL*beta)
ELSE
$P1_REF=0
$P0D1=($PL*beta)
ENDIF
ENDIF
ELSE
$P1_REF=$Pd1_REF
ENDIF
```